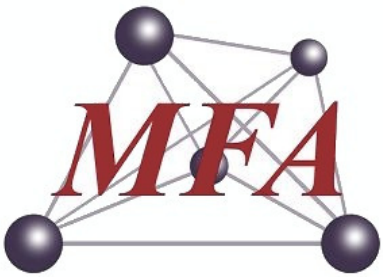

Yearbook

2009

Research Institute for Technical Physics and Materials Science

Hungarian Academy of Sciences

http://www.mfa.kfki.hu/

Research Institute for Technical Physics and Materials Science
Hungarian Academy of Sciences

Director: Prof. István Bársony

Address: Konkoly-Thege Miklós út 29-33,
H-1121 Budapest, Hungary
Postal: P.O.Box 49, H-1525 Budapest, Hungary
Phone: +36-1-392 2225
Fax: +36-1-392 2226
E-mail: info@mfa.kfki.hu
URL: http://www.mfa.kfki.hu/

MTA MFA Yearbook 2009

Editors: Miklós Menyhárd, Csaba S. Daróczi, Zsolt Zolnai, György Z. Radnóczi
Published by: MTA MFA, Budapest, Hungary, 2009

CONTENTS

DIRECTOR'S FOREWORD

Harvesting the preliminary results of agreed research profile, and a stable research strategy, the improved qualification and rejuvenation of research staff, as well as the continuous improvement of infrastructure *as a consequence of a supportive research policy*. This is the summary of the activities of the Research Institute for Technical Physics and Materials Science *in 2009,* where *the institute again achieved its highest financial turnover so far of ca. € 6.3M*. All this happened in a year of worldwide economical crisis, hitting a generally weakened Hungary - a country in disarray, awaiting a change for the better - more than any other country in the EU.

Creativity in science has its roots in individual talent or ability. Successful innovation, however, i.e. how to make the results to work for the benefit of society, is the result of collective effort. Hungarian scientists usually always excel whenever and wherever they have to prove their individual creativity in the World. Concerning the collective performance of our society, however, Hungary is less praiseworthy. This year's success at MFA is therefore all the more valuable, as it reflects the collective effort of our researchers and the excellent technical and administrative support, together with the general acceptance of self-imposed discipline and the regulations and rules of the ISO quality assurance system. All these efforts not only manifest themselves in the good performance of 2009, but more importantly in the strengthening of the institute's collective as such. We at MFA have all the reasons to believe that the continuous striving of our colleagues for high quality in project execution, the training of postgraduate students, the involvement of graduate and undergraduate students at an early phase of their studies in MFA activities, the notable "customer satisfaction" with all our partners from R & D and industry alike, are key factors in this remarkable progress. This has led well beyond the research obligations to new initiatives, with several successful events organised in 2009 again.

The two years old organisation scheme of MFA proved to be adequate to support the coordination and organisation of research efforts. The young colleagues entrusted with responsibilities grew up to the requirements and became efficient drivers of novel initiatives. A long prevailing shortcoming at MFA was that due to lack of information or simple ignorance, existing capabilities and knowledge were not utilized for the benefit of the whole scientific community. A significant improvement in this regard is meanwhile obvious. Among the six research departments within the institute a dense network of collaboration became an efficient driver of the scientific achievements.

We marked a big step forward in the development of public relations for MFA, by publicising the most remarkable new scientific results, and news about supported projects and organised events. Over 150 references were made to our 10 press-releases (some of them as part of the statements of the National Technology Platform for Integrated Micro/nanosystems – IMNTP, coordinated by MFA) in the electronic and printed media – a most reasonable 'echo'. In this regard we also enjoyed the steady attention and support of the news-page of the Hungarian Academy of Sciences, being an important source of reference itself. As an indirect consequence

of it, MFA became rather well known and respected in the materials field, many students and potential customers visited us motivated by those reports.

In 2009 eight young colleagues came to work and study at MFA and a further two Ph.D. stipend owners started their projects at the institute, while only one colleague left us, and three of them retired.

We had again reasons to be proud of the achievements of our colleagues:

Zsolt József Horváth obtained the D.Sc. (MTA Dr.) title from the Hungarian Academy of Sciences for his thesis: "Semiconductor structures – novel effects, new approximations". Péter Basa and Ágoston Németh received their Ph.D. degree from the Budapest University of Technology and Economics.

On March 15, 2009 the financial director of MFA, Mrs. Vera Somogyi was awarded the Golden Cross of Merit of the Hungarian Republic by the President of the Republic, László Sólyom for her "excellent financial direction and achievements in the utilisation of MFA research results by license transfer and spin-off generation".

László Honty received the "Distinction by the General Secretary" on November 26, 2009 for his "excellent and selfless work of over four decades both in his function as scientific secretary of MFA and the representative of the colleagues at the KFKI campus in social matters".

György Gergely, Professor Emeritus Instituti of MFA received his "Diamond diploma" from the Budapest University of Technology and Economics, where he obtained his dr. techn. degree 60 years ago. He was also awarded on November 3, 2009 in "recognition of his life achievements in surface physics" the "Engineering Prize Károly Simonyi".

József Gyulai, past director and Professor Emeritus Instituti of MFA was awarded the "Medal of the Roland Eötvös Physical Society of Hungary".

Antal Gasparics won the "Genius-Europe Jubilee Gold Medal" in 2009 for the development of the control software for the invention of the 'magnetic mouse'.

We are especially proud of the success of our students in different competitions.

At the European Materials Research Society Spring Meeting in Strasbourg, June 8-12, 2009, two of our students won the Best Student Paper Award: in the Section 'Bio- and chemical sensors and transducers: from materials to systems' Péter Kozma (supervisors: Péter Petrik and Róbert Horváth); and in the section 'Carbon nanotubes and graphene - low dimensional carbon structures' Péter Nemes Incze (supervisor: László Péter Biró).

Furthermore, both of the 2009 prizes of the "György Ferenczi Memorial Foundation" were handed over to MFA Ph.D. students, Anita Pongrácz (supervisor: Gábor Battsitig) and Gergely Dobrik (supervisor: László Péter Biró).

Fanni Misják (supervisor: Péter Barna and György Radnóczi) obtained the "Materials Science Prize of the Hungarian Foundation for Microscopy" along with the stipend of the European Microscopy Society.

There was also a 'rain' of prizes at different university and national scientific student contests for the undergraduate and graduate students conducting their training at MFA. Just to list the name of the winners of viarious distinctions: Gábor Dobrik, Gábor Piszter, Zoltán Fekete, Dorina Kocsis, Andrea Németh, Gábor Magda, Mihály

Tóth, Tibor Gerlai, Gergely Márton. After graduation they hopefully will continue their studies as Ph.D. trainees at our institute.
Meanwhile a 'traditional' event, from June 22-27, 2009 the MFA summer camp for high school students was organised again under the motto 'Let's learn from each other!' (http://alag3.mfa.kfki.hu/mfa/nyariiskola/). Using its own means the institute financed the participation of 20 students this time. Applicants were selected from the Hungarian language High Schools of the whole Carpatian-basin, five youngsters came from Transylvania were also supported. The enthusiasm of the participants and mentors, coordinated by Csaba Sándor Daróczi, was a full compensation for the unfavourable weather conditions. As a consequence, at the event "Night of the researchers" on September 24, 2009 two of the participating children, Ervin Habel from Nyíregyháza, and Milan Janosov from Veszprém emerged as winners of the scientific movie-contest.
Another, well visited initiative of the institute on November 13, 2009 was the traditional "Open Day of MFA", hosting some hundred, interested, mostly young attendees at the popular lectures and laboratory visits.
Upon request of the president of HAS, MFA colleagues also participated in the technical design and supervision of the construction of the demonstration-cabinets for physics, biology and chemistry education at the High School János Arany in Budapest.
A continuing task of a management is the steady improvement of research conditions by renovation and extension of existing facilities and new investment of preparatory and analytic equipment. Besides, this is the only means that will enable the participation of MFA in international scientific collaboration as an interesting partner, and of making the institute an attractive place for scientific work – despite the crisis and the relatively low wages of civil servants.
This MFA made a big step by the completion of the microtechnology complex. A new 100 m^2 CVD laboratory for thin-film solar cell technology development was constructed, and at the same time the air conditioning, closed-loop cooling and gas supply of the whole clean-room complex was reconstructed. Also five new laboratories (for liquid-phase-epitaxy, optical and electrical testing as well as device assembly) and 5 working cabinets were newly constructed. Also a notable result of this year is the construction and the inauguration of the joint laboratory for Biosensorics (with the Faculty of Information Technology of University of Pannonia) and for Chemical Nanostructures (with the Faculty of Chemical and Bioengineering of Budapest University of Technology).
This Yearbook is an account of the research progress at MFA in 2009. These introductory remarks are meant to highlight the efforts of the management of the institute to ensure the right conditions to support high quality research work and the birth of scientific achievements by providing an all-around favourable atmosphere despite circumstances beyond our own control.

Budapest, January 2010

István Bársony

GENERAL INFORMATION

Organisation

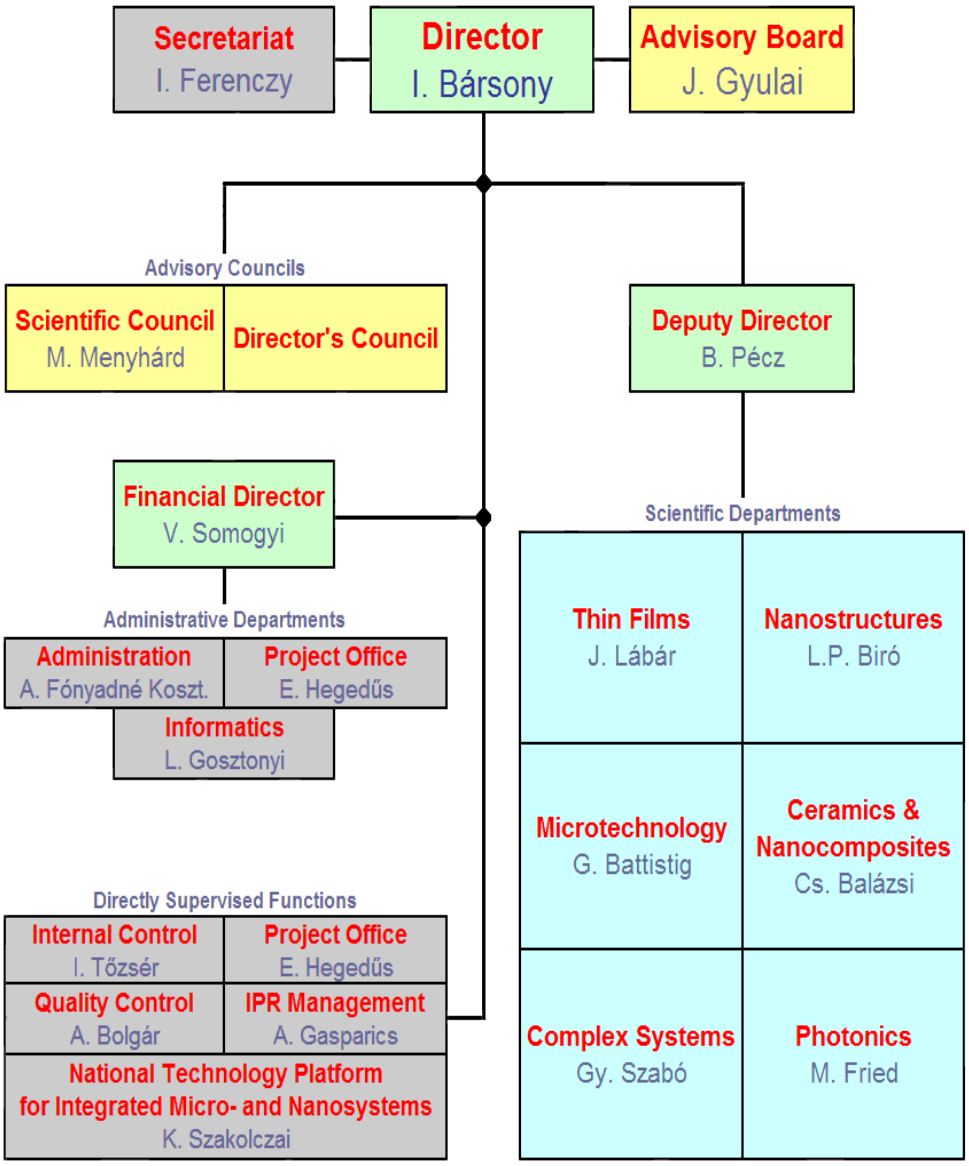

Key Financial Figures

The total budget of MFA in 2009 reached a similar level of about € 6.5 million as in the previous year with significantly improving indices. Beside the decreasing subsidies in 2009 the higher level of the budget of the Institute was mainly facilitated by the increasing success in the participation in international projects.

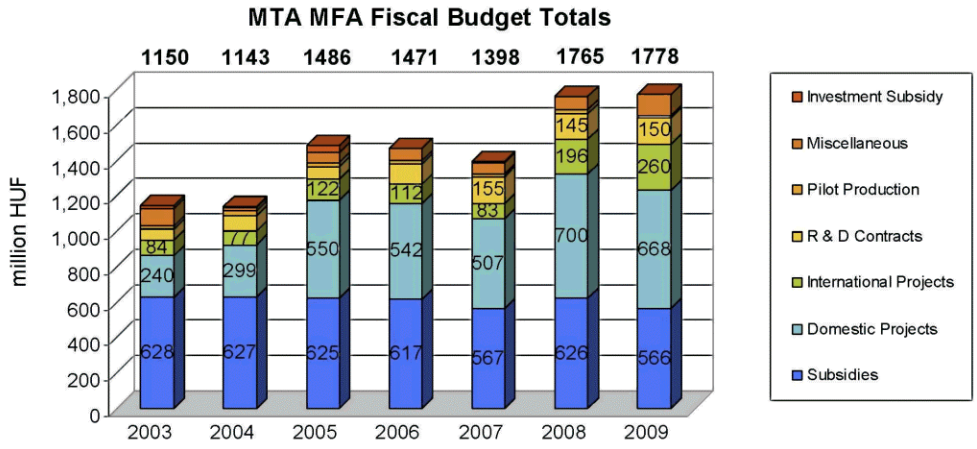

Despite the marginal central investment support, in the last period the research infrastructure of the Institute developed substantially, and in 2009 a significant restoration and extension of the clean room area has been also processed.

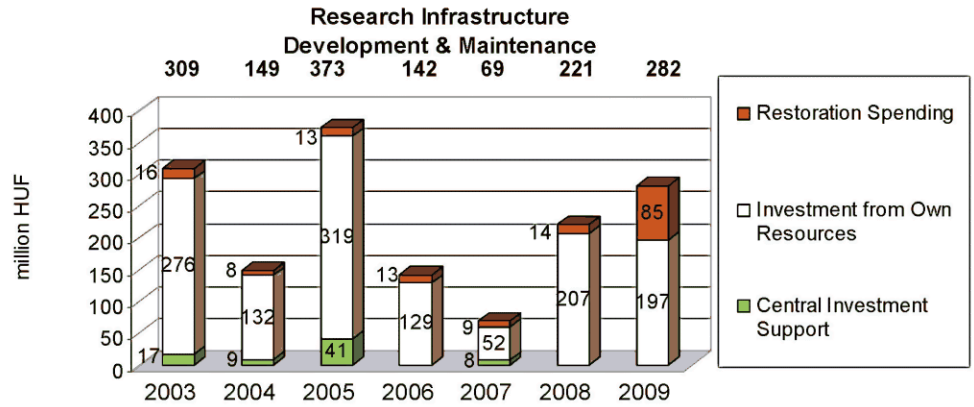

Publications & Citations of MFA

According to the independent internet database of *The Thomson Reuters* (http://isiknowledge.com/), MFA keeps up an average publication activity of 100 scientific papers yearly in the last decade. Fluctuations arise due to the phases of strategic infrastructural development and establishment of new fields of research.

***Publications** of MFA (source: ISI Web of Science)*

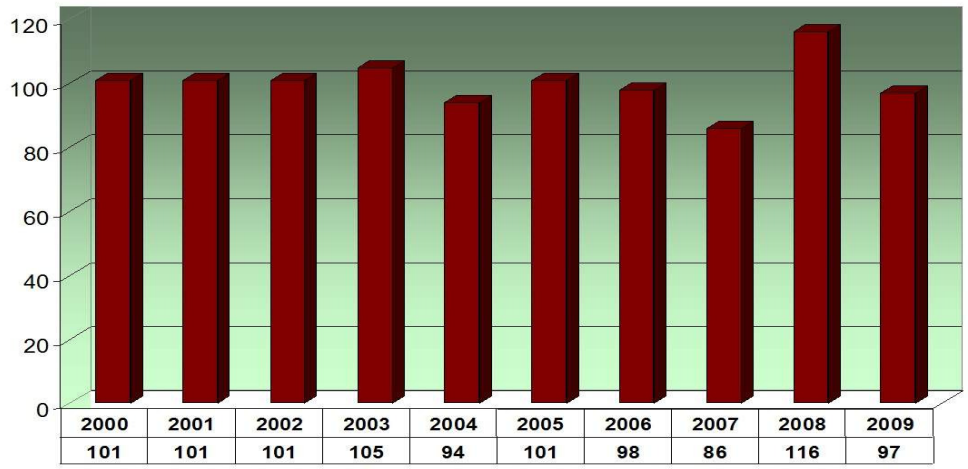

A good measure of the recognition of MFA's scientific activity is the *Hirsch-index* value of **49**, and it can be clearly seen in the yearly growth of independent citations.

*Publication **citing** of MFA (source: ISI Web of Science)*

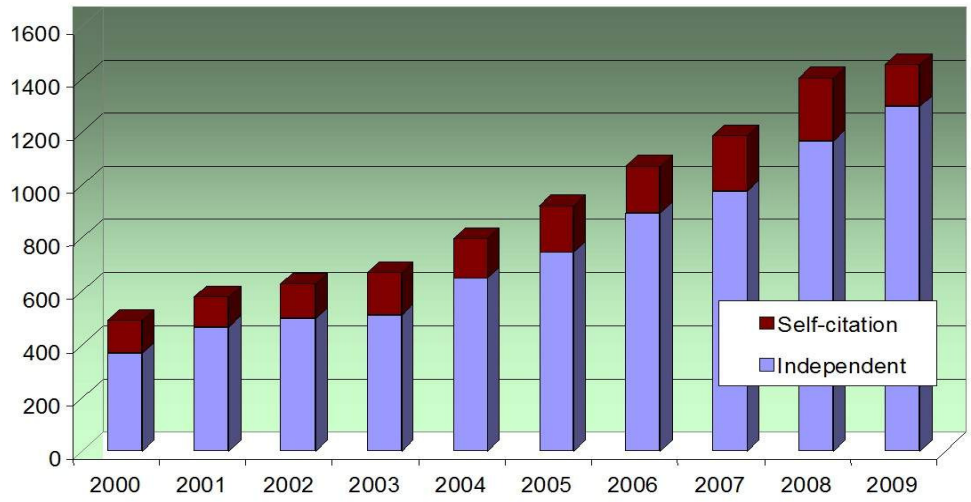

Prizes and Honours

Istvánné SOMOGYI: *Golden Cross of Merit of the Hungarian Republic - for the outstanding control of the institute's administration and successful business utilisation of research results as financial director of MFA*

László HONTY: *Distinction by the Secretary-General of the Hungarian Academy of Sciences for his decadelong excellent professional work and social engagement as scientific secretary of MFA*

József GYULAI: *Prize of the Roland Eötvös Physical Society*

György GERGELY: *Diamond Diploma, Budapest Univ. of Technology and Economics, Charles Simonyi prize*

László BARTHA: *Doctor Honoris Causa (Univ. of Miskolc)*

Csaba BALÁZSI: *Bolyai Plaquette, János Bolyai Postdoctoral Grant, Board of Trustees*

Antal GASPARICS: *Genius Gold Prize for inventors*

Péter KOZMA and Péter NEMES-INCZE: *Outstandig Young Scientist Award, European Materials Research Society, Spring Meeting 2009*

Fanni MISJÁK: *(1) Pócza Jenő Electron Microscopy Prize, Microscopy Society of Hungary, (2) Best Poster Award, Microscopy Conference 2009*

Anita PONGRÁCZ: *Ferenczi György Memorial Prize*

Gergely DOBRIK: *(1) Ferenczi György Memorial Prize, (2) II Prize, Hungarian Student Scientific Competition – Physics, Budapest Univ. of Technology and Economics*

Gábor PISZTER: *(1) Special Prize, Hungarian Student Scientific Competition – Physics, (2) II Prize, Hungarian Student Scientific Competition – Physics, Budapest Univ. of Technology and Economics*

Gábor MAGDA: *I Prize, Student Scientific Competition – Physics, Budapest Univ. of Technology and Economics*

Dorina KOCSIS: *I Prize, Student Scientific Competition – Physics, Roland Eötvös Univ.*

Andrea NÉMETH: *I Prize, Student Scientific Competition – Physics, Roland Eötvös Univ.*

Béla SZENTPÁLI and Gábor VÉRTESY: *MFA Prize*

Péter NEMES-INCZE: *MFA junior prize*

Antal SÜVEGES: *MFA special prize for excellent research support*

Scientific Promotions

Zsolt József HORVÁTH: *Doctor of Science (D.Sc.) degree of the Hungarian Academy of Sciences*

Péter BASA *and* **Ágoston NÉMETH:** *Successful Ph.D. defences in 2009*

Conferences and Symposia Organised with MFA Contribution

- National Technology Platform for Integrated Micro/Nanosystems (IMNTP) Conference, *(March 27, 2009, Budapest, Hungary, Organiser: Krisztina SZAKOLCZAI)*
- 11th European Workshop on Modern Developments and Applications in Microbeam Analysis (EMAS), *(May 10-14, 2009, Gdynia, Poland, Organising Committee Member: János LÁBÁR)*
- Conference of the Hungarian Microscopy Society, *(May 21-23, 2009, Siófok, Hungary, Organising Committee Member: Béla PÉCZ)*
- E-MRS 2009, Syposium M: Bioinspired and Biointegrated Materials as New Frontiers Nanomaterials, *(June 8-12, 2009, Strasbourg, France, Chair: László Péter BIRÓ)*
- 11th International Conference and Exhibition of the European Ceramics Society, Engineering Ceramics section, *(June 21-25, 2009, Cracow, Poland, Organising Committee Member: Csaba BALÁZSI)*
- Summer School at MFA "Let's learn from each other!", *(June 22-26, 2009, Csillebérc, Budapest, Hungary, Organiser: Csaba Sándor DARÓCZI)*
- Bioinspired Photonic Nanoarchitectures, Workshop on "Bio-Inspired Photonic Structures", (*July 9-15, 2009, Donostia-San Sebastian, Spain, Chair: László Péter BIRÓ)*
- Microscopy Conference 2009, MC2009, (*Aug 30-Sept 4, Graz, Austria, Co-organising Committee Members: János Lábár, Béla Pécz, György RADNÓCZI)*
- EMRS2009 Fall Meeting "Novel Bio & Chemosensing Materials for Health, Safety and Security Applications", *(September 14-18, 2009, Warsaw, Poland, Organising Committee Member: Csaba BALÁZSI)*
- XXI Conference on Applied Crystallography (XXI CAC), *(September 20-24, 2009, Zakopane, Poland)*
- Summer School on Diffraction-Based Structure Analysis in TEM, *(September 25-27, 2009, Zakopane, Poland, Director: János LÁBÁR)*
- 1st Joint Advanced Electron Microscopy School & Workshop on Nanomaterials (AEM-NANOMAT), *(Sept 28-Oct 2, 2009, Saltillo, Mexico)*
- Thermal Investigations of ICs and Systems (THERMINIC) 2009 Conference, *(October 7-9, Leuven, Belgium, Program Committee Member: István BÁRSONY)*
- 7th Hungarian Conference and Exhibition on Materials Science Testing and Informatics, *(October 11-13, 2009, Balatonkenese, Hungary, Co-organiser: Csaba BALÁZSI)*
- Open Day at MFA, *(November 13, 2009, Csillebérc, Budapest, Hungary, Organiser: Csaba Sándor DARÓCZI)*
- ENIAC SE2A Project Meeting, (*November 25-27, 2009, Budapest, Hungary, Organiser: Gábor BATTISTIG*)

HIGHLIGHTS

Structure and morphology of two component films

(OTKA 048699)

F. Misják, Gy. Radnóczi, and P. Barna

Technological applications often aim at multifunctional utilisation of thin films and coatings. For the achievement of this, especially in nanolayers for contact or interconnect application in IC or memory structures as well as corrosion protection or tribological applications, generally two- or multicomponent films are used. The appropriate structure and morphology of them has to be created in one technological step and formed by self-organisation mechanisms because the 10-50 nm size dimension of trenches e.g. does not allow subsequent deposition of materials and multilayer structures.

In the two component films, the mapping of the phase separation processes can be an important key to the understanding of self-organised nanostructures and morphologies. Using model systems, a comprehensive view has been worked out to describe the main atomic mechanism of phase separation resulting in diverse morphological features in different thin film systems. The phase separation mechanisms have been investigated in Cu-Ag as well as carbon metal co-deposited films as the function of composition and other parameters.

There are two known mechanisms for the phase separation in multiphase thin film systems formed by simultaneous condensation of their components, non-mixing at equilibrium conditions: the kinetic segregation process and spinodal decomposition. In the kinetic segregation process the separation of components and the formation of phases take place by atomic movements on the surface of the growing film. No atomic rearrangements and consequently no measurable changes take place in the bulk of the film. The formation of phases can be described by the classical nucleation theories. When the surface processes are hindered (e.g. at too high deposition rates the surface is buried before the separation processes could start) unstable or metastable structures can form. Then the thermodynamically more stable configurations can form only by atomic rearrangements in the bulk of the film by bulk diffusion. Bulk diffusion, however, is limited at the technologically applicable temperatures of film growth. Nevertheless, when the phase formation process has no thermodynamic barrier (no critical nucleation size is needed to decrease the energy of the system) short range rearrangements will be possible also in the bulk of the film.

As a result, the phase separation process starts by formation of compositional fluctuations on the nm scale, i.e. by spinodal decomposition. The comparison of the two mechanisms is summarised in Table 1.

The phase separation processes are not easy to observe in-situ during film growth, as we are talking about movements on atomic scale. In most cases we can make conclusions for the operating kinetics only from detailed structural analysis of the as grown structures. Using this approach, in the Cu-O system we could spectacularly demonstrate that kinetic segregation works with surface processes. In Fig. 1 we can clearly see the pinning and bunching of growth steps and the formation of macrosteps on the growth surface of a large Cu grain. Appearance of second phase Cu-oxide nuclei is due to segregation and accumulation of oxygen atoms/molecules on the growth surface of Cu. These particles of the new phase, contrary to adsorbed species, are not mobile on the surface and serve as pinning points for the growth steps. This can lead to various effects changing the growth morphology of the film. In general, accumulation (segregation) of the minority component on the growth surface of the majority phase can get to compositional conditions facilitating and consequently leading to the nucleation of a second phase.

mechanism	*The process*		*formation of the new phase*
	place	*kinetics*	
Kinetic segregation	*surface*	*surface diffusion, (step movement)*	*nucleation*
spinodal decomposition	*bulk*	*short range bulk diffusion*	*spinodal decomposition (+ nucleation)*

Table 1 *The main features of the two phase-separation kinetics, operating in thin film growth processes*

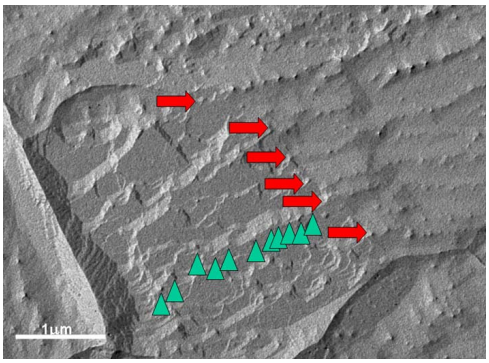

Figure 1 *The image of a C-Pt replica taken from the surface of a Cu film grown at 500 °C temperature and 1000 nm/s deposition rate. The arrows point to the oxide particles pinning the growth steps. The green arrows show the pinning of a macrosteps while the red arrows mark a small angle grain boundary, where the surface morphology changes remarkably.*

The structure and morphology of the forming two phase film depends on growth mode (two or three dimensional) of the growing phases, differences in melting points, compound formation capability and so on. So, the kinetic segregation processes may lead to different and unexpected morphologies. For example in the Al-Sn system, contaminated by oxygen the lamellar growth of the Al crystallites occurs (Fig. 2a). In the Cu-C (Fig. 2b) and Al-C systems (Fig. 3.) the covalent amorphous or nanocrystalline phases (a-C, Al_4C_3) growing in 2D mode lead to the segregation of the metallic component resulting in the self-organised formation of layered structures. At the same time in the Cu-Ag system (Fig. 4.) at ~5-20 at% Ag or Cu concentration

a bimodal grain size nanocomposite forms. In Cu-Ag films besides of the kinetic segregation process we could first identify another phase separation process. This process takes place in the bulk of the film and was identified as spinodal decomposition (i.e. a nano-scale phase separation process of the metastable solid solution formed by co-deposition of components).

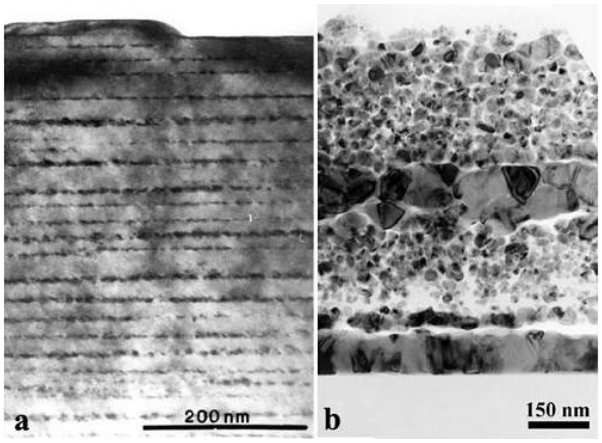

Figure 2 *Lamellar structure in the Al-Sn system (a), and layered structure in the Cu-C system (b) both formed by self organisation*

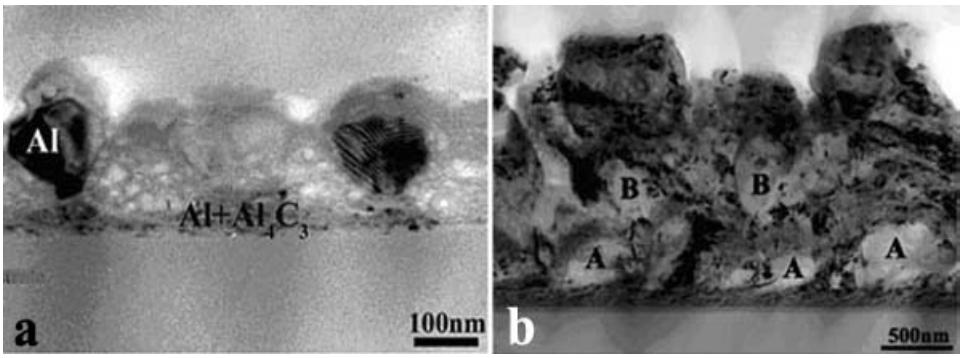

Figure 3 *Cross section images of 200 nm thick (a) and 1.5 μm thick (b) co-deposited Al-C films showing composite structure consisting of large Al crystals embedded in Al-Al4C3 nanocomposite. In the thick layer (b) a layered morphology develops. Large Al grains in the first layer are marked by A, in the second layer by B.*

By carefully analysing morphological, structural and texture properties of Cu-Ag films we were likely to show first the simultaneous existence of different phase separation mechanisms – alone or in common action, depending on the film composition- in the same system, namely in the co-deposited Cu-Ag thin films. We have shown that competition between these phase separation processes can lead to quite different structure and consequently different properties (e.g. nanohardness) in films grown at the same temperature but different composition. For the presentation of the interdependence of all these properties and atomic mechanisms we have

suggested an extended, multidimensional structure zone diagram for the composite Cu-Ag films (Fig. 5).

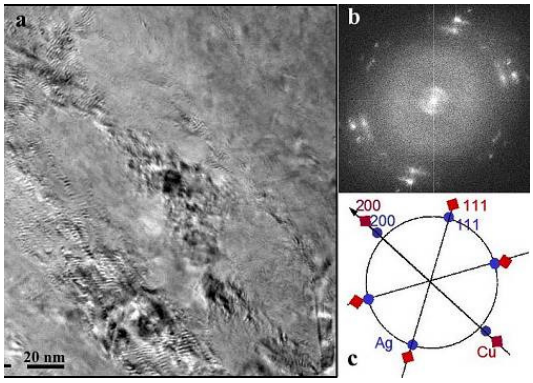

Figure 4 *High resolution image of a Cu-Ag layer containing 10 at% of Ag (a), the Fourier transform of the image (b) and its schematic pattern showing the indexes of the reflexions (c). The large grains in (a) are Cu grains, while in the intergrain area, showing Moire patterns, a two phase nanostructure formed by spinodal decomposition.*

In general, for being capable to describe structural and morphological development in two component films as well as to understand structure-property relations similar multidimensional structure zone diagrams must be built for material systems intended for functional applications. We consider this kind of information to be a necessary tool in application-oriented research of multicomponent films and coatings.

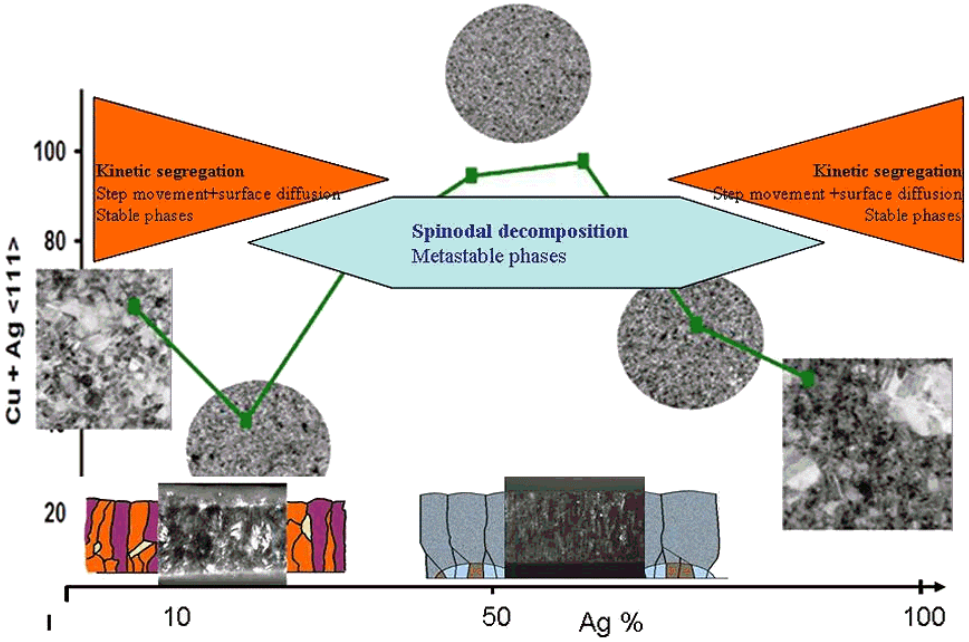

Figure 5 *The sections of the multidimensional structure zone diagram of the Cu-Ag system, placed above each other: morphology in cross section and in lateral view, texture fraction (green line) and the acting phase separation mechanisms are shown as the function of film composition.*

Novel multichannel silicon electrode for high quality laminar neural recordings

(A co-operation between the Microtechnology Laboratory of MFA and the Institute for Psychology of the Hungarian Academy of Sciences)

A. Pongrácz, É. Vázsonyi, G. Battistig, L. Grand (Institute for Psychology), and G. Márton (BME-VIK)

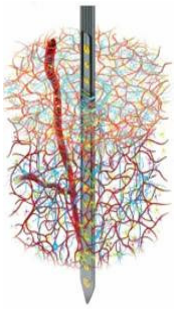

Studying physiological processes at the cellular level is essential in order to elucidate complex brain mechanisms. Simultaneous observation of activities of large number of cells might be the key factor for better understanding of neuronal systems. Modus operandi of different neuronal networks, communication between various neuronal population and functional connectivity between different brain areas can be uncovered by using *simultaneous multisite recording* techniques.

The efficiency of the silicon substrate as a brain electrode carrier was confirmed due to the biocompatibility of the material and its thin films like silicon dioxide and silicon nitride with the brain tissue. Although silicon based probes have appropriately small dimensions, a number of electrical contacts can be placed at different locations along the probe. Moreover, they offer the potential of integrating signal processing circuitry on the probe itself.

A novel, minimally invasive yet mechanically robust silicon-based multichannel brain electrode was developed. For the construction of multisite neural interface an advanced MEMS process flow consisting of 38 steps is used. In Fig. 1 the schematic plan of the probe can be viewed with a single shaft projecting from the base.

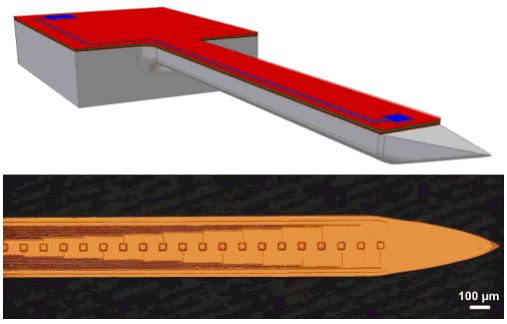

Figure 1 *The simplified 3D view of the probe with the Pt contact placed close to the tip of the shaft, and the corresponding Pt lead and the bonding pad is (top). The manufactured electrode holds 24 separate Pt contacts (bottom).*

Figure 2 *Scanning Electron Micrograph of the completed silicon probe reveals the tip shaped like the bow of a boat and three out of 24 of the Pt recording sites*

For probe manufacturing standard [100] oriented, p-type 3 inch silicon wafer of the thickness of 200 µm, was used - polished on both sides. The fabrication consisted of four phases: the deposition of thin-films to form the insulating layers on the bottom, the electrodes, the passivation layer, followed by the formation of the contact holes and bonding pads. In the subsequent two phases different types of wet chemical Si etching steps were applied to obtain the characteristic shape of the probe: the sharp tip with rounded profile (Fig. 2). The special isotropic etching method results in the required minimally invasive probe shaft of the shape of the hull of a boat, having rounded edges and a sharp tip.

The specially developed etching method allows the formation of neural interfaces with varying thickness and length dimensions. The current probe (see in Fig. 3) was designed with definite geometry, the length of the probe was in excess of 12 mm, the height and width were 80 µm and 280 µm, respectively. The distance from the tip to the centre of the first contact window was designed to be 660 µm, as the tip length itself is 620 µm long. The sharp angle of the probe tip was 26 degrees. The probe body to be inserted into the brain tissue has a length of 7 mm. The present design supports 24 square shaped Pt sensing sites of 30×30 μm^2. The site spacing (pitch) is 100 µm.

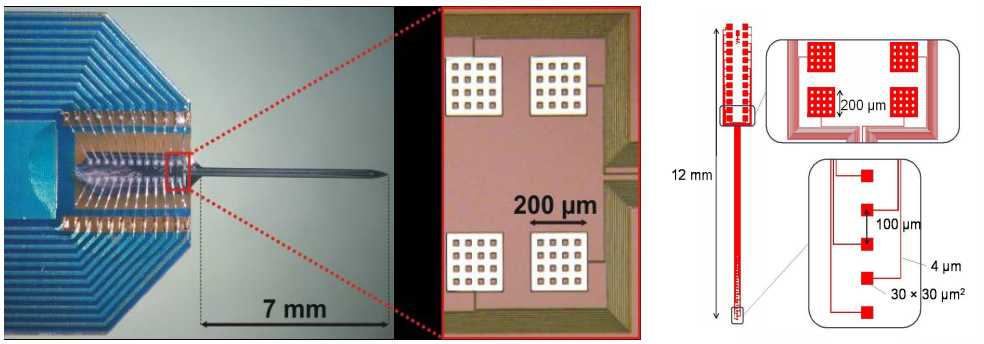

Figure 3 *The assembled probe with its support and contact wiring, along with the dimensions of the probe, bonding pads and Pt sensing sites.*

The functional test of the minimally invasive probe provided high resolution and good quality recording. The body of the rounded probe can easily be cleaned and reused owing to its excellent mechanical properties. During insertion it could simply penetrate through dura and pia mater without bending or causing serious bleeding. The tested electrodes exhibit excellent in vivo performance in Local Field Potential (LFP), Multi-unit (MUA) and Single-unit (SUA) activity recordings.

The newly developed design and manufacturing technique facilitates the scaling of length, width and thickness of the probe according to the mechanical and geometrical performance demanded by the specified biological task. In view of the characteristics

and degrees of freedom obtained in dimension scaling and shaping of the silicon probes by the described technique, the development of deep brain recording/stimulation arrays as well as multiple shank probes looks encouraging as well.

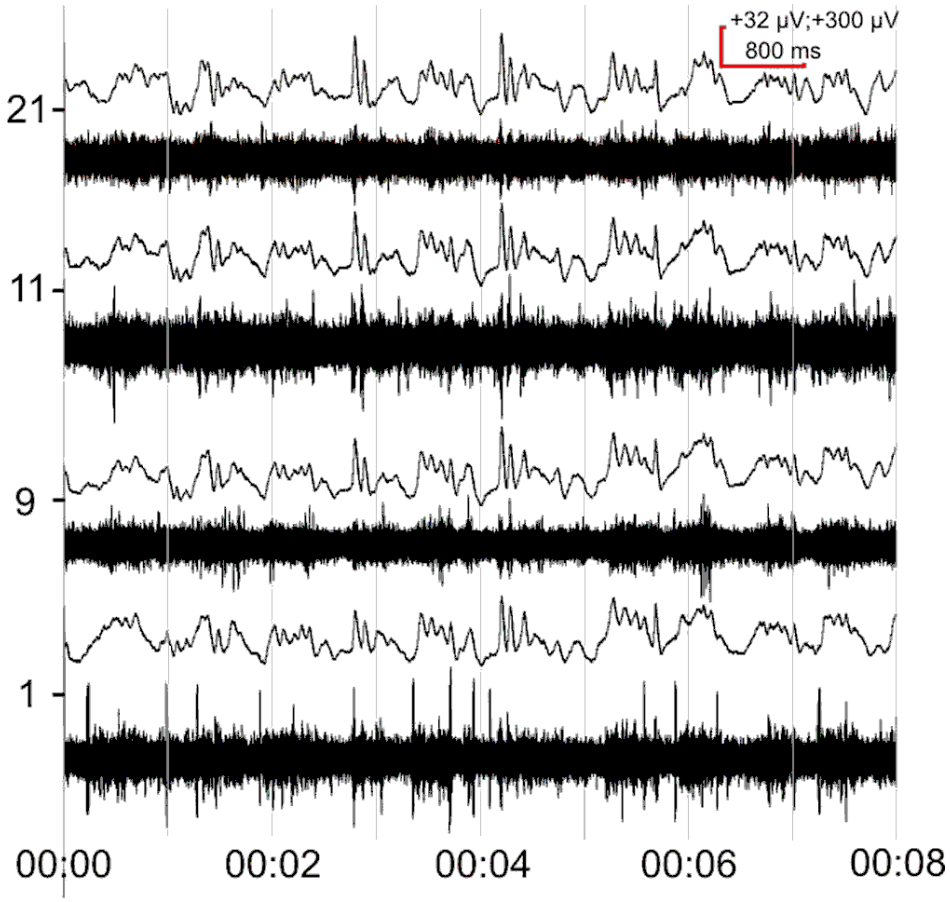

Figure ***4*** *High quality LFP and MUA activity recordings obtained. A remarkable single-unit activity is observed in the signal that was acquired at the site located closest to tip. The vertical scale bar represents two values, one belonging to MUA (+32µV) and the other to LFP (+300µV,) respectively. Gain: EEG (1k), MUA (50k).*

NOTABLE EVENTS

MFA Members Honoured in 2009

Istvánné Somogyi, the financial director of the Institute MFA was decorated by the Golden Cross of Merit of the Hungarian Republic handed out by Prof. József Pálinkás, the President of the Hungarian Academy of Sciences, *for the outstanding control of the institute's administration and successful business utilisation of research results as financial director of MFA.*

László Honty, the Scientific Secretary of the Institute MFA was honoured with the Distinction by the Secretary-General of the Hungarian Academy of Sciences, *for his decadelong excellent professional work and social engagement as scientific secretary of MFA.*

Conference on Micro/Nanosystems

The National Technology Platform for Integrated Micro/Nanosystems (IMNTP) co-ordinated by the Research Institute for Technical Physics and Materials Science (MFA) was established in 2008. The aim of this organisation is to support the competitiveness of the Hungarian micro- and nanoelectronics and photovoltaics technology sector. The main goal is to elaborate a Hungarian R&D roadmap for the respective fields and to come up with a feasible strategic research plan, based upon the Strategic Research Agendas (SRA) of the European Technology Platform for Nanoelectronics (ENIAC) and the European Photovoltaic Technology Platform (PV), respectively.
The SRA combines the knowledge and experience of enterprises, higher educational and research institutes as well as other stakeholders, while covering R&D actions and technology domains from frontier/theoretical research towards application and manufacturing. The IMNTP platform also supports the incubation of unique developments utilising nano-functionality in high added value electronic products, the exploitation of special Hungarian knowledge and opportunities in solar technology and integrated sensors/actuators.

On March 27, 2009 IMNTP organised a conference with the motto: 'The technology of the future today'. The aim of the conference was to introduce the SRA dealing with potential breakthrough possibilities, and disseminate best practices of this community. The event also offered an opportunity for participating companies and research groups to exhibit and demonstrate their latest research and development results.

Manufacturers and developers of tactile and gas sensors, measurement systems and also photovoltaic demonstration systems visited the exhibition

Dr. Ilona Vass (Vice president of the National Office for Research and Development NKTH) opened the event emphasising the importance of R&D connections within Hungary and in Europe to increase the competitiveness of SMEs and R&D institutes.
The two invited speakers introduced the European platform activities: Prof. Dr. Kouchi Zhang, member of the Scientific Committee of ENIAC has held a lecture on Europe's nanotechnology vision. Prof. Dr. Wim Sinke, Head of the Working Group on Science, Technology & Applications of the PV Technology Platform was talking about the new and emerging technologies in the photovoltaic industry. Selected talks from Hungarian research and higher education institutions as well as industrial companies demonstrated their capabilities, results and plans. More than 100 guests from microelectronic and photovoltaic field visited the conference and the product and technology exhibition which was a great success of the IMNTP and of the MFA.

The invited speakers Prof. Dr. Wim Sinke and Prof. Dr. Kouchi Zhang and the participants of the IMNTP Conference in Hotel Gellert

High School Relations

While the number of university students are solidly increasing world wide, it is an unfavourable phenomenon, that the share of the natural science is constantly decreasing. Nowadays even the absolute number of students in science and engineering is becoming critically small – and Hungary is not an exception, either. Obviously, the universities alone can not rectify this problem, because the effective practice of natural sciences requires many years of deep study *years before* the university. So, a couple of years ago here at MFA we decided to open up opportunities especially created for *high school students* to let them near to the "big science" before they determine their future profession.

MFA summer camp for high school students:
Between June 22-26, 2009 we have organised this program already second time (trying to make it a tradition), under the motto '*Let's learn from each other!*' (co-ordinated by Csaba Sándor Daróczi). At our home page (http://alag3.mfa.kfki.hu/mfa/nyariiskola/), there were more than 20 scientific themes offered for the students to select from in advance, to work on under the supervision and guidance of our colleagues (called '*mentors*'). From the several dozen applicants from Hungarian language High Schools of the whole

Figure 1 *Student participants and the organiser at the MFA Summer Camp 2009*

Carpatian-basin 20 students (15 youngsters from Hungary and another 5 from Transylvania, Fig. 1) were selected. During the training period, the institute fully financed their participation (travelling, subsistence, evening social programs, etc.) from own means. The students turned out to be very enthusiastic at practicing real scientific work (Fig. 2) for a whole week! Everybody found this week very exciting and fruitful!
Trainees of the last years (2008) summer-event already joined us this year as university students just for this reason! Also the 2009 year's summer practice bore fruits already: on September 24, 2009 at the countrywide event of "Night of the researchers" two of 'our' summer-camp students, Ervin Habel from Nyíregyháza, and Milan Janosov from Veszprém emerged as winners of the scientific movie-contest. Several months later Ervin won another **1st** prize of the Nanotechnology Competition:

http://www.nanopaprika.eu/group/nanopalyazat/, while Milan won the **1st** prize of the ELTE's Mathematical modelling competition (not to name many others): http://www.cs.elte.hu/math/news/jelentes.pdf

Figure 2 *Brain-storming about the result of an interesting experiment in the nanotechnology laboratory (left)…*

…and the next generation of microtechnology professionals (right)

Patronage of the Budapest High School 'János Arany':
Upon request of the president of HAS, the colleagues of MFA participated in the technical design and supervision of the modernisation of the classrooms for natural sciences (physics, biology and chemistry) of the High School 'János Arany', Budapest (Figs 3-4). MFA, being a multidisciplinary research institute itself

Figure 3 *High School 'János Arany'*

Figure 4 *Planning the reconstruction.*

is involved in physics, chemistry, biology, engineering, computer science and mathematics, too. Therefore, we constantly experience the importance of experiments and demonstration in science education. This project of establishing new cabinets for science education was a good opportunity to support a school, that might be an example to follow for many others. Started in May, the work had to be executed pretty fast before taking the new classrooms in use in September 2009 (Figs. 5-7).

Figure 5 *Waiting for the 'bang' in the new chemistry classroom…*

Figure 6 *Some of the observers kept the safe distance…*

Figure 7 *While in the physics classroom some real 'big bang' was expected…*

Open Day of MFA:
Our institute is operating in a guarded area at the KFKI campus, which is generally *not* accessible freely for everyone. However, for a better social acceptance of our work we regularly organise the 'Open Day of MFA'. On this occasion the institute can be visited by any interested person from the country. The MFA Open Day on November 13, 2009 was hosting some hundred interested, mostly young attendees (mainly secondary school students, occasionally several complete classes) at the popular lectures and laboratory visits (Fig. 8). This time the institute is also open to journalists, TV and radio reporters, which helps us a lot to make more people to think of science.

Figure 8 *During the open day we have visitors for almost every corner of our laboratories.*

SCIENTIFIC REPORTS

Nanostructures Department

Head: Prof. László Péter BIRÓ, D.Sc., scientific advisor

Research Staff

- Zsolt Endre HORVÁTH, Ph.D., Deputy Head of Department
- Prof. József GYULAI, Member of the HAS (Professor Emeritus)
- Antal Adolf KOÓS, Ph.D. (on leave)
- Géza István MÁRK, Ph.D.
- Zoltán OSVÁTH, Ph.D. (on leave)
- Levente TAPASZTÓ, Ph.D. (on leave)
- Zofia VÉRTESY, Ph.D.

Technical Staff

- Zoltánné SÁRKÁNY, technician

Ph.D. students / Diploma workers

- Enikő HORVÁTH, Ph.D. student
- Gergely DOBRIK, Ph.D. student
- Krisztián KERTÉSZ, Ph.D. student
- Péter NEMES-INCZE, Ph.D. student
- Péter Lajos NEUMANN, Ph.D. student
- István TAMÁSKA, Ph.D. student
- Dorina KOCSIS, diploma worker
- Gábor PISZTER, diploma worker
- Gábor MAGDA, diploma worker
- Kitti RATTER, diploma worker
- Péter VANCSÓ, diploma worker

The Nanostructures Department has an almost two decades expertise in the production and characterisation of various nanostructures. In recent years in the focus of work were various carbon nanostructures (carbon and haeckelite nanotubes, nanotube junctions, graphene and few layer graphite) their nanoarchitectures, bioinspired photonic nanoarchitectures and potential applications of these nanoobjects in various fields in nanotechnology, nanoelectronics, sensorics and environmental protection. The most relevant results in 2009 are detailed below:

We developed a new etching method based on a solid state reaction allowing crystallographic control of the orientation of graphene nanoarchitectures.

Graphene and few layer graphite samples were prepared by a CVD type reaction on Ni. We showed that the thickness of the grown layer has crystallographic orientation dependence.

SWCNT bundles were contacted by e-beam lithography, electrical transport and gas sensing experiments were carried out.

A new type of intercalated photonic crystal was discovered in beetle elytra and a bioinspired artificial structure exhibiting similar behaviour to the natural “blueprint” was successfully produced by thin film deposition and nanomachining.

A new method was developed to characterise the photonic nanoarchitectures occurring in the scales of various butterflies and showing various degrees of order from single crystalline to amorphous.

For more details, please feel free to visit the web page of the Nanostructures Department (link: http://www.mfa.kfki.hu/int/nano/index.html).

Biologic and bioinspired photonic nanoarchitectures

(OTKA-NKTH grant K-67793)

L. P. Biró, K. Kertész, Z. Vértesy, G. I. Márk, E. Horváth, I. Tamáska, G. Molnár, A. Kun (HNHM), Zs. Bálint (HNHM), J-F. Tsai (NCHU), and J-P. Vigneron (FUNDP)

While human thinking is often guided by widely accepted concepts, random natural evolution can outperform man-made devices and materials. Bioinspiration opens new directions in materials science, nanotechnology, photonics and several other fields of science and technology.

An unusual, intercalated photonic nanoarchitecture was discovered in the elytra of Taiwanese *Trigonophorus rothschildi varians* beetles. It consists of a multilayer structure intercalated with a random distribution of cylindrical holes normal to the plane of the multilayer. The nanoarchitectures were characterised structurally by scanning electron microscopy and optically by normal incidence, integrated, and goniometric reflectance measurements. They exhibit an unsaturated specular and saturated non-specular component of the reflected light. Bioinspired, artificial nanoarchitectures of similar structure and with similar properties were realised by drilling holes of submicron size in a multilayer structure, showing that such photonic nanoarchitectures of biologic origin may constitute valuable blueprints for artificial photonic materials.

One of the most remarkable features *T. rothschildi varians* beetles is that in the same habitat and in the same period, one may encounter various colours ranging from orange to violet or even black (Fig. 1). Field observation yields an 80% occurrence of the green variant, 10% for the orange variant and around 5% for the violet variant.

Figure 1 *A "crowd" of Trigonophorus rothschildi varians beetles (Taiwan) feeding in their natural habitat. One may remark the various different colorations, the most frequent color being green.*

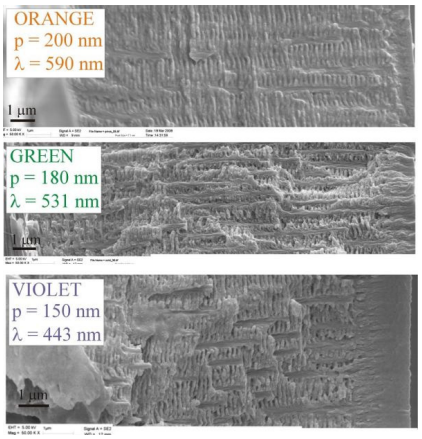

Figure 2 *SEM images of cross-sections through the elytra of orange, green and violet T. rothschildi varians beetles. One may remark the intercalated photonic nanoarchitectures in all three cases.*

We showed that the epicuticle has a multilayer type structure (1D photonic crystal), with different layer periodicities p (see Fig. 2) but the nanoarchitecture constituted of chitin and air is more complex than a simple multilayer, or Bragg mirror. A random arrangement of columns penetrating through 10–20 chitin/air layer pairs can be observed in all three colourations, Fig. 2. The wavelength of the reflectance maximum as computed with a simple multilayer model is given in the insets of Fig. 2. Surprisingly enough, the normal incidence reflectance spectra do not show these characteristic maxima, only the measurements carried out with an integrating sphere showed reflectance maxima in good agreement with the computed wavelengths, Fig. 3. The curious behaviour is attributed to the presence of the columns which together with the multilayer structure constitute an intercalated photonic nanoarchitecture.

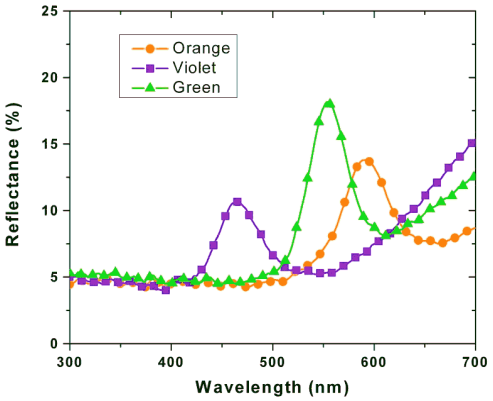

Figure 3 *Reflectance spectra acquired with an integrating sphere on the elytra of orange, green and violet beetles. The colours originate from non-specular reflection. The normal incidence of reflectance spectra do not show a saturated colour, but a plateau type reflectance trough the visible range.*

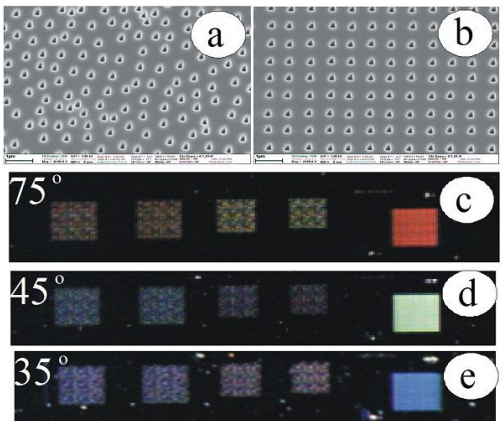

Figure 4 *Bioinspired artificial nano-architectures. (a) & (b) SEM images of the random and square FIB hole patterns. (c)–(d)-(e) Reflectance of various hole patterns under changing angles of illumination. Only the rightmost patterns have the square array of holes.*

Intercalated photonic nanoarchitectures are understood as complex nanostructures that can be decomposed into two or more distinct nanostructures, each with its characteristic dimensionality (1D, 2D or 3D). The individual nanostructures composing the intercalated nanoarchitecture occupy the same volume, interpenetrating each other [L. P. Biró et al., J. R. Soc. Interface published online before print November 18, 2009, doi:10.1098/rsif.2009.0438]. As shoved by experimental data and by computer simulation, the global optical response of the intercalated nanoarchitectures is determined by both of its constituting parts. The colour is primarily decided by the periodicity of the multilayer, while the angular visibility is determined by the presence of the holes nanomachined transversally through the multilayer. It is worth to point out: if the holes are arranged in a regular square pattern – the rightmost column in Fig. 4c to d – the hole array will act as a 2D diffraction grating.

New method for discriminating blue Polyommatine lycaenid butterflies by wing reflection spectra

(OTKA-NKTH grant K-67793)

K. Kertész, G. Piszter, Zs. Bálint (HNHM), Z. Vértesy, and L. P. Biró

The wing colour of a butterfly is produced by the complex chemical and physical properties of the wing scales. Our earlier studies demonstrated various roles of the butterfly wing coloration. Reflectance measurements can equally reveal information about the pigment-based chemical colours and the effect of nanoarchitectures occurring in wing scales, the so called "structural colour". For the accurate measurement of wing reflectance a detached and frame mounted wing is needed. This sample preparation allows different measurement setups (perpendicular, integrating sphere, transmittance, goniometer), but because of its destructive nature, it is not suitable for unique or rare specimens stored in collections or for large numbers of museum specimens. Frequently the angle dependent reflectance is pronounced, in these cases one can obtain averaged reflectance data only by using an integrating sphere [K. Kertész et al., Phys. Rev. E 74, 021922, (2006)]. Here we propose a new equipment to get reliable reflectance data without sacrifying the specimens. The instrument is inspired by the wooden spreading board used by the entomologists. A perpendicular illuminating/pick-up fiber optic is mounted normal to the wing surface to be measured. In this manner, moving horizontally the fiber holding arm, one can measure reproducibly several specimens placed on the board (Fig. 1.) without the need to detach the wings.

Figure 1 *(Color on-line) Photo of installed spectroboard. In the left side there is the Avantes white reference standard. The butterflies are from museum collections, mounted on pins.*

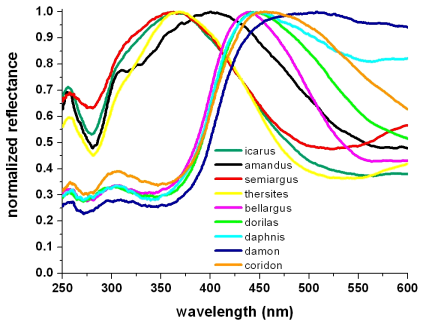

Figure 2 *(Color on-line) Normalized reflectance of the nine investigated Polyommatus species. Each curve represents the average reflectance of 10 exemplars.*

In this study we measured a selection of nine Polyommatine species, 10 or 20 specimens each. Averaged reflectance curves for these species are shown in Fig. 2. As the curves show features characteristic for the species, we tried to find an automated discrimination mode.

Species classification was done using an artificial neural network (ANN). An ANN is an adaptive system that changes its "structure" (the values of the coupling coefficients between "neurones") based on external or internal information that flows through the network during the learning phase. In order to prepare the input data for the ANN, each spectrum was processed: we extract a series of parameters (reflectance peak maximum position, FWHM, etc.) characteristic to the spectral shape. In the learning phase we entered these parameters for half of all specimens (5 or 10 samples). With the remaining 55 specimens we tested the network, 53 of them were classified correctly, this means 96% accuracy. This shows that the studied nine blue Polyommatine species have a characteristic hue. By measuring the visible reflectance of the wing, a properly trained neural network can identify an unknown specimen from a "library" of previously stored species characteristic spectra.

In a further step, we compared the interval of time when the butterflies fly in their habitat and their wing colour. The spectra were first transformed into CIE XYZ tristimulus values, then the derived x and y parameters were represented in CIE 1931 colour space chromaticity diagram (Fig. 3.). Each point in this diagram represents a specimen; the points assemble in domains marked with coloured elliptical shapes. The determination of flying time intervals was based on data stored in museum collection: we represented the exact time in days (month noted on y axis) when the specimens were collected for each species (Fig. 4.).

Considering the butterfly species of the year in the order of their appearance, P. icarus, P. amandus, P. dorylas and P. bellargus, their ellipses in the chromaticity diagram are disjunct. In other words the simultaneously flying butterflies possess different hues of blue. The same way we can prove that two coincident ellipses e.g. blue and green on Fig. 3. belong to two species that are not flying in the same time: P. icarus and P. thersites, see Fig. 4.

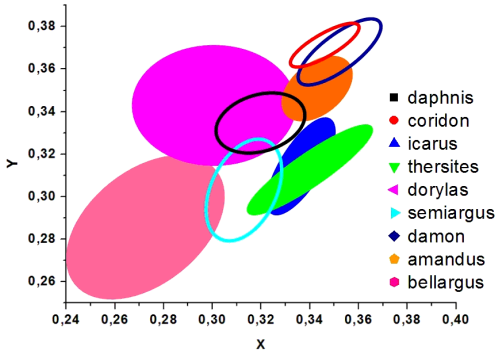

Figure 3 *(Color on-line) Part of chromaticity diagram. The specimens for each species are located inside the elliptical shapes. The filled ellipses are discussed in the text.*

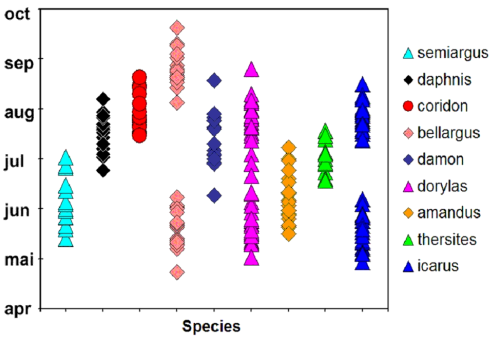

Figure 4 *(Color on-line) Flying intervals of nine species. The color coding is the same as in Fig. 3. Data from the collection of the Hungarian National History Museum.*

Order-disorder effects in structure and colour relation of photonic-crystal-type nanostructures in butterfly wing scales

(EU6 NEST/PATHFINDER/BioPhot-12915, OTKA-NKTH grant 067793, and HAS-Belgian FNRS)

G. I. Márk, K. Kertész, Z. Vértesy, Zs. Bálint (HNHM), and L. P. Biró

The optical reflectance of butterfly wings often shows peculiar features, i.e. their Bidirectional Reflectance Distribution Function (BRDF) is different from that of matt "painted" surfaces, with diffuse reflectance. These non-lambertian BRDF functions are generally not produced by pigments, but by a micro- or nanostructure whose optical properties change on the length scale of the wavelength of the light. Colours produced by this mechanism are called "structural colours". Butterfly scales are nanocomposites built of mostly two basic components, air and chitin. The inside of the scale is often filled by nanostructured chitinous material, which causes the structural colours [L. P. Biró et al., Phys. Rev. E 67, 021907 (2003)]. If this spatial variation is periodic, the structure may be called a photonic crystal. 3D photonic crystals are found in the scales of many butterflies [K. Kertész et al., Phys. Rev. E 74, 021922 (2006)].

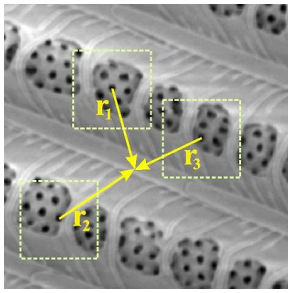

Figure 1a *The real space averaging algorithm. The selected holes are translated to a common origin and their neighborhoods averaged.*

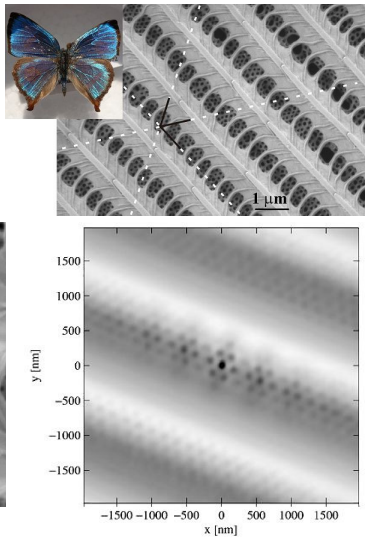

Figure 1b *(Upper): SEM image of a dorsal wing scale of Cyanophrys remus butterfly. (Lower): Result of the real space averaging algorithm applied to the SEM image in the upper panel.*

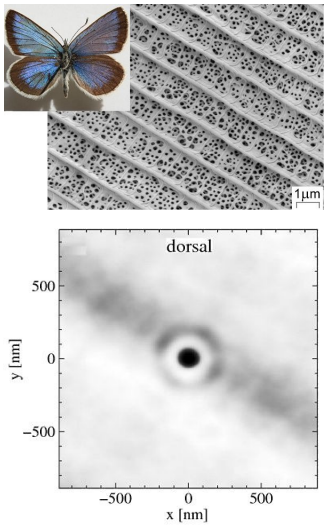

Figure 1c *(Upper): SEM image of a dorsal wing scale of Albulina metallica butterfly. (Lower): Result of the real space averaging algorithm applied to the SEM image in the upper panel.*

In order to study the local order in SEM images of butterfly scales, we developed a direct space algorithm [G. I. Márk et al., Phys. Rev. E 80, 051903 (2009)], based on averaging the local environments of the scattering sites. The algorithm is illustrated on Fig. 1. We demonstrated this algorithm for three characteristic examples, having long-range order (dorsal scales of the *Cyanophrys remus* butterfly), medium-range order (ventral scales of the *Cyanophrys remus* butterfly), and short-range order (*Albulina metallica* butterfly), see Fig. 1.
In order to reveal the in-depth structure of the scales, TEM investigations were taken. Optical spectrum of a butterfly scale is closely related to its reciprocal space structure. The scales are thin structures with moderate refractive index contrast, hence, the first Born approximation is applicable. Results calculated within this framework agree well with measured reflectance spectra (Fig. 2.) because of the small width and moderate refractive index contrast of butterfly scales [G. I. Márk et al., Phys. Rev. E 80, 051903 (2009)].

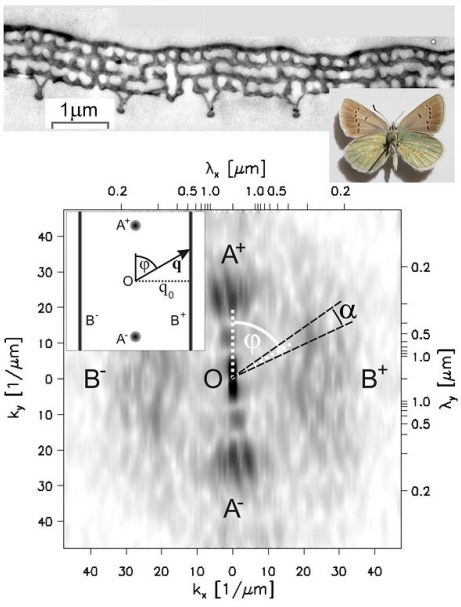

Figure 2a *(Upper): TEM image of a ventral scale of Albulina metallica. (Lower): FFT power spectrum of the TEM image. The inset shows the FFT image and the procedure of the spectrum calculation for a model image.*

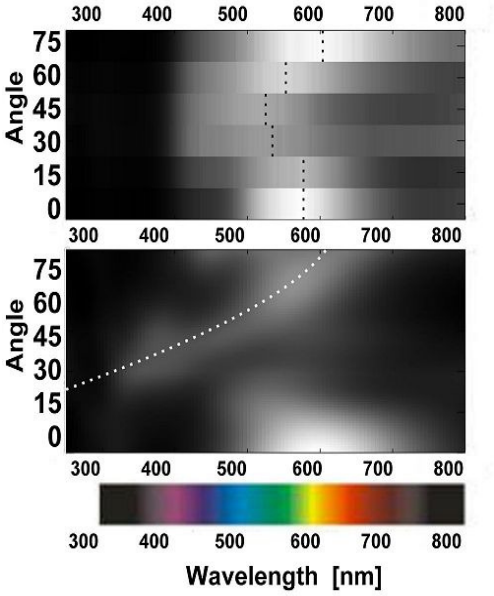

Figure 2b *(Upper): Measured goniometric backscattered spectra for Albulina metallica. (Lower): Goniometric spectra calculated from the FFT image of Fig.2a, the light shades indicate high light intensity, dark shades indicate low light intensity.*

The experimental spectra (Fig. 2b, upper) and the spectra computed (Fig. 2b. lower) according to the model in Fig. 2a, show a good agreement.

Zigzag graphene nanoribbons made easy

(OTKA-NKTH grants 67793, 67851 and 67842)

P. Nemes–Incze, G. Magda, K. Kamarás (RISSPO), and L. P. Biró

Graphene has many advantageous properties, but its lack of an electronic band gap makes this two dimensional material impractical for many nanoelectronic applications, for example field effect transistors. This problem can be circumvented by opening up a confinement induced band gap, through the patterning of graphene into ribbons having widths of a few nanometers. The electronic properties of such ribbons depend on their size and the crystallographic orientation of the ribbon edges [L. Tapasztó et al., Nature Nanotechnology 3, (2008) 397].

Therefore, etching processes that are able to differentiate between the zigzag and armchair type edge terminations of graphene are highly sought after. Our group has shown for the first time that such an anisotropic, dry etching reaction is possible and we used this reaction to obtain graphene ribbons with zigzag edges [P. Nemes-Incze et al., Physica Status Solidi C, in press and P. Nemes-Incze et al., Nano Research, in press].

Using the carbothermal reaction of the graphene layer with the SiO_2 substrate itself we can produce hexagonal etch pits into graphene layers, with the pit edges having zigzag edge terminations. During carbothermal etching the carbon of the graphene layer edges reduces the SiO_2 substrate material into SiO itself being oxidised at 700 ^{o}C in an argon atmosphere (see Fig. 1).

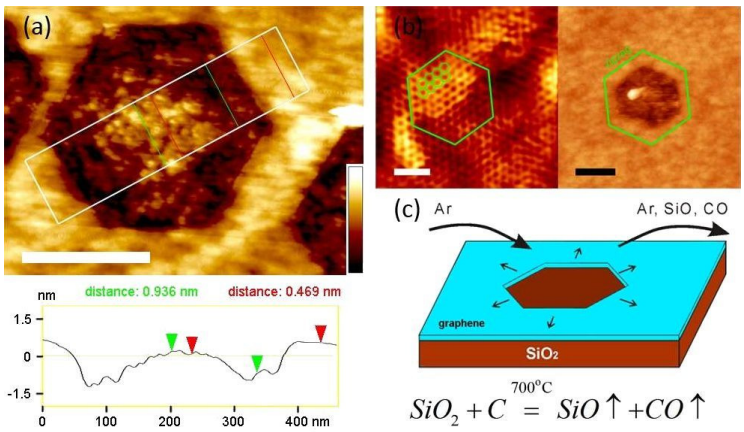

Figure 1 *(a) AFM image of a hexagonal etch pit and height profile. In the height profile we can clearly identify that the SiO_2 substrate has been etched away along with the graphene at the oxidation hole edges. (colour bar 3 nm, scale bar 200 nm). (b) STM image (scale bar 1 nm) and AFM image (scale bar 150 nm), showing the atomic lattice of the graphene sample and the orientation of the etch pit. The as obtained pit edges have zigzag terminations. (c) model structure and carbothermal reaction.*

We have also demonstrated that the starting positions for the carbon removal reaction can be tailored at will with precision. We have shown that this can be achieved by introducing defects on purpose into the graphene layer in a controlled fashion. This can be easily achieved by piercing the surface of the graphene layers using an AFM tip (see Fig. 2a and 2b). This makes our etching technique a straightforward and powerful tool to tailor graphene layers in a crystallographically oriented manner by using the hexagonal holes as building blocks for more complex graphene structures, such as graphene nanoribbons (Fig. 2c and 2d). The process described here shows great promise in the fabrication of graphene devices having zigzag edges, helping to unlock the experimental aspect of a field of graphene research which up to now has only been the subject of theoretical study.

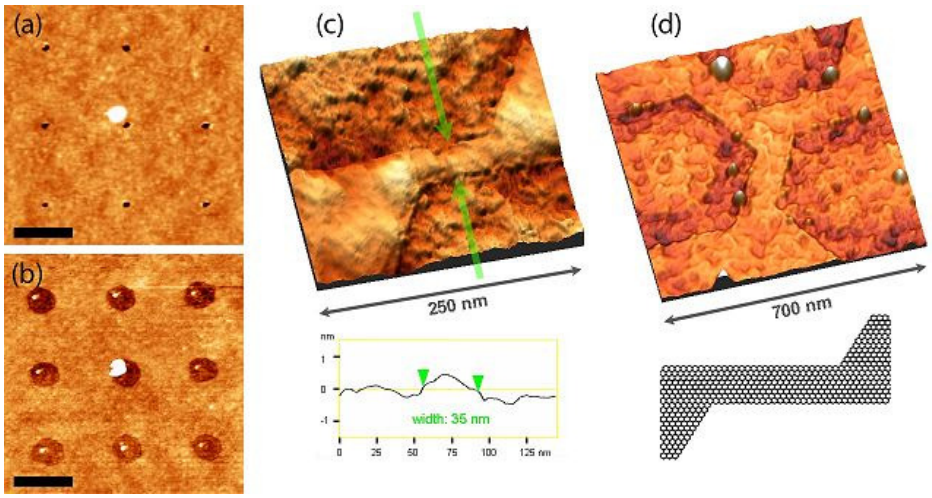

Figure 2 *(a) The result of AFM indentation: a 3×3 matrix of holes in graphene. (b) AFM micrograph of the hexagonal holes grown from the defects induced by indentation. Scale bars: 500 nm. (c) The image shows a 3D AFM image of a graphene nanoribbon of about 35 nm. The AFM height profile has been acquired at the place shown by green arrows. The inset in the right lower corner shows a scheme of the corresponding atomic structure. (d) The image shows a junction of 3 nanoribbons, with the ribbons having widths of: 93, 100, 101 nm (starting from the upper left ribbon, going clockwise).*

The great advantage of the new carbothermal etching method resides in the fact that the edges of the graphene nanoarchitectures are not formed in energetic processes generating strong disorder like e-beam lithography, or to a lesser extent STM lithography, too, but in a slow chemical reaction close to the equilibrium. Therefore these edges are expected to produce significantly less scattering, which may constitute a crucial issue if practical, device applications are envisaged. Furthermore, the etching process can be easily controlled by the reaction time, thus significantly reduces the time during which a skilled operator and scanning probe microscope have to be involved in the pattering process.

Few layer graphite grown on Ni by chemical vapour deposition

(OTKA-NKTH grants 67793, 67851)

P. Nemes–Incze, A. Darabont (BBU), L. Tóth, Z. E. Horváth, K. Kamarás (RISSPO), and L. P. Biró

In order to integrate graphene into practical devices, methods are needed to reliably produce this two dimensional carbon crystal. The great success of the CVD method to produce carbon nanotubes and tailor their properties, sets this method into the

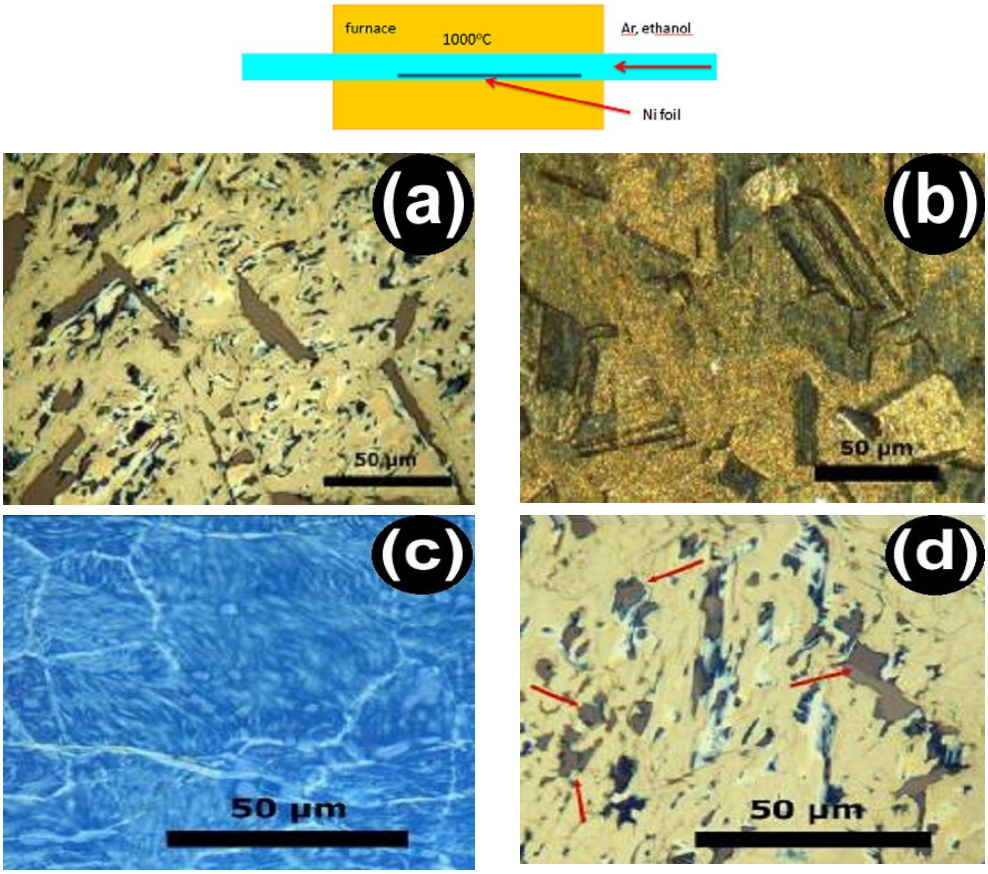

Figure 1 *Graphite and FLG layers deposited onto SiO_2 substrates. (a, d) Optical micrograph of graphite layers grown on the nickel surface using gradual cooling and (b) the nickel surface after removing the graphite and FLG layers. One can observe that on certain grains (red arrows in (d)) little or no FLG is formed. (c) Optical micrograph of the FLG layer obtained by quenching the Ni film. As opposed to the samples obtained by gradual cooling (a, d), the thickness of the layers obtained by quenching (c) is homogeneous. The blueish colour of the layers is due to the fact that the FLG is formed of only a few graphene layers.*

limelight of graphene growth research. Indeed various groups have reported successes in the growth of graphene and few layer graphite layers on nickel and copper surfaces [*Nano Lett. 9 (2009) 30 - 35*].

Following our successes in growing carbon nanotubes by CVD, using ethanol as a carbon feedstock we have set out to explore the possibilities of graphene and few layer graphite (FLG) growth using this straightforward technique. The growth experiments were carried out in a quartz tube furnace setup (see Fig. 1) at 1000°C, using ethanol vapours. In Fig. 1 we present optical micrographs of graphite and FLG layers grown on polycrystalline Ni surface. These layers grow by the formation of a solid solution at high temperature, followed by carbon precipitation during the cooling of the sample. After growth we have transferred our FLG layers to a SiO_2 substrate for further examination.

We have obtained for the first time FLG on Ni, using ethanol vapours. We have demonstrated that by slowly cooling our Ni layers, the amount of carbon that precipitates is dependent on the grain orientations of the Ni (see Fig. 1a-b). Furthermore, we have confirmed that thinner FLG layers may be obtained by rapidly cooling the sample after carbon dissolution. This is due to the drastic difference in growth kinetics at high cooling rates, where diffusion is suppressed, effectively limiting the amount of carbon that is able to precipitate, forming fewer graphene layers. We have also shown that at high cooling rates the FLG thickness is more uniform (see Fig. 1c), which means that a suppression of crystallite orientation dependence occurs.

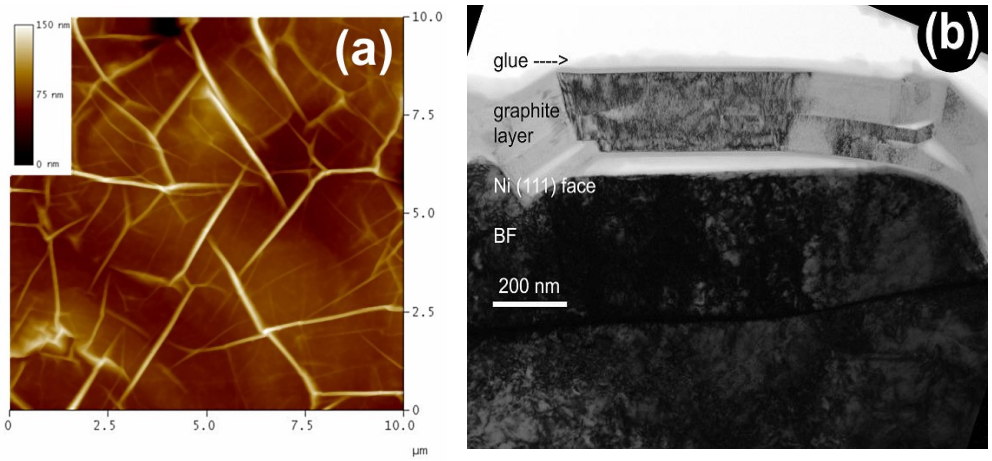

Figure 2 *(a) Atomic Force Microscope image of the grown FLG layers, which shows ripples formed on the surface possibly due to the different thermal expansion coefficients of the FLG and Ni. (b) Cross–sectional transmission electron microscope image of the graphite layers on top of the polycrystalline Ni film.*

Raman spectra show that the quality of the few layer graphite films grown by our method is comparable to the quality of samples obtained by HOPG exfoliation.

Contacting and electrical testing of individual single wall carbon nanotube bundles

(OTKA T049182, OTKA-NKTH K67793 & NI67851)

G. Dobrik, Z. E. Horváth, V. Obreczán, P. Neumann, I. Lukács, K. Kertész, Gy. Molnár, and L.P. Biró

Gas sensing properties of carbon nanotube (CNT) mats has been intensively studied in our laboratory in the last couple of years. The change in gas ambient of these layers can modify their electrical conductivity. The amplitude and course of the conductivity change depend not only on the kind and concentration of the applied gas or vapour but on the type of CNTs and the way of sample preparation, too [Horváth ZE et al: Appl. Phys. A 93 (2008) 495-504]. In order to differentiate between the intrinsic properties of CNTs and the effect of the network, we started to investigate the electrical and gas sensing properties of individual carbon nanotube type objects, at first single wall CNT (SWCNT) bundles. While the sample preparation of CNT mats can easily be solved by spraying or drop-drying CNT suspension on macroscopic substrates with predeposited metallic electrodes, in case of individual objects, a precision of about 100 nm is needed in locating objects and depositing contacts. Diluted suspension of COOH-functionalized SWCNT bundles with diameters of 10–20 nm was spin-coated on marked Si/SiO_2 substrate. Atomic Force Microscopy (AFM) was used to locate a few separated bundles on the surface. 2, 3 or 4 contacts were deposited on them, depending on their length using a standard electron beam lithography process. The contacts were prepared from 5 nm thick Cr and 35 nm thick Au films. *Figure 1* shows AFM images of a SWCNT bundle before (left) and after (right) contacting.

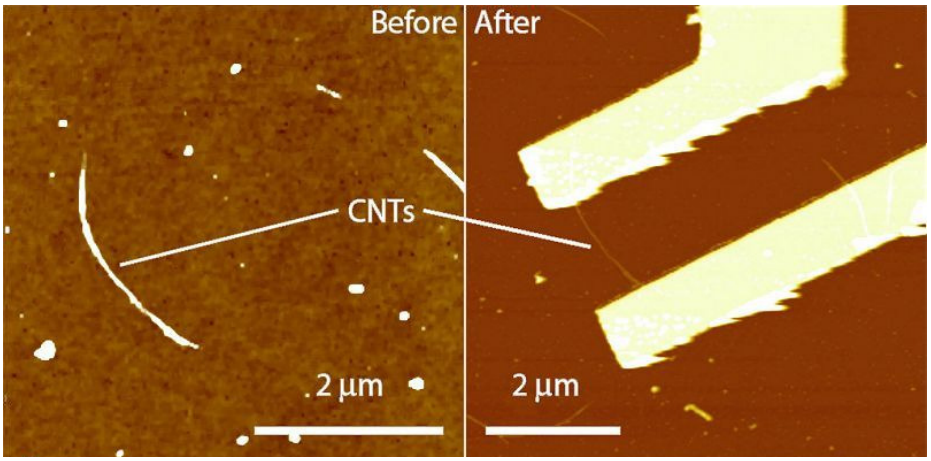

Figure 1 *Tapping mode AFM images of a SWCNT bundle. Left side: a 2,5 µm long bundle is visible on marked SiO_2 substrate, before lithography process. Right side: the same bundle with two Cr-Au contacts.*

Figure 2 shows an I-V curve (black) and its derivative (grey) measured on a SWNT bundle with two contacts. Current was ramped from -250 nA to 250 nA and the voltage recorded. All I-V diagrams were recorded at room temperature and in dark. The curves are approximately symmetric to zero, and monotonic. The derivative curve shows a pair of peaks symmetric to zero at 80 meV, indicating the presence of a band gap in the electronic structure of the system. This can belong either to the semiconducting tubes or the tube-contact interface.

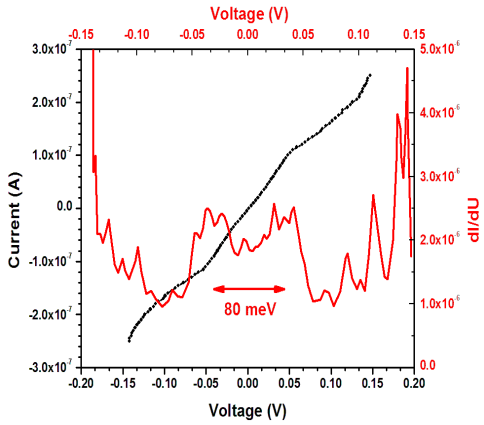

Figure 2 *I-V curve (black) and its derivative (gray) measured on a contacted SWCNT bundle.*

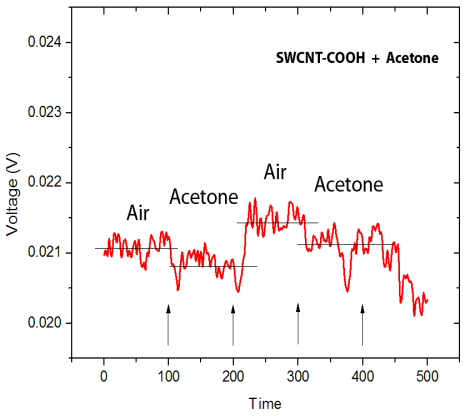

Figure 3 *Voltage measured on a SWCNT bundle in alternately changed air/acetone vapor ambient.*

Preliminary chemical sensing measurements were carried out on one of the contacted bundles by modifying gas ambient periodically in every 50 seconds. Keeping the current constant at 50 nA, the voltage was measured with a sampling frequency of 2 Hz. The measured voltage is proportional to the resistance. As an example, *Figure 3* shows the measured voltage in case of acetone vapour, the changes of gas ambient are denoted by arrows. Though the measurement is rather noisy, it is clearly visible that the changes in vapour concentration are always followed by an abrupt change of resistance. However, the level of resistance can not be correlated with the concentration. Compared to the case of macroscopic networks, a reversed behaviour can be observed: the appearance of acetone vapour makes the resistance of the network raise, just the opposite as in case of a single bundle.

Photonics Department

Head: Miklós FRIED, D.Sc., scientific advisor

Research Staff

- Péter PETRIK, Ph.D., Head of Ellipsometry Laboratory
- Miklós SERÉNYI, C.Sc., Head of Semiconductor Photonics Laboratory
- János BALÁZS, Ph.D. (part-time)
- Antal GASPARICS, Ph.D.
- Norbert NAGY, Ph.D.
- András HÁMORI, dr. Univ.
- Róbert HORVÁTH, Ph.D.
- György JUHÁSZ, dr. Univ.
- Zsolt LACZIK, Ph.D. (on leave)
- Tivadar LOHNER, C.Sc.
- János MAKAI, C.Sc. (part-time)
- György KÁDÁR, D.Sc.
- Sándor KURUNCZI, Ph.D.
- Olivér POLGÁR, Ph.D.
- Miklós RÁCZ, Ph.D. (part-time)
- Ferenc RIESZ, C.Sc.
- Gábor VÉRTESY, D.Sc.
- Péter TÖRÖK, D.Sc. (on leave)

Technical Staff

- Rózsa Mária JANKÓNÉ, technician

Ph.D. students / Diploma workers

- Csaba MAJOR, Ph.D. student
- Péter KOZMA, Ph.D. student
- Emil AGÓCS, Ph.D. student

Development of non-destructive study of Carbon Fiber Reinforced Plastic (CFRP) materials: Presentation of the results in Frankfurt, at the AIRTEC 2009, 4th „Supply on Wings" Conference. The new Fluxset sensor assembly successfully operated at low frequency (15…20 kHz) and measured significant signals on CFRPs.

Magnetic measurements were performed on low-carbon steel in the frame of an international collaboration (Universal Network for Magnetic Non-destructive Evaluation), which aim to disseminate magnetic methods in the practice of nondestructive material testing, mainly in power plants. Our method was proven as the most sensitive tool to show the structural degradation in ferromagnetic materials.

Realisation of grating-coupled hybrid waveguide interferometry (without moving parts): In co-operation with Creoptix GMBH (Switzerland), MFA performs feasibility studies about a new patent. The study aims the realisation of grating-coupled hybrid waveguide interferometry (without moving parts) for highly sensitive optical sensing. The results in 2009 were published in Applied Physics B. Péter Kozma was awarded with the "Graduate Student Award" at the "European Materials Research Society Spring Meeting".

We have new results in the field of immobilisation of bacterial flagellar filaments with the help of in situ ellipsometry and AFM. We established that more flagellar filaments can be bounded to the surface using chemical immobilisation. The deposited protein layer can be described using a multi-layer model that accounts for the total thickness of the film of 500 nm with decreasing protein density away from the surface: the first 100 nm contains lying filaments, the upper (lower density) layers contain different orientation filaments.

Optical waveguide lightmode spectroscopy/interferometry has been used to observe successfully the Z-domain bonding receptors. Our investigations were in good agreement with the calorimetric measurements performed at the Pannon University.

We are involved in two "National technology development" projects: "Development of integrated process monitoring metrology for the 32 nm technology node of IC processes" and "Development of metrology tools based on electrical and optical techniques for in-line and laboratory qualification of thin film solar cells"

The Ellipsometry Laboratory is part of a newly formed joint European Laboratory of the EU FP6 ANNA consortium (http://www.i3-anna.org/) providing analytical services in a wide range of characterisation techniques. The laboratory has been accredited with excellent ratings:
(http://nat.hu/adatbazis/reszletes-oldal.php?azon=2695).

New patent pending (in Hungarian: Nagy Norbert, Deák András, Hórvölgyi Zoltán, Bársony István; *"Eljárás maszk kialakítására általános alakú test felületén és alkalmazásával felületi struktúra létrehozása orvosi implantátumon"*).

Various nanostructures on macroscopically large areas prepared by tunable ion-swelling

N. Nagy, A. Deák, Z. Zolnai, G. Battistig, and M. Fried

A series of experiments were carried out by Xe^+ and Ar^+ ion implantation into (100) Si substrates using monoparticulate colloidal nano-masks for the investigation of various ion–nanoparticle interactions, furthermore to utilise new data analysis capabilities of the RBS-MAST [Z. Hajnal et al., Nucl. Instr. and Meth. B 118 (1996) 617-621] (for details please see: *"A 3D RBS study of ordered nanosystems prepared by irradiated nanoparticulate masks"*). Additionally to these results various nanostructures were achieved on macroscopically large Si areas based on ion-swelling effect in the nanometer range. The nanostructures were prepared by ion irradiation of 40 keV Ar^+ or 500 keV Xe^+ ions through nano-masks composed from silica particles with the diameter of 450 nm. The AFM images of the surface patterns can be seen in Fig. 1 and Fig. 2. The character of the surface topography can be tuned by setting the parameters of the masking and irradiation step.

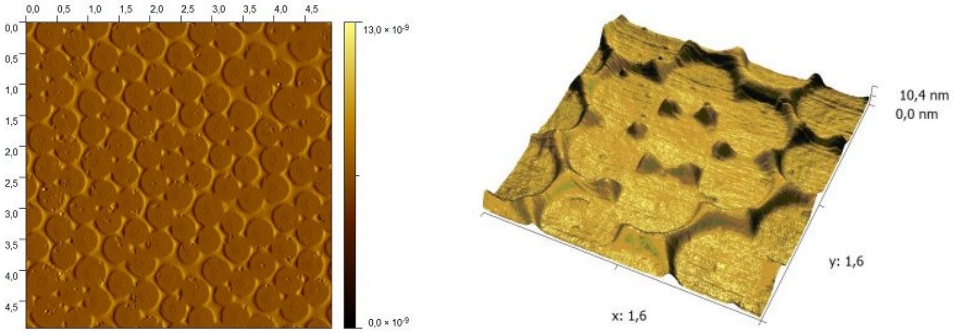

Figure 1 *AFM images of Si surface topography achieved by irradiation of 40 keV Ar^+ ions with fluence: $1x10^{15}$ Ar^+cm^{-2} using nanoparticulate mask with diameter of 450 nm*

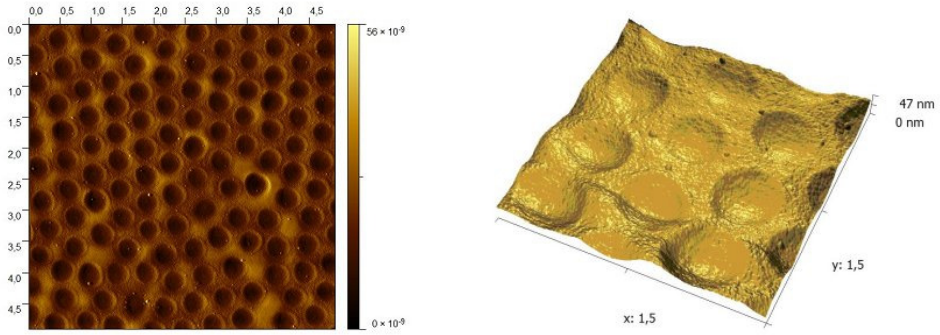

Figure 2 *AFM images of Si surface topography achieved by irradiation of 500 keV Xe^+ ions with fluence: $2.4x10^{16}$ Xe^+cm^{-2} using nanoparticulate mask with diameter of 450 nm*

Makyoh topography

(OTKA K 68534; HYPHEN, EU FP6 IST 027455; ANNA, EU 026134 (RII3); MORGaN, EU 214610)

F. Riesz, and J. P. Makai

Makyoh topography is an optical tool for the qualitative flatness testing of specular surfaces, based on the defocused detection of a collimated light beam reflected from the tested surface. By inserting a square grid into the path of the illuminated beam, the height map can be calculated by integrating the gradients obtained from the distortion of the grid's reflected image (quantitative extension).

From the methodological point of view, the relation between the spectral properties of the Makyoh image and that of the studied surface was investigated through ray-tracing simulations of the imaging of periodic and quasi-periodic surfaces and theoretical considerations. It was found that the dominant periodicity of the image depends on the slope of the power spectrum of the surface height map.

Research activities were concentrated also on applications, mostly within the framework of the ANNA transnational access program and other EU funded projects. Investigations were made for in-house research purposes as well.

Deformation and surface morphology measurements were performed on Si substrates and SiC/Si heterostructures grown by vapour phase epitaxy at IMEM–CNR, Parma The final aim was to establish the optimum growth parameters to obtain stress-free layers having low surface defect density and appropriate flatness.

The characterisation of the bare Si substrates indicated that the majority of the localised surface defects observed for the epiwafers are present in the wafers, that is, they stem from substrate preparation procedures. Namely: the carburisation process induces small point-like detects, and the thermal annealing develops line-like defects, possible by thermally etching bunches of dislocation slip lines. The epiwafers are found to be deformed into a concave overall shape, most probably due to thermal stresses. The epilayers possess a fine-scale roughness not present in the Si substrate.

MEMS wafers and elements, fabricated from the SiC/Si heterostructures, were also studied tentatively. We concluded that the deformation of the whole wafer is in line with that of the non-patterned wafers. The deformation of individual square membranes indicated an essentially flat membrane with a slightly concave surrounding area. In addition, a definite morphology of the membrane were observed, possibly due to the wet backside etching.

The deformation of Si wafers was measured to assess the stress generated by deposited dielectric layers of different technologies (within the ANNA project).

Deformation and morphology measurements were also performed on Si/SiC-based composite substrates used for GaN growth (for the HYPHEN project) as well as on polycrystalline diamond, GaN/Si and Si/diamond substrates (for the MORGaN project).

For in-house research, curvature measurements of dielectric-covered Si substrates as well as an in-depth study of the effects of different polishing etchants on Si wafers must be mentioned. As an example, Fig. 1 shows the Makyoh images of four Si wafers subjected to polish etch using etchants of different compositions. The images show point-like defects (etch pits) and a large scale morphology, characteristically to the different etchants.

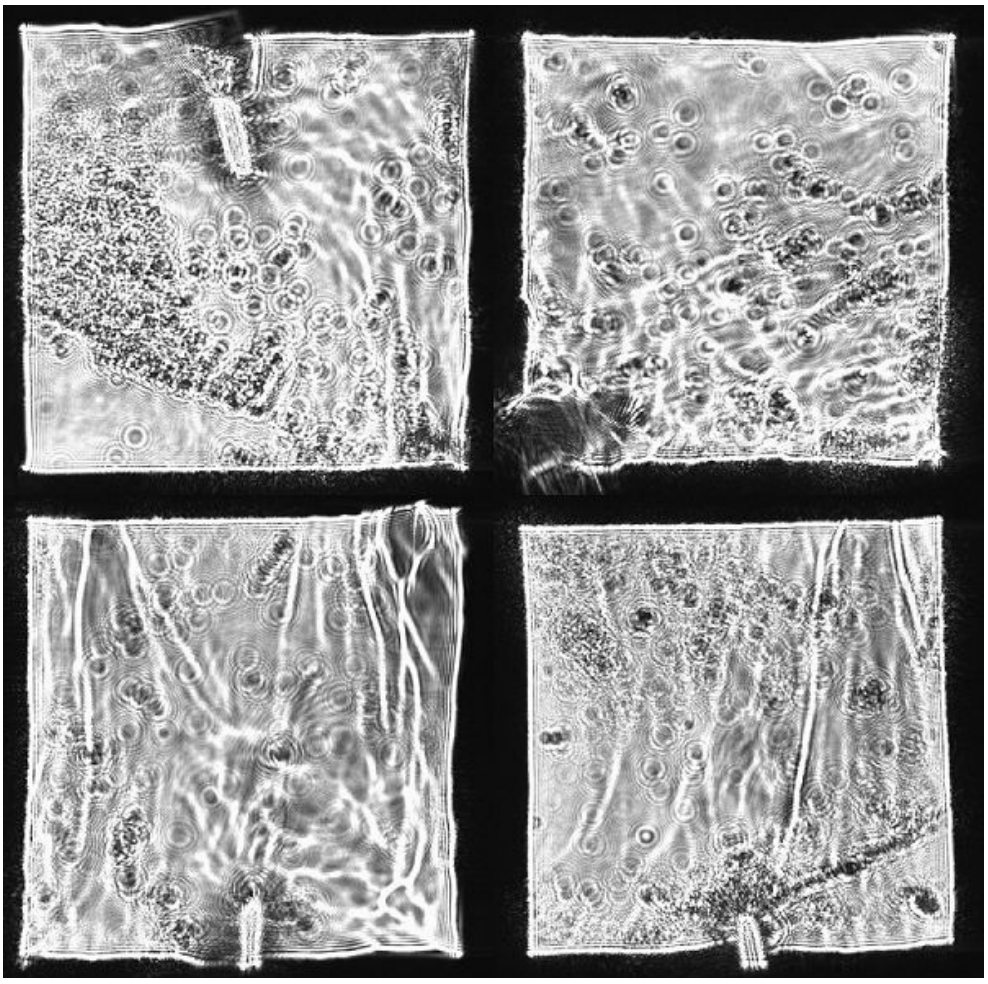

Figure 1 *Makyoh images of Si wafer pieces subjected to polish etch using different etchants*

Inspection of steel degradation by Magnetic Adaptive Testing

(OTKA K62466)

G. Vértesy

A novel, nondestructive magnetic measurement method has recently been developed, which is based on systematic measurement of minor magnetic hysteresis loops. This technique can serve as a powerful tool for comparative measurements, and for detection of changes, which occur in structure of the inspected ferromagnetic material during their lifetime or during a period of their heavy-duty service. It has been shown previously that this method, Magnetic Adaptive Testing (MAT), is significantly more helpful than that of the traditional major loop studies.
In the present work MAT was applied for a series of carbon steel (SS400) and austenitic stainless steel (SUS316L) materials. Residual strain was added by tensile loads. For illustration, the stress-strain diagram of the stainless steel sample is shown in Fig. 1.

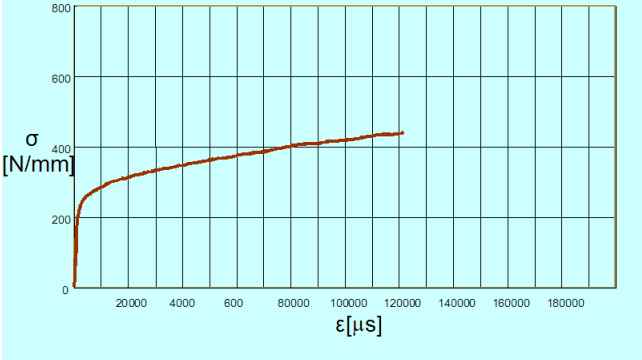

Figure 1 *The stress-strain diagram of the SUS sample*

All samples in the two series were measured by MAT method. Both directions of magnetisation in parallel and perpendicular to tension direction were examined. A specially designed Permeameter with a magnetising yoke was applied for measurement of families of minor loops of the magnetic circuit differential permeability. The experimental raw data are processed by an evaluation program. Each calculated $\mu_{ij}(BH)$-element represents one "MAT-descriptor" of the investigated material structure variation. The consecutive series of μ-matrices, each taken for one sample with a value of the strain, ε_k, of the consecutive series of the more-and-more deformed steel, describes the magnetic reflection of the material plastic deformation. Integrating the permeability along the field, h_a, hysteresis loops and B-matrices can be obtained. The B-matrices contain in principle the same information as the μ–matrices, however, presentation of the ε-dependences is different and sometimes advantageous.
In the case of carbon steel, definite differences were found in the directly measured permeability of differently deformed samples, however, the calculated μ_{ij}-degradation functions did not reveal systematic correlation with residual strain. However, B_{ij}-

degradation functions shows good correlation, as shown in Fig. 2. Here all the B_{ij} values are normalised by the reference (not deformed sample). Note, that significant difference was found if the direction of magnetisation was taken with parallel or perpendicular direction with respect to the elongation. The most deformed samples had about 5 times larger MAT descriptors than not deformed sample.

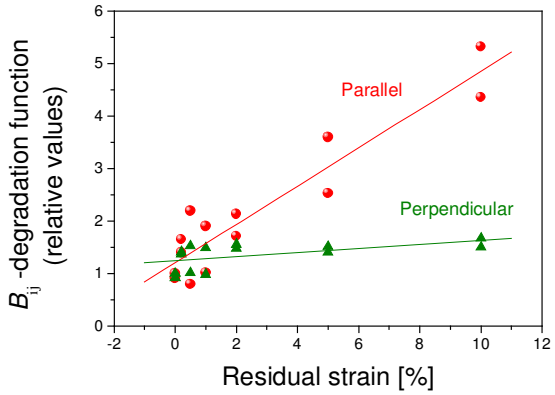

Figure 2 *$B_{ij}(\varepsilon)$-degradation functions vs. residual strain of carbon steel for parallel and perpendicular magnetization with respect to the elongation*

In the case of austenitic stainless steel practically no difference was observed in the permeability as a function of deformation. It is not surprising, because these samples have very low magnetisation. But calculating again B_{ij}-degradation functions, a definite correlation has been seen between the residual strain and the magnetic descriptors as shown in Fig. 3.

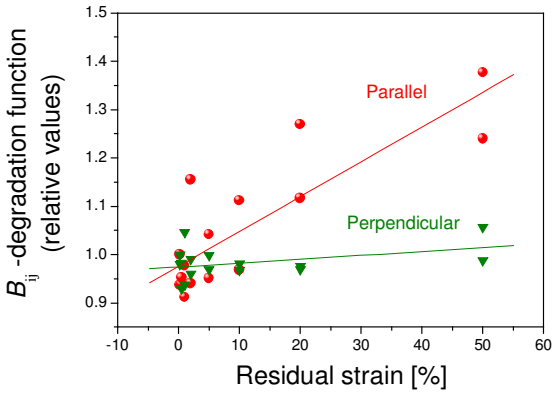

Figure 3 *$B_{ij}(\varepsilon)$-degradation functions vs. residual strain of stainless steel for parallel and perpendicular magnetization with respect to the elongation.*

In the perpendicular direction no influence of elongation was found on MAT descriptors, but in parallel one this parameter was about 30% larger compared with reference sample. The scatter of points is rather large, but the tendency is clearly seen. These results shows the capability of Magnetic Adaptive Testing very well and give a good chance for future practical application.

NANOMAGDYE: Magnetic nanoparticles combined with submicronic bubbles and dye for oncologing imaging

(EU FP7 – GA No 214032)

G. Vértesy, and A. Gasparics

The objective of NANOMAGDYE consists in developing tailored biocompatible magneto-optical nanosystems based on magnetic iron oxide nanoparticles with dimension between 2 and 100 nm. The project comprises elaboration of the nanosystems and characterisation of their structural, optical and magnetic properties. The opto-magnetic nanoparticles will be tested in a medical application and a dedicated magneto-optical probe will be fabricated for oncologing imaging. Combining optical and magnetic labelling into a single biocompatible nanosystem will provide increased spatial resolution and will avoid currently used ionising radiation based method to improve patient safety and medical effectiveness.

MFA has the role to develop suitable magnetic sensing technology for indicating the presence of the submicron sized magnetic particles. These iron-oxide based particles are close to (or already in) super-paramagnetic state due to their dimension. However, the real challenge of the detection is the low mass of the accumulated particles in a typical lymph node. Novel Fluxset sensor based method has been developed to sense with acceptable signal/noise ratio 0.7 mg of aggregated nanoparticles even from 7 mm distance. The figures below show the magnetic field distribution, detected by the Fluxset probe in the vicinity of the typical lymph node sized capsules filled with different amount of magnetic nanoparticles. The total weights of nanoparticles within one capsule (Ch1, Ch2, etc.) are also given in Figs. 2 and 3.

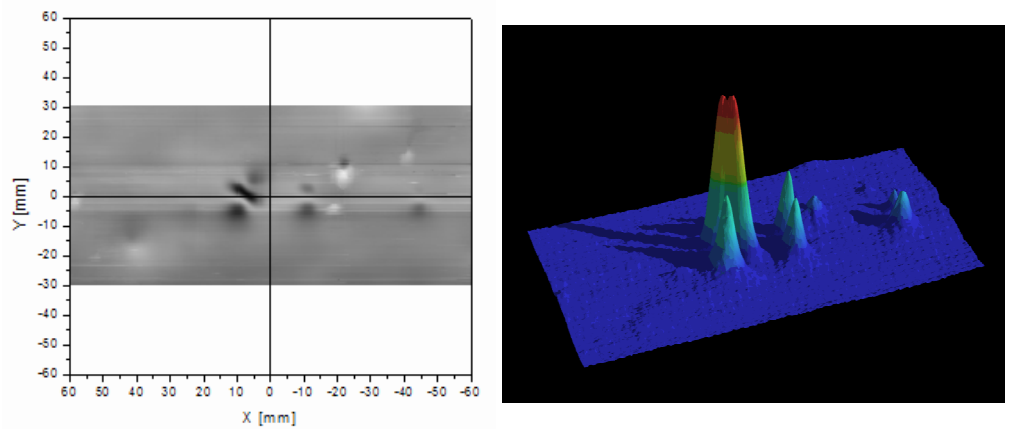

Figure 1 *Magnetic field map of the sensed nanoparticles at 20 kHz (left: 2D, right 3D representation)*

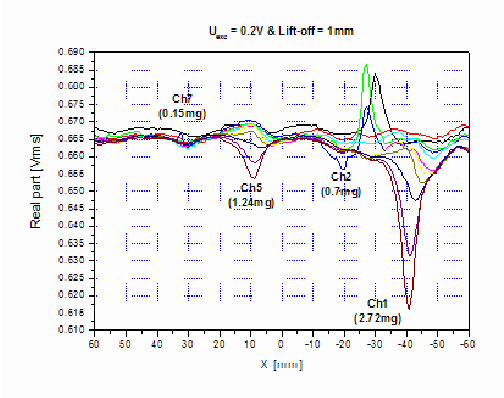

Figure 2 Feasibility tests on Fluxset sensor based probe

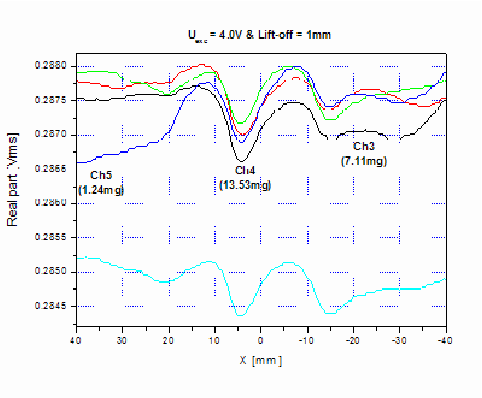

Figure 3 Feasibility tests on Magneto-resistive sensor based probe

Comparative study has been performed on the Fluxset system performance. The sensitivity of the Fluxset probe (Fig. 2) was compared to the commercially available Magneto-resistive (MR) sensor (Fig. 3). The curves with different colours represent parallel scan lines of Fig. 1. Only the capsules with low amount of particles were selected in the Fluxset experiment, while only the other ones could produce valuable response in the MR system. The Fluxset probe was found to have an order of magnitude higher sensitivity meanwhile the MR sensor failed in the detection of the targeted capsule with 0.7 mg nanoparticles. These results establish opportunity for developing new surgery hand tool for the detection of the affected human tissue to be removed and which eliminates the ionising radio nuclide based markers. MFA has begun the co-development of the Fluxset probe industrial prototype with EURORAD. The ultra low power miniaturised front-end electronics (Fig. 4), which operates the Fluxset sensor has been developed and manufactured. The Fluxset sensor based probe prototype (Fig. 5) was designed in accordance to the needs of the recently used surgeon tools. This way, the user can easily replace the nuclide detectors with the magnetic probe without the need of modifying any practice in the surgery.

Figure 4 *Mini front-end electronics that operates the Fluxset sensor*

Figure 5 *Manufacturing the industrial prototype of the Fluxset probe (Ø 10 mm)*

Bioellipsometry

(OTKA K 61725, OTKA PD 73084, FP7 OPTIBIO)

P. Kozma, A. Németh, T. Hülber, S. Kurunczi, P. Petrik, R. Horváth, and M. Fried

Bioellipsometry is a new research direction in the Ellipsometry Laboratory of MFA (http://www.ellipsometry.hu/). A strong basis is provided by the complementary competence of our staff covering physics, bio-physics, chemistry, and device fabrication, as well as by our new tool, a Woollam M-2000DI rotating compensator spectroscopic ellipsometer that is capable of taking full spectra in a liquid cell within 1 s (http://jawoollam.com/m2000_home.html) with high accuracy. We purchased and built liquid cells (Fig. 1), and performed extensive studies for testing the performance of our tools through *in situ* investigations during deposition of reference protein molecules (like fibrinogen) or advanced structures like flagellar filaments (Fig. 2) intended to be used in waveguide sensors.

Our results have been presented at the Spring Meeting (prize of Graduate Student Award for P. Kozma) and at the Fall Meeting of the European Materials Research Society, at the TDK-2009 conference of the Eötvös Loránd University (I. prize for A. Németh), as well as submitted for publications.

Figure 1 *Self-made 0.2-ml liquid cell.*

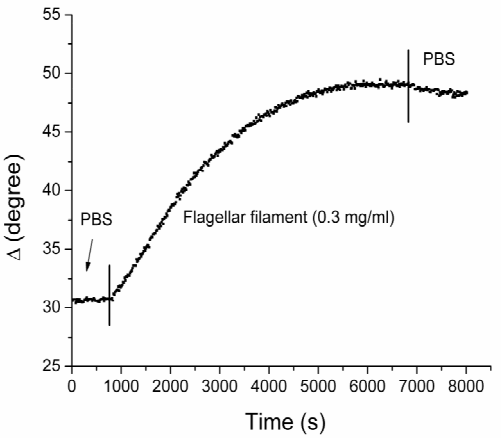

Figure 2 *Flagellar filament adsorption on clean Si-wafer. Δ denotes the ellipsometric phase shift at a wavelength of 600 nm.*

ANNA - European Integrated Activity of Excellence and Networking for Nano and Micro- Electronics Analysis

(EU I3, ANNA Project Nr. 026134)

P. Petrik, T. Lohner, M. Fried, A. Bolgár, and F. Riesz

The aim of the ANNA project (http://www.i3-anna.org/) is the formation of a joint European Laboratory including partners from all over Europe. The ANNA Laboratory provides access to instrumentation and analytical services at first class European analytical laboratories. Until the end of 2010 the users can apply for free access supported by the EU. Most of the ANNA laboratories have been accredited, including MFA. Apart from the accreditation, the laboratories have been improved, optimised, and demonstrated their capabilities through so called Joint Research Activities (JRA) covering topics like characterisation of ultra thin films, ultra shallow junctions, or nanocrystals – the latter activity being co-ordinated by MFA.

In frame of the Joint Research Activities we have shown that ultra thin HfO_x layers (Fig. 1), ultra-shallow ion implantation profiles (Fig. 2) and nanocrystals in porous silicon and silicon rich oxide can be measured with high sensitivity using ellipsometry. We have also studied 3C-SiC layer growth on silicon substrates with respect to their large-scale deformation and surface defects depending on the growth conditions as well as the curvature of Si substrates covered by different dielectric films to assess the layer stress.

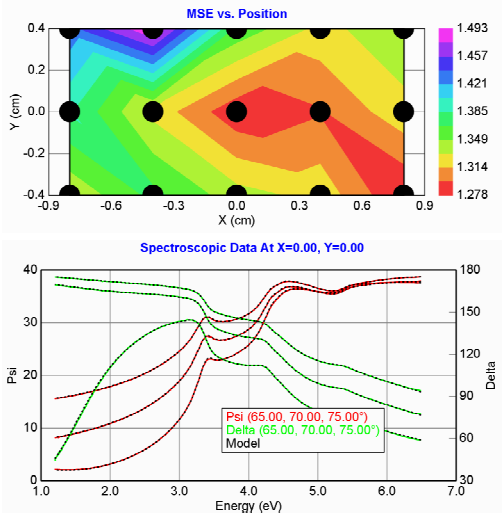

Figure 1 *Map (top) on 2 nm HfO_2 deposited on 1.7 nm SiO_2 on c-Si. In the bottom graph, the solid and dotted lines show the measured and calculated spectra, respectively.*

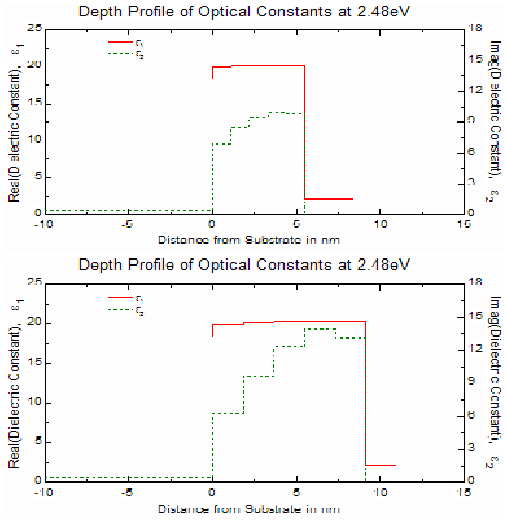

Figure 2 *Step-like damage depth profile models for c-Si implanted by 1 keV (top) and 3 keV (bottom) As at a fluence of 10^{15} cm^{-2}. The solid and dotted lines denote, respectively, the real and imaginary parts of the pseudo-dielectric function.*

Development of integrated process monitoring metrology for the 32 nm technology node of IC processes

(NKFP-07-A2-ICMET_07)

M. Fried, G. Juhász, P. Petrik, and G. Battistig

The aim of this project (leaded by Semilab Inc.) is to develop such a measurement technology and equipment, which will enable the process control of the 32-65nm generation integrated circuit production complying with the clean room and automation standards. The equipment, which will be delivered by the project, enables one of the most important technological processes in the semiconductor dopant (resistance and type adjustment) monitoring in several steps: after the implantation and thermal activation of the dopant species.

MFA's task is in the project to prepare ion-implanted reference samples (ultra-low-energy implantation, ULE-imp), and to perform reference measurements.

Ellipsometry is very sensitive for changes but the detection is limited from two directions. The lower limit is the minimum detectable lattice-disorder depending on the atomic mass of ions and the implantation energy. The upper limit is the full amorphization, also depending on the atomic mass and energy, two orders of magnitude higher than the lower limit. The precision is better than 1 % between the two limits if it is calibrated with ion-backscattering technique (RBS, available in MFA). RBS needs expensive accelerator and vacuum system but ellipsometry being an optical method can be used in-situ or in-line. Note, that ellipsometry cannot be applied for the determination of electrically active dopants after high temperature annealing. Ellipsometry shows increasing damage thickness with increasing energy. Similarly, the series of increasing dose show an increasing damage. After calibration (ion type, energy), dose-map with typically better than 1 % precision can be achieved.

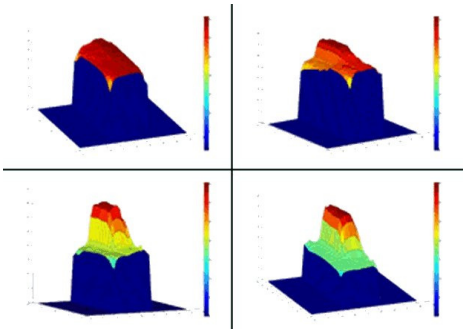

Figure 1 *4 different dose-levels on 4-inch wafers: wafer had ¼ of virgin part, ¼ of the "center dose" (5e12, 5e13, 5e14, 5e15 20-keV BF2 /cm2 ¼ of 90% of the "center dose" and ¼ of 110% of the "center dose".*

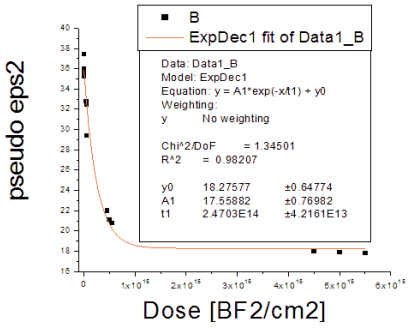

Figure 2 *The first direct optical transition of the c-Si at 365 nm (E1) was used for the analysis. Imaginary part of the complex pseudo dielectric function of the 20 keV BF2-implanted samples. At E1 <ε2> decreases systematically with increasing dose.*

Development of metrology tools based on electrical and optical techniques for in-line and laboratory qualification of thin film solar cells

(TECH_08_ D2(2008) PVMET_08)

M. Fried, C. Major, G. Juhász, and P. Petrik

The aim of this project (leaded by Semilab Inc.) is to develop an equipment and measurement technology family, which is capable to perform electrical and optical measurements for in-line and laboratory qualification of thin film solar cells. MFA's task is in the project to make applicable spectroscopic ellipsometry for this purpose.
We develop optical models for different types of amorphous silicon (p-a-Si, n-a-Si, i-a-Si) We used the Cody-Lorentz function suggested by R. W. Collins's group (A. S. Ferlauto, G. M. Ferreira, J. M. Pearce, C. R. Wronski, R. W. Collins, Xunming Deng, Gautam Ganguly: "*Analytical model for the optical functions of amorphous semiconductors from the near-infrared to ultraviolet*" Applications in thin film photovoltaics, JOURNAL OF APPLIED PHYSICS V92(5) p.2424, 2002). As it is shown in Fig. 1 we can fit the measured spectra very well in the whole spectral region (1.1-5 eV). In Fig. 2 the i-a-Si layer complex dielectric function is shown.

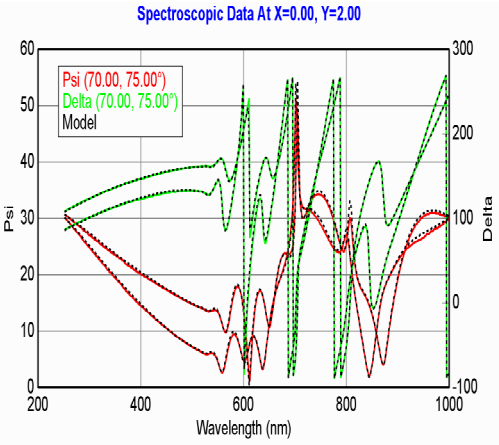

Figure 1 *The fit of the p-i-n-a-Si layer structure ellipsometric spectra.*

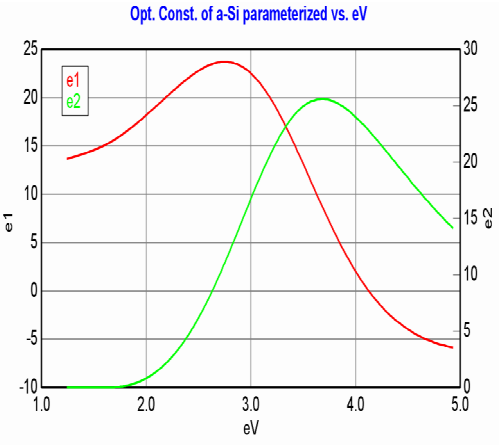

Figure 2 *i-a-Si layer complex dielectric function.*

Grating coupled interferometry for optical sensing

(OTKA PD 73084, FP7 OPTIBIO)

P. Kozma, A. Hamori, K. Cottier*, S. Kurunczi, and R. Horvath

*Creoptix GmbH, Wädenswil, Switzerland

An interferometric sensor based on gratings on a planar waveguide is introduced. The device combines the advantages of known interference-based waveguide sensors with the simplicity of grating couplers. In the presented configuration, two parallel and coherent light beams, laterally separated in the direction of mode propagation, are coupled into a planar waveguide through a grating. One of the coupled beams is phase modulated using a periodically relaxing liquid crystal modulator, resulting in a time varying intensity signal at the end facet of the waveguide. Refractive index changes within the waveguide section between the two coupling regions are monitored by observing characteristic changes in the intensity signal. We determined that the present refractive index resolution of the device is potentially better than 10^{-5}.

Our results have been presented at the EMRS 2009 Spring Meeting (P. Kozma received the graduate student award of the conference in section "L") and published in Applied Physics B (Lasers and Optics Volume 97, Number 1, 2009).

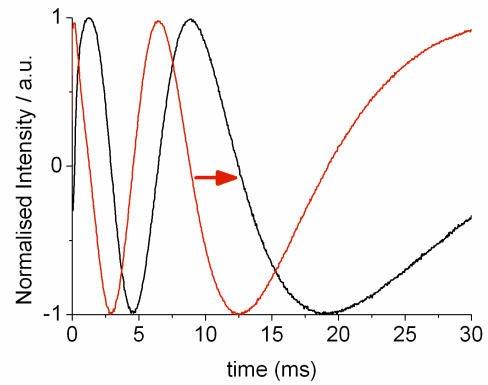

Figure 1 *The time shift of the interference signal when the water in the cuvette was replaced to 0.25% glycerol solution (4.6x10-4 refractive index increase).[2]*

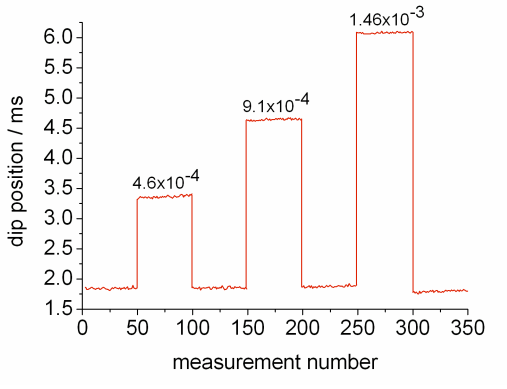

Figure 2 *The measured dip position (from Fig. 1.. when the water in the cuvette was replaced to various glycerol solutions and back to pure water (see text). The corresponding refractive index increments are indicated.[2]*

Ellipsometric characterisation of compound semiconductors

P. Petrik, M. Fried, Z. Zolnai, T. Lohner, and N. Q. Khanh

We have developed optical models for the characterisation of ultra thin thermal oxides on SiC. We have investigated the properties (including density, roughness, and transition layers) of the oxide layer as a function of thickness using a combination of ellipsometry, ion beam analysis, and atomic force microscopy (Fig. 1, Ref. 1). We performed a comparative investigation by ellipsometry and ion beam analysis to measure the damage formation in SiC ion implanted by 100-keV Xe and P (measured at the BESSY synchrotron facility in Berlin, to be published in 2010) as well as CdTe ion implanted by 350-keV Bi ions at different fluences to build ellipsometric models for photovoltaic thin film CdTe measurements (Fig. 2). We found extended defects with concentrations linearly increasing with fluence (Ref. 2).

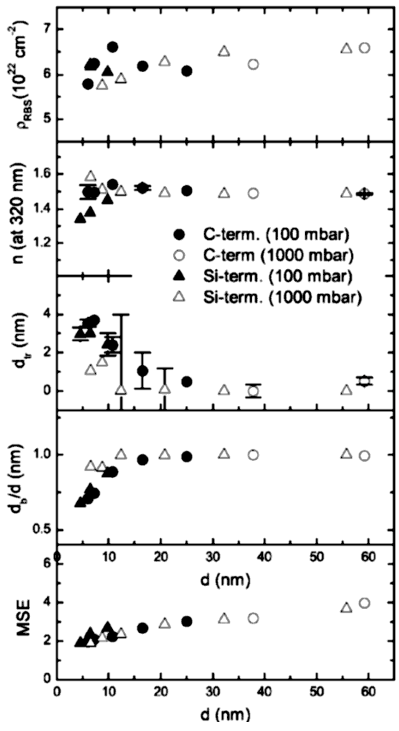

Figure 1 *Fitted parameters as a function of oxide thickness on SiC. n, d_{tr}, d_b, and MSE denote the refractive index, the thickness of the transition layer, the thickness of the bulk layer, and the mean squared error of the fit, respectively. The density, ρ, was calculated combining ellipsometry and ion beam analysis.*

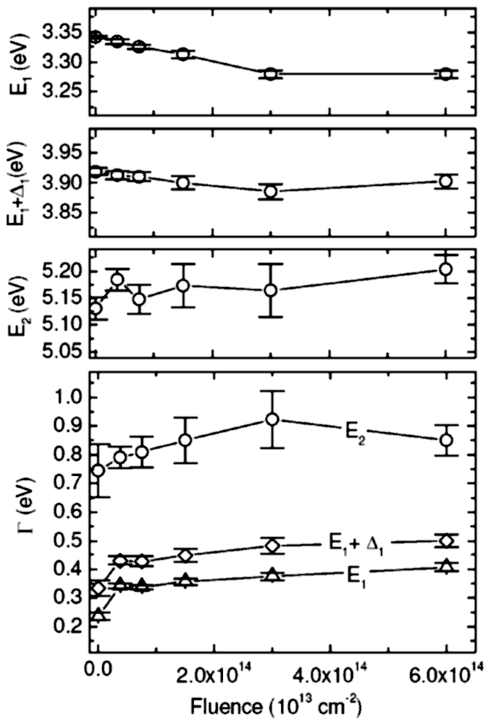

Figure 2 *Fitted critical point energies (E) and broadening parameters (Γ) as a function of fluence for CdTe single-crystals implanted by 350-keV Bi ions.*

Influence of Hydrogen on the Structural Stability of Annealed Ultrathin Si/Ge Amorphous Layers

(Scientific Cooperation Agreement between CNR and MTA under the contract MTA 1102)

M. Serényi, and C. Frigeri[1]

[1] CNR- IMEM Institute, Parco Area delle Scienze 37A, 43100 Parma, Italy

Hydrogen can be used to compensate individual dangling bonds in Si, Ge and SiGe alloys. Hydrogenation can thus improve the electro-optical properties of those materials, in particular for their application as solar cells, by reducing the deep electronic levels in the band gap. One way of preparing the amorphous hydrogenated SiGe alloy is to deposit very thin alternating layers of Si and Ge and then form the alloy by intermixing the Si and Ge elements via diffusion. Ultrathin (thickness 3 nm) alternating amorphous layers of Si and Ge were deposited on Si substrates by radio frequency sputtering in an argon atmosphere. The crystalline Si and Ge targets were powered at 1.5 kV. The samples consisted of multilayer stacks made of 50 pairs of Si/Ge layers for a total thickness of 300 nm. Hydrogenation was carried out by letting hydrogen to flow into the deposition chamber with different flow rates and the samples were annealed in argon at 350 C.

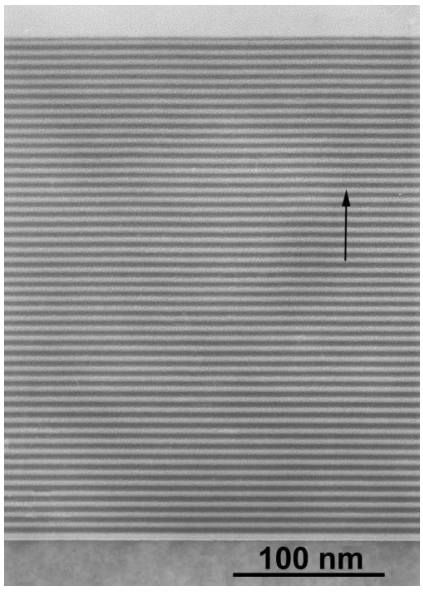

Figure 1. *Typical TEM image of the investigated amorphous Si/Ge multilayers. The substrate (outside the field of view) is on the bottom side of the picture*

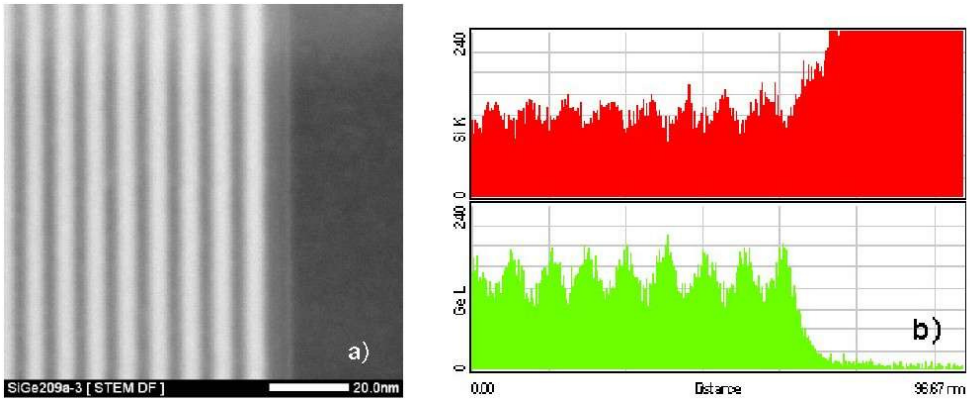

Figure 2. *Hydrogenated a-Si/Ge:H multilayer annealed at 350 °C. a) TEM image, b) EDX line scan profiles for Si (top) and Ge (bottom) across the zone in a). The Si substrate is visible on the right part of a).*

The structure of the amorphous Si/Ge multilayers is shown in the Fig. 1 which is representative of both not-hydrogenated and hydrogenated samples. The TEM image of a hydrogenated sample submitted to heat treatment at 350 °C and EDX line scan profile can be seen in the Fig. 2. After annealing the EDX signals of Ge and Si are quite distinguishable though much more for Ge. The peaks of Ge emerge quite well from the background at well defined positions corresponding to the nominal Ge layers. After annealing of a non-hydrogenated sample (Fig. 3) the peaks of both elements are much more diffused out, especially those of Si, suggesting a greater interdiffusion of the elements. The experimental fact the diffusion intermixing is slower in the hydrogenated sample as compared to the non-hydrogenated one can be interpreted by the effect of still remaining hydrogen. This can inactivate the dangling bonds and decrease the diffusion coefficient.

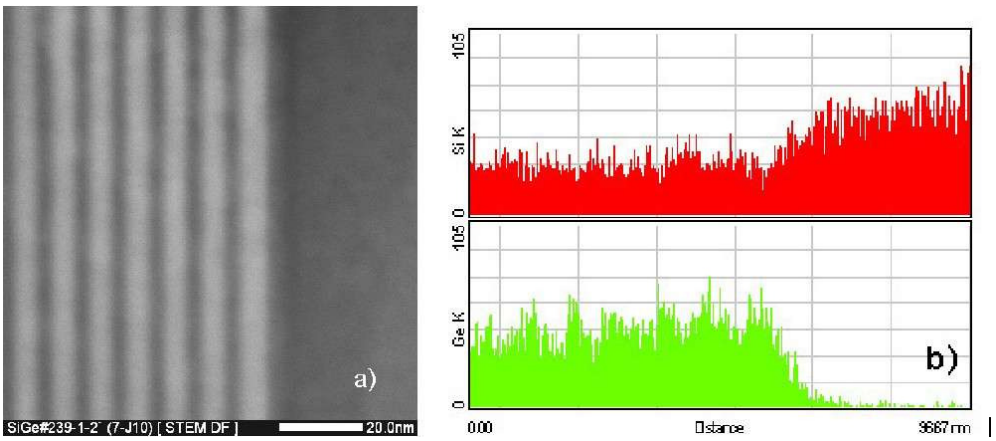

Figure 3. *Non-hydrogenated a-Si/Ge multilayer annealed at 350 °C. a) TEM image, b) EDX line scan profiles for Si (top) and Ge (bottom).*

Microtechnology Department

Head: Gábor BATTISTIG, Ph.D.

Research Staff

- István BÁRSONY, D.Sc.,
- Péter BASA, Ph.D.,
- László DÓZSA, Ph.D.,
- Péter FÜRJES, Ph.D.,
- Zsolt József HORVÁTH, D.Sc.,
- Zoltán LÁBADI, Ph.D.,
- György MOLNÁR, Ph.D.,
- Ágoston NÉMETH, Ph.D.,
- Andrea Edit PAP, Ph.D.,
- Vilmos RAKOVICS, Ph.D.,
- Zsolt ZOLNAI, Ph.D.
- Ferenc BELEZNAY, D.Sc., Emeritus
- Gábor PETŐ, D.Sc., Emeritus
- Antalné ÁDÁM, M.Sc., (part-time)
- Albert KARACS, M.Sc., (part-time)
- Tibor MOHÁCSY, M.Sc., (part-time)
- Ákos NEMCSICS, Ph.D., (part-time)
- István PINTÉR, Ph.D., (part-time)
- Bálint PŐDÖR, Ph.D., (part-time)
- Béla SZENTPÁLI, Ph.D., (part-time)
- Éva VÁZSONYI, M.Sc., (part-time)
- Vo Van TUYEN, Ph.D. (on leave)

Ph.D. students / Diploma workers

- Zoltán FEKETE, Ph.D. student
- Anita PONGRÁCZ, Ph.D. student
- Zsófia BAJI, Ph.D. student
- László GRAND, Ph.D. student
- Tamás KÁRPÁTI, M.Sc. diploma w.
- Katalin GILLEMOT, M.Sc. diploma w.
- Gergely MÁRTON, M.Sc. diploma w.
- Sydney GOIAME, M.Sc. diploma w.
- Gábor LÖVEI, B.Sc. diploma w.

Technical Staff

- Edvard BADALJÁN, engineer
- György ALTMANN, technician
- Csaba LÁZÁR, engineer
- Gabriella BIRÓ, technician
- Ákos MAJOROS, engineer
- Sándor CSARNAI, technician
- Ábel DEBRECZENY, engineer
- Magdolna ERŐS, technician
- István RÉTI, engineer
- Károlyné PÁYER, technician
- Imre SZABÓ, engineer, dr. Univ.
- Csilla FARAGÓ, technician
- Tamás SZABÓ, engineer
- János FERENCZ, engineer
- Ádám SZENDREY, engineer
- Tamás JÁSZI, engineer
- József WAIZINGER, engineer
- András LŐRINCZ, engineer
- Katalin Veresné-VÖRÖS, engineer
- Attila NAGY, technician
- Róbert HODOVÁN, engineer
- Magda VARGA, technician
- Sándor PÜSPÖKI, engineer, dr. techn, (part-t.)
- Zsuzsa PÜSPÖKI, engineer (part-t.)

The main task of the Microtechnology Department is the research, development and system integration of physical, chemical/biochemical sensors and systems:

- MEMS and MEMS related technologies, with special emphasis on development of Si MOS embedding circuits.
- Development and functional testing of different MEMS gas, chemical, 3D force, biology related sensors and sensor systems
- Development of microfluidic systems
- Development and applications of near IR light emitting diodes and detectors.
- Development of solar cells and their competitive technology.

Fundamental research on:

- sensing principles
- novel materials and nanostructures
- novel 3D fabrication techniques
- ion-solid interaction for supporting MEMS development.

Device and material characterization widely used in our projects:

- Ion beam analysis methods
- IR and Raman scattering
- Scanning Microprobes
- SEM, TEM, EDX
- Spectroscopic Ellipsometry
- Electrical characterisations

The Microtechnology Department of MFA runs the 300 sqm clean lab (Class 100-10000) with the complete Si-CMOS technology together with a mask shop. A rather new and developing large facility of the Department is the CIGS solar cell technology laboratory equipped with a pilot line of sputtering, evaporation and laser scribing modules for 30×30 cm^2 glass substrates.
The technology base of the clean lab has been further improved in the recent year. Two new technologies were introduced into our Si technology line:

- Oxford Instruments Plasmalab 100 type deep reactive ion etching system was purchased and installed in order to facilitate the works on 3D Si based MEMS devices (Fig. 1).
- Atomic layer deposition (ALD). In the frame of the CIGS solar cell project a SUNALE type ALD system was purchased from PICOSUN. By this technology the buffer ZnO layer between the TCO and CIGS layers can be deposited in a controlled way. The method can also be used in 3D MEMS technology (Fig. 2).

Figure 1 *Oxford Instruments Plasmalab 100 DRIE system installed in the clean room*

Figure 2 *PICOSUN SUNALE ALD equipment*

Chemically modified solid-state nanopores for sensing

(Supported by Hungarian Scientific Fund OTKA, NF69262)

P. Fürjes, S. Goiame (BME), A. L. Tóth, and R. E. Gyurcsányi (BME)

Sensing with chemically-modified nanopores is an emerging field that is expected to have major impact on bioanalysis and fundamental understanding of nanoscale chemical interactions down to the single-molecule level. The main strength of nanopore sensing [R. E. Gyurcsányi, TrAC-Trends in Analytical Chemistry 27 (7) (2008) 627-639] is that it implies the prospect of label-free single-molecule detection by taking advantage of the built-in transport-modulation-based amplification mechanism. Here we are presenting a line of nanopore based sensor development, including methodologies for fabrication of single and multi channel solid state nanopores with diameters ranging from 5 to 100 nm, their chemical modification and application for bio(chemical) sensing.

Solid-state single gold nanopore structures were fabricated by the combination of the silicon based 3D MEMS/NEMS technology, and special subsequent nanofabrication techniques, such as subtractive nanoscale modification of the existing microstructure by focused ion beam etching.

The various strategies and their performances in terms of size, shape and reproducibility are addressed in detail. Multichannel gold impregnated nanopore membranes were also fabricated and characterised. For interfacing the nanopore membranes special crossing microchannel structure was designed and fabricated combining the silicon 3D micromachining and PDMS (poly-dimethyl-siloxane) polymer structuring as presented in Fig. 1.

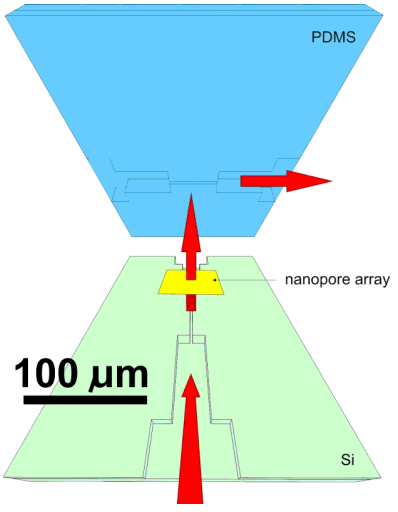

Figure 1a *Schematic view of the assembling of interfacing structure*

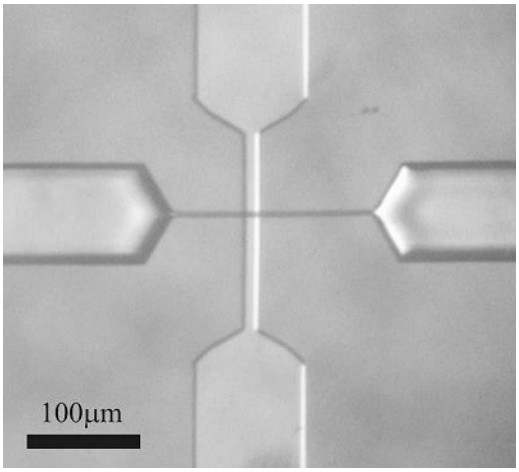

Figure 1b *Realised and sealed crossing microchannels*

To use nanopores as selective detectors their surfaces must be chemically modified. The functionalisation of the nanochannels passing through the gold layer and the method of transport-modulation-based selective molecule detection were developed by the Research Group for Technical Analytical Chemistry of the Hungarian Academy of Sciences at Budapest University of Technology and Economics.
Besides introducing specific receptors chemical modification can be also used to protect surfaces from biofouling, or to induce specific transport modulation effects. Aspects of thiol (dithiolan, disulfide) chemistries for building up self-assembled molecular architectures with molecular recognition capabilities are discussed in detail. Introducing surface charge by chemical modification in asymmetrically shaped nanopores results in current rectifying effects and diode type behaviour which was modelled by using multiphysics and coarse grained molecular modelling to allow the characterisation of self assembled monolayers formation within the nanopore. The quantitative determination of nucleic acids by peptide nucleic acid modified gold nanopores was also demonstrated (see Fig. 2 a and b).

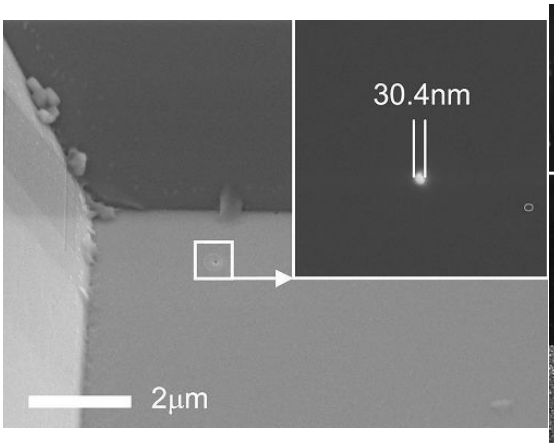

Figure 2a *Solid-state single nanopore.*

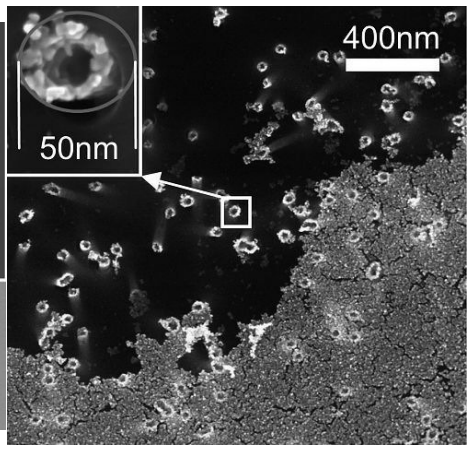

Figure 2b *Multichannel nanopore membrane*

The capabilities of nanopore based sensors in terms of detection limit are explored by using random walk simulation and multiphysics modelling. Apparently, the detection limit of single nanopore based affinity sensor is determined by the probability of a successful encounter between the nanosensor and analyte. Since a single molecule can be in principle detected by nanopore sensors the limit of detection of such sensors has also explored in terms of concentration. However, significant improvements are obtained upon directing the analyte by means of an electrical field or pressure gradient into the sensing zone of the nanopore.

Investigation of actuation phenomena and controllable moving microstructures

(Supported by Hungarian Scientific Fund (OTKA) F61583)

P. Fürjes, G. Lővei, and P. Csíkvári (BME)

Free standing, suspended 3D MEMS compatible microstructures constitute a major contribution to the actuated devices, which also can be significant elements of active micro-systems. Realisation and application of controllable moving microstructures are the milestones of development active optical or microfluidic systems.
The practicability of the actuation phenomena (electrostatic, magnetic, thermal) and the predictability of functional parameters of the designed structures (deformation, driving frequency, residual stresses of the layer structures) were analysed by Finite Element Modelling as presented in Fig. 1. Test structures were manufactured by development and application of the adequate MEMS techniques, as bulk and surface silicon micromachining, respectively, and analysed considering the functional aspects.
Micromachined suspended membranes (Fig. 2) utilising the capacitive sensing or electrostatic actuation phenomena can be basic components of numerous sensors and actuator structures, e.g. as photo-acoustic gas detectors or micro-mirror arrays respectively. The most frequently used structural materials are polycrystalline and crystalline silicon, silicon-nitride, silicon-dioxide and multilayered combination of these materials. Minimisation of the residual stress and initial deformation of the structured membranes is a crucial object of the realisation. In preferential applications additional metal layers are deposited on the top of the membrane as reflective material.

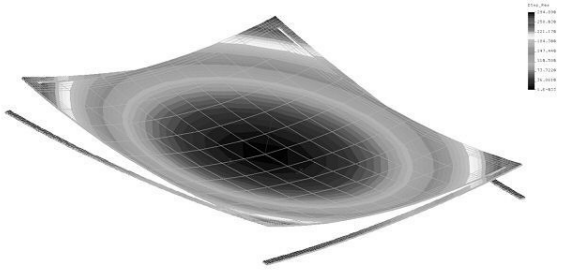

Figure 1 *Finite Element Modeling of a thermally actuated microfluidic valve.*

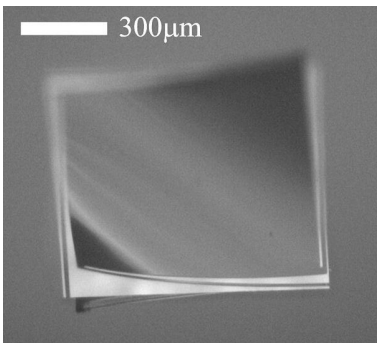

Figure 2 *Deformed multilayer cantilever structure*

Smart microfluidic devices are built up with active elements, typically heaters, sensors of various type and valves containing moving components for injection or facilitating the fluid flow in the required direction or in the reactor micro-vessel.
The developed multi-channel structure demonstrates the combination of porous silicon MEMS technology and structured PDMS formation facilitating the integrated

manufacturing of active devices and the interfacing channel system, respectively. The active part of the 3D MEMS structure was manufactured by silicon bulk micromachining applying platinum microheaters embedded in CVD deposited layer structure. The microchannels were formed by porous silicon micromachining and PDMS formation. Fig. 3 shows the manufactured valve structure. The complex micro-fluidic system is developed for intelligent fluid control in multi-parameter analysis platforms.

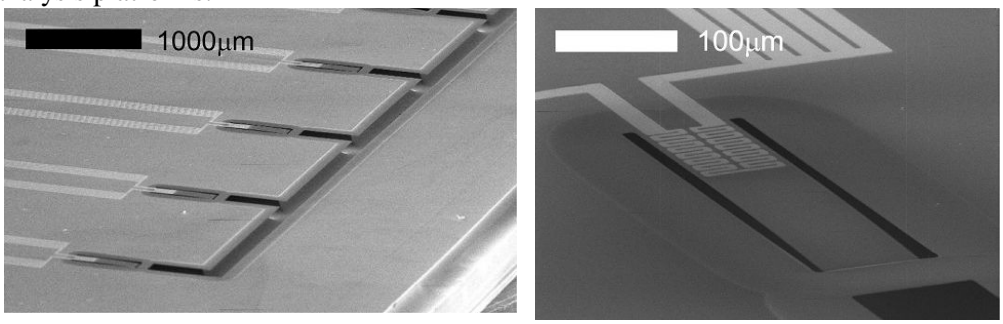

Figure 3 *Micro-fluidic multi-channel system (left), and with thermally actuated control valves (right)*

Characterisation of thermo-mechanical properties of structural materials of MEMS

(Supported by Hungarian Scientific Fund (OTKA) F61583)

P. Fürjes, and P. Csíkvári (BME)

Micro-heaters are basic components of sensors and lab on a chip devices, e.g. as sensors of calorimetric principle, or heaters in chemical micro-reactors. The most frequently used structural materials are silicon-nitride, non-stoichiometric silicon-nitride, silicon-oxinitride, silicon-dioxide and multilayered combination of these materials.

In the micro-heater design the most important parameters to be considered are the thermal conductivity, the thermal capacitance, linear expansion and the residual stress in the applied layers in order to select the optimum functionality of the device. While appropriate data are available for the widely used materials (SiO_2, Si_3N_4) this is far not being the case for the non-stoichiometric materials or deposited poly-crystalline silicon, diamond and DLC layers. Their properties are process dependent, i.e. both their composition and structure are determined by the given individual process. The thermo-mechanical properties were extensively analysed for proper prognostication of the functional parameters and behaviour of the active elements of the microstructures. Non-stoichiometric silicon-nitride and MWCVD diamond layers

were used for reliable micro-machined hotplates in order to provide effective chemical and mechanical protection of the MEMS elements as presented in Figs. 1-2.

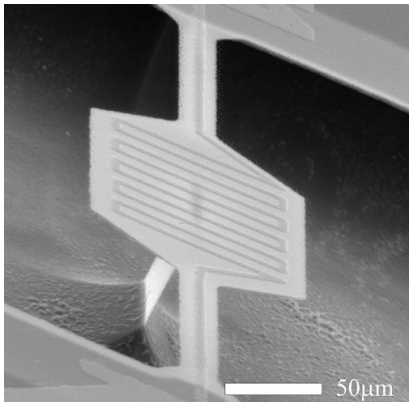

Figure 1 *Silicon-nitride based micro-filament heater as basic element of a calorimetric type sensor.*

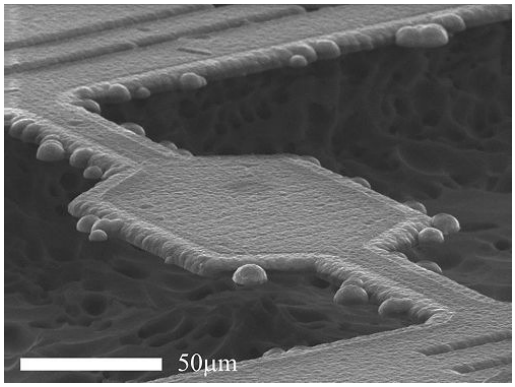

Figure 2 *UltraNano Crystalline Diamond layer forming the micro-hotplate deposited by SAD technique*

Alternative structures were applied to determine the thermal parameters of CVD layers by comparison the results of thermal measurements and FEM simulations. By fitting the parameters applied for calculations, the static and dynamic behaviour of the model structure was synchronised to the experimental results to extract physical properties of the structural materials.
The proposed method provides uncomplicated and reliable determination of thermal parameters without fabrication of complex test structures. Therefore, it facilitates both structure design and material characterisation by using the functional MEMS devices.

Si micro-turbine by proton beam writing and porous silicon micromachining

(Supported by Hungarian Scientific Fund (OTKA) T047002)

P. Fürjes, Cs. Dücső, Z. Fekete, and I. Rajta (ATOMKI, Debrecen)

Integrated microfluidic elements are essential components of lab-on-a-chip devices. The complexity of such devices depends on their application and covers a wide range from simple mixers composed of just a few passive elements: e.g. opened or embedded channels, cavities, up to miniaturised chemical reactors or sample feeding/pumping systems composed of additional active components as well. These MEMS with complex functions are preferably formed from Si or combination of Si and other materials.

The most promising technique for the formation of high aspect ratio, vertically positioned, actuated or moving structures in the recessed channel is the DRIE (Deep Reactive Ion Etching). In the last few years proton beam writing in combination with porous silicon processing has been proposed by a few research groups for formation of fixed high aspect ratio 3D Si structures. Our group has demonstrated the capability of this technique for formation of vertically positioned mobile elements by fabricating a silicon micro-turbine. This work was the first demonstration of a silicon device containing a moving part made by proton beam writing. The operation of the encapsulated device fabricated is successfully demonstrated (Figs. 1-2).

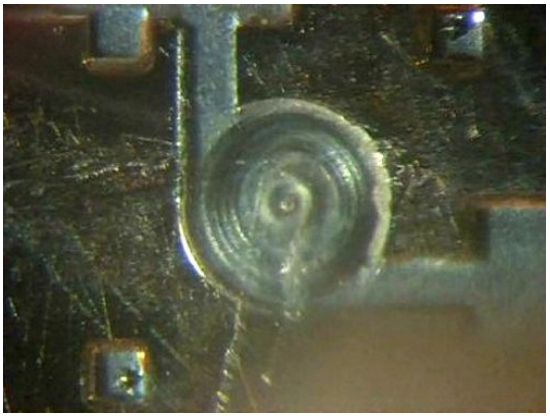

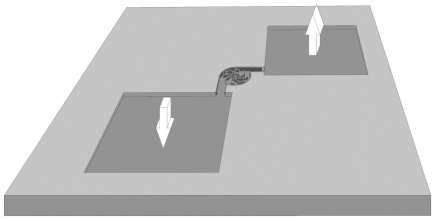

Figure 1 *The schematic structure of the micro-turbine Si chip*

Figure 2 *Photograph of the rotating micro-turbine. Here you can see the turbine in action*: http://iba.atomki.hu/video/

3D Si micro-turbine characterised by vertical walls of high aspect ratio was formed by combination of proton beam writing (PBW) technique and subsequent selective porous Si (PS) etching. Crystal damages generated by the implanted protons result in increased resistivity, thereby limit or even cease the current flow through the implanted area during electrochemical etching. Characteristic feature of the proposed process is that the shape of the micro electro-mechanical (MEMS) components are defined by two implantation energies, i.e. a higher energy is applied for defining the frame of the device while the lower energy is used to write the moving components. The implantation energies were selected such as to result appropriate difference between the two projection ranges, taking into consideration the thickness of the walls of the moving component and the isotropic etching profile of the electrochemical PS formation. The electrochemical etching is led until the sacrificial PS layer completely under-etches the moving components but the etching front does not reach the bottom of the frame. Therefore, the dissolution of PS results in a ready-to-operation device with a released moving component embedded in the cavity as shown in Figs. 3-4.

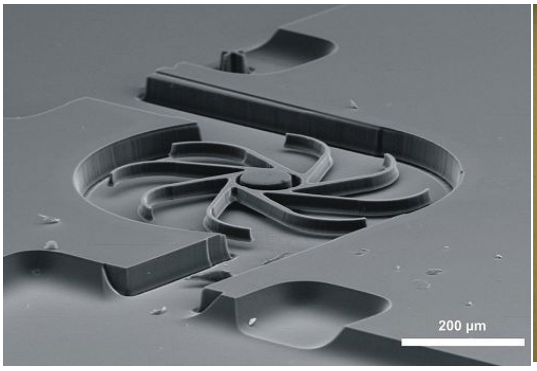

Figure 3 *Crystalline silicon micro-turbine developed by the combination of PBW and subsequent Porous Silicon formation.*

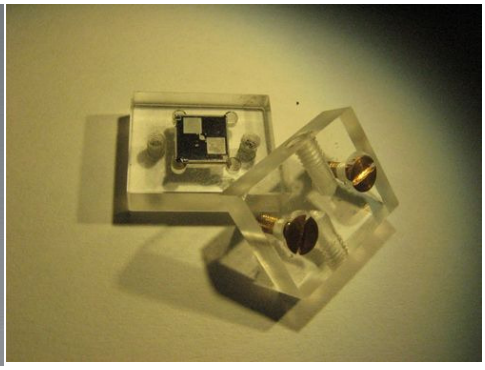

Figure 4 *Plastic housing of the micro-turbine chip*

However, the proposed combined technology has been successfully used for realisation of microfluidic MEMS components, an inherent disadvantageous property of ion scattering in the end-of-range region is still a great issue, since the widening geometry caused by the presence of Bragg-peak limits the perfect functionality of the designed microstructures. The phenomena at the end-of-range volume and the effects on the realisation of micro-components by PBW and subsequent PorSi etching were analysed by both experimental and simulation (MatLab, Comsol) results. A MEMS process sequence enabling the elimination of widening at the bottom of the microstructures was developed. The elaborated technology provides a complete removal of the disadvantageous volume without any preliminary requirement for changes in geometric design as presented in Fig. 5.

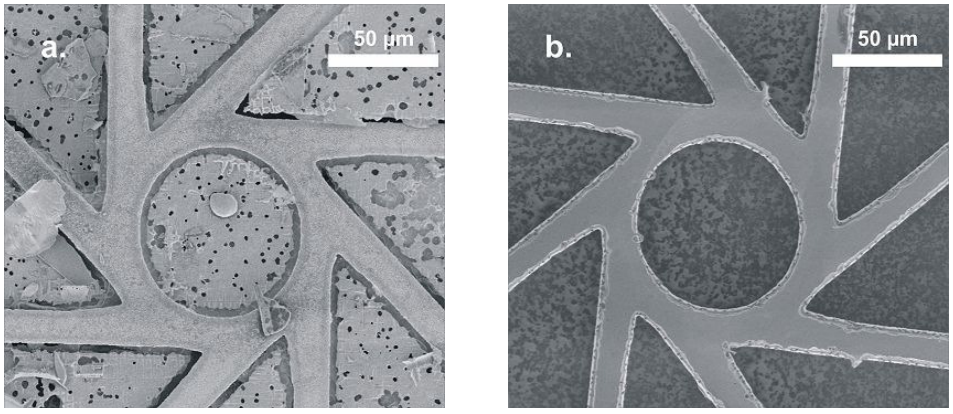

Figure 5 *The plan-parallel and suitably smooth top (a) and bottom (b) surface of the micro-turbine realised. (SEM view)*

As a result, the beneficial properties of the combined technique can exploited more effectively and less compromise is necessary to make during the realisation of complex 3D silicon microstructures

Hard coating of mobile 3D silicon microstructures

(Supported by Hungarian Scientific Fund (OTKA) T047002)

P. Fürjes, and Z. Fekete

The growing need for MEMS of complex structure and function requires continuous development of novel processing techniques as well as application of materials with tailored properties. Recently, the technological evolution led to the fabrication of MEMS with embedded mobile elements, such as micromotors, microgears, microengines. Mechanical degradation (Fig. 1) of mobile components of complex micro electromechanical systems (MEMS) reduces device reliability and operation time. Although the considerable abrasion of the surface micromachined poly-crystalline or metallic elements can be reduced by substitution of their crystalline silicon equivalent, there is still room for further improvement in device durability.
The significant wear rate of the most commonly used crystalline-Si and poly-Si initiated extensive research in development and adaptation of hard coating techniques for increased life-time. In view of the required function conformal coverage, good homogeneity, hardness, low coefficient of friction and wear rate in combination with small internal stress and surface roughness are the essential parameters. One of the greatest challenges is the deposition of the appropriate coating material on microstructures of high aspect ratio and vertical sidewalls. Beside conventional materials, like Si_3N_4, SiC, DLC or TiN, nanocomposites and multilayers has also been investigated to improve tribological properties.

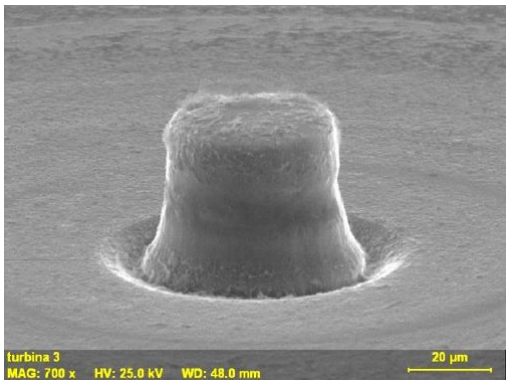

Figure 1 *The degradation of the planar surfaces of the microturbine-pit and the vertical wall of the axle.*

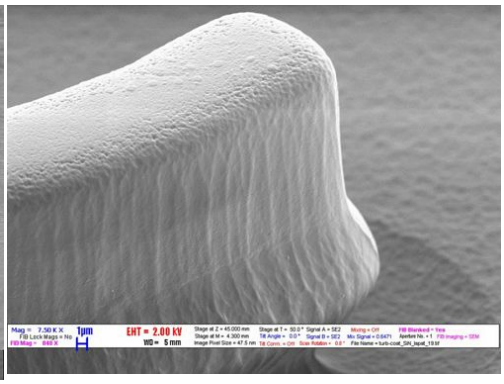

Figure 2 *Conformity of the selected SiN_x coating are shown by the coverage of the high aspect ratio turbine wing.*

The LPCVD Si_3N_4 process was successfully integrated in a MEMS fabrication sequence. The demonstration device was the recently presented 3D crystalline silicon micro-turbine formed by the combination of proton beam writing (PBW) and subsequent selective porous silicon (PorSi) etching. The 3D silicon components were uniformly covered with LPCVD Si_3N_4 protective layer. The Si_3N_4 coating improves

the chemical and mechanical properties; strength, hardness and chemical resistance. The elaborated processing technology can easily be adapted for deposition of protective materials of superior properties, e.g. TiN and diamond-like carbon (DLC).
Beside ALD technique the low pressure CVD method is known to provide the best conformity as presented in Fig. 2. The advantageous effect of the Si_3N_4 thin film on the life-time of friction at 3D structure was demonstrated. Detailed analysis of step coverage, conformity, hardness, elastic modulus and fracture toughness as well as the effect device in wear rate measurements demonstrates the feasibility of the proposed process.

Epitaxial cubic SiC nanocrystals on Si

A. Pongrácz, D. Beke, and G. Battistig

Epitaxial formation of SiC nanocrystals on single crystal silicon surfaces by a simple and cheap reactive annealing in CO has been discovered and patented by BME AFT and MTA MFA. We have investigated the CO diffusion and SiC nanocrystal (NC) formation on different silicon based systems after 100% CO treatment at elevated temperatures (T >1000°C).
It has been shown that epitaxial and void-free 3C-SiC NCs can be formed at the Si side of a SiO_2/Si interface. Based on experiments in isotopically labelled $^{13}C^{18}O$ gases we have found that ^{13}C and ^{18}O accumulates at the SiO_2/Si interface at 1100 °C. The amount of ^{13}C is proportional to CO gas pressure and the annealing time. These results have been proved experimentally by isotopic tracing using SIMS and NRA.

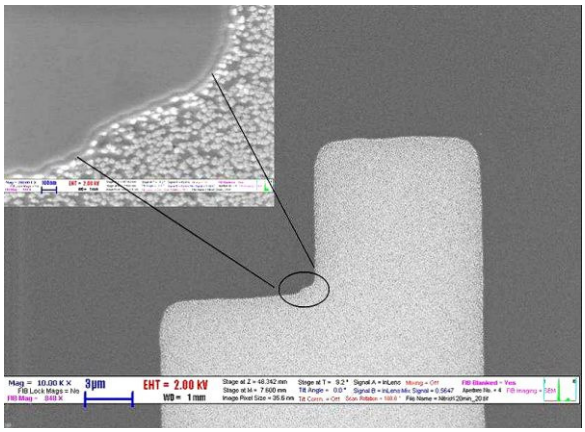

Figure 1 *Selective SiC NC growth can be achieved by applying Si_3N_4 layer as a diffusion barrier. The sample was heat treated in 10^5 Pa CO at 1100 °C for 2 hours. Before the SEM investigation Si_3N_4 (grey area) and SiO_2 (white area) layers have been removed in HF. SiC NCs can be seen on the area which was covered by SiO_2, while nitride acted as a masking layer.*

The first step to form SiC NCs on the Si side of the SiO_2/Si interface is the diffusion of CO through the thermally grown silica. Applying a Si_3N_4 capping layer as a diffusion barrier, CO diffusion can be hindered so well that no SiC can be formed at the interface. Fig. 1 shows the masking property of a 20 nm thick Si_3N_4 layer against CO diffusion at 1100 °C for 8 hours. No SiC NCs can be observed after removing the nitride in HF.

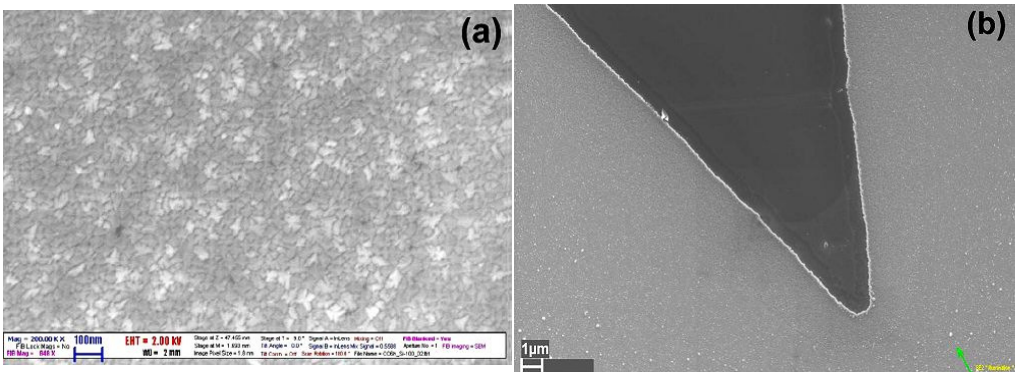

Figure 2 *(a) Plan view SEM image of a nanocrystalline SiC layer grown by reactive CO annealing of a Si(100)/SiO_2 structure at 1100 °C for 6 hours.*

(b) Selective growth of SiC nanocrystalline layer by applying a Si_3N_4 layer as diffusion barrier. The darker area was covered by Si_3N_4 while the lighter area was covered by SiO_2 during the CO annealing. SEM image was taken after the removal of both Si_3N_4 and SiO_2.

A continuous polycrystalline SiC layer formation as protective coating can have a great interest in harsh environment MEMS applications. By optimising the annealing time a continuous, approximately 25 nm thick polycrystalline SiC layer can be formed. Fig. 2 (a) shows the structure of the polycrystalline SiC layer, while Fig. 2 (b) shows the selective growth of the SiC layer.

A 3D-RBS study of ordered nanosystems prepared by ion irradiated nanoparticulate masks

Z. Zolnai, A. Deák, N. Nagy, A. L. Tóth, E. Kótai, and G. Battistig

The emergence of nanotechnology leads to the production of 3D objects having submicron size on both the depth and lateral scale. Besides the fabrication of such systems there are continuous efforts to find suitable characterisation tools for their investigation. We have shown that conventional Rutherford Backscattering Spectrometry (RBS) supported by the enhanced data analysis capabilities of the RBS-MAST spectrum simulation code is a suitable technique to provide 3D information on the shape, size and atomic composition of ordered nano-objects, moreover, geometrical changes of the system can be followed as well.

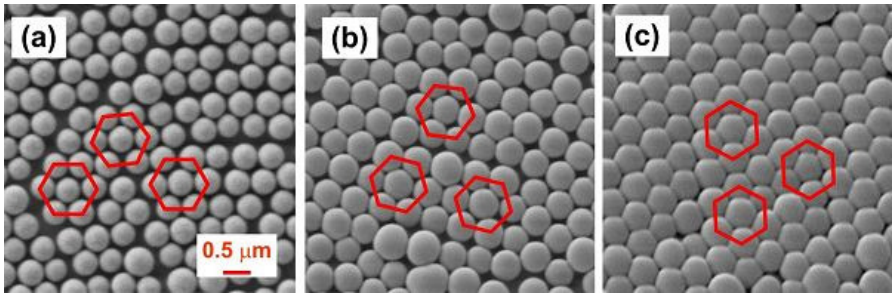

Figure 1 *SEM micrographs of a colloidal nanomask of hexagonally arranged silica particles deposited on Si substrate: (a) unirradiated monolayer of spheres with diameter of 450 nm, similar layers irradiated with (b) 6×10^{15} Xe^{2+}/cm^2 and (c) 1.2×10^{16} Xe^{2+}/cm^2, respectively. Transformation from spherical to oblate ellipsoidal shape occurs under the ion bombardment.*

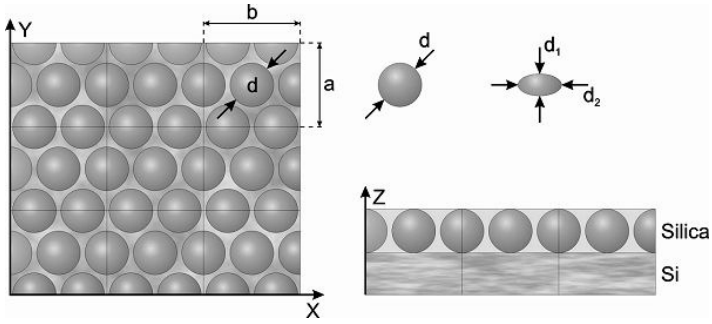

Figure 2 *The 3D model cell of the hexagonally ordered silica monolayer/Si substrate system as used in the RBS-MAST spectrum simulation program. The cell parameters, a, and b, and the sphere diameter d (for unirradiated case), or the longitudinal and transverse diameters, d_1 and d_2 (for irradiated case), of the ellipsoidal particles can be varied to fit the measured data.*

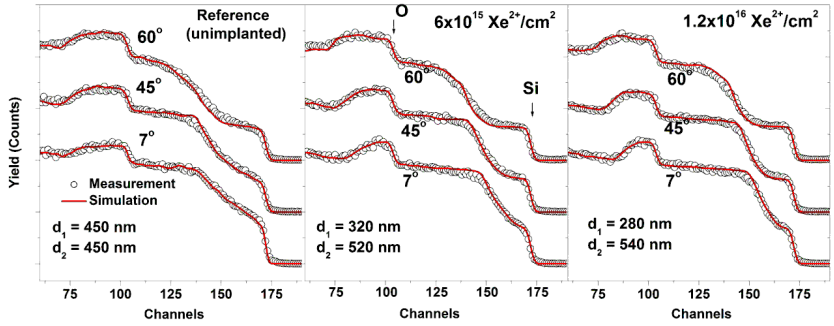

Figure 3 *Measured and simulated 2 MeV He RBS spectra of colloidal silica nanoparticulate masks. The corresponding SEM micrographs can be seen on Fig. 1. Experiments at different measurement geometries, i.e. sample tilt angles of 7°, 45°, and 60°, with respect to the analysing He beam, provide 3D geometrical information on submicron scale. The particle diameters fitted with RBS-MAST are represented, and they are in good agreement with the results of SEM analysis.*

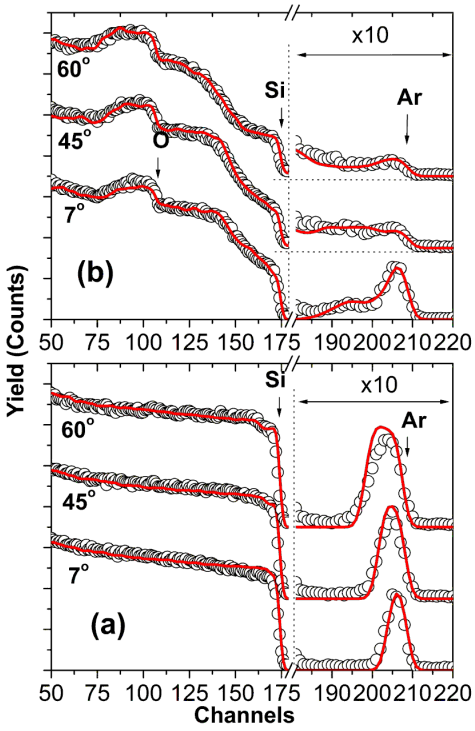

Figure 4 *Measured and simulated RBS spectra of a colloidal silica nanomask/Si substrate system irradiated with 40 keV Ar^+ ions. The two panels show the spectra recorded on the same sample when the colloidal silica monolayer (a) was, and (b) was not removed from the Si substrate.*

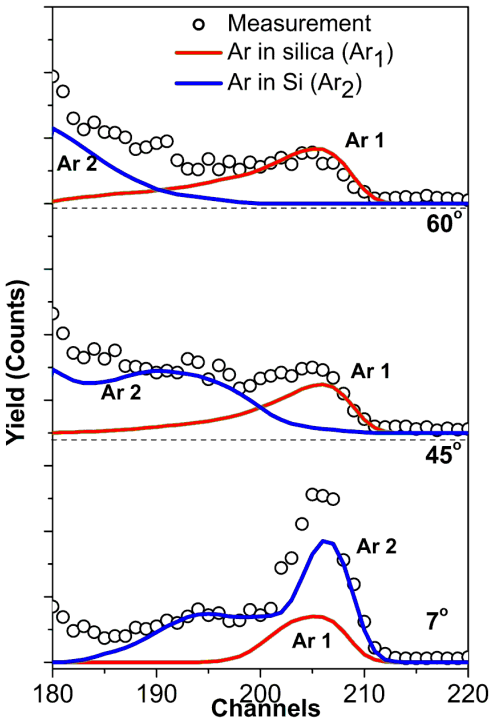

Figure 5 *The two Ar components of the simulated RBS spectra shown in Fig. 4(b). The height and shape of spectrum Ar2 show drastical change with tilting the sample off from 7° because the view of the Ar atoms buried in the Si substrate is determined by the 3D nanostructure of the system (see Fig. 6).*

Figure 6 *Schematic picture of the 3D model cell of the Ar^+ irradiated sample as used in RBS-MAST simulations. In this case significant deformation of the spherical particle shape does not occur during the irradiation process. The Ar atoms are distributed in the upper shells of the nanospheres and in the unmasked regions of the Si substarate.*

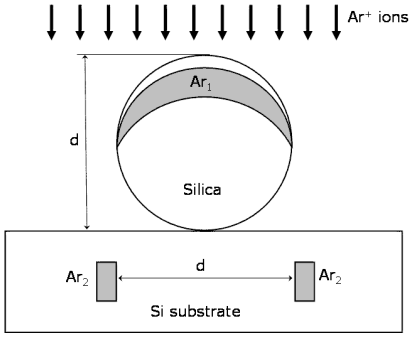

A monolayer of hexagonally packed colloidal silica nanospheres with diameter of less than 1 μm and with uniform size distribution (ca. ±7%) is an ideal system to be investigated. Even so the size of the analysing beam is as large as 500 μm × 500 μm

in an RBS experiment, the local nature of the individual He ion trajectories makes it possible to extract information on the dimensions of only one unit cell containing a single nano-object and its first neighbour environment. Fig. 1 shows a monolayer of silica nanoparticles before and after irradiation with Xe^{2+} ions. The ion-nanoparticle interactions lead to an anisotropic shaping effect. In this case spherical silica colloids contract parallel to the ion beam and expand perpendicular to the ion beam thus changing their shape to oblate ellipsoidal. As Figs. 2-3 show, building up an appropriate 3D model cell with variable geometrical parameters the measured RBS spectra - showing the anisotropic deformation process in function of the Xe^{2+} fluence - can be followed with the simulation. The results extracted for the transverse particle diameters in Fig. 3 are in good agreement with SEM observations.
We have shown that even more complicated systems can be described in 3D. A sample shown in Fig. 1(a) was irradiated with 40 keV Ar^{+} ions perpendicular to the Si surface. Here anisotropic deformation of the nanospheres does not occur, and the Ar ions are distributed in 3D spherical shells (in the silica mask) and in buried planar areas with lateral dimensions of ca. 100 nm (in the Si substrate). As Figs. 4-6 show, not only the geometry of the system but also the different Ar components can be determined by RBS when applying different sample tilt angles.
Note that regular nanopatterns with special properties on the Si surface can be observed after irradiation with Xe^{2+} or Ar^{+} ions through ordered silica nanomasks. For details, please, see in this yearbook: Various nanostructures on macroscopically large areas prepared by tuneable ion-swelling.

Charge injection and storage in semiconductor nanocrystals embedded in dielectrics

P. Basa, and Z. J. Horváth

Semiconductor nanocrystals (NCs) are widely studied for non-volatile memory purposes. During this year our activity in this field was devoted to study the influence of the varying distance between the layer containing Si nanocrystals and the Si substrate on the charge injection and storage. The layer structure of the examined samples is shown in Table 1. These thicknesses were determined by evaluation of spectroscopic ellipsometry measurements. The total layer thickness of the samples was chosen to be equal, while the vertical position of the layer with NCs was varying (note, that an additional reference sample with no NCs was also prepared). Characteristic cross-sectional transmission electron microscopy (XTEM) image of Sample AR15 is shown in Fig. 1. The XTEM study confirmed the thicknesses obtained by ellipsometry and verified the existence of NCs in the layer.
The memory window width of the examined samples as a function of programming voltage pulse amplitude is shown in Fig. 2. The results show that the memory window width increases if the NC-substrate distance decreases. It is in good agreement with the physical picture that significant part of the injected charge is stored in the NCs,

which causes the memory window to increase with decreasing bottom layer thickness. In case of Sample TR49 (reference), only the nitride traps store the charge, with charge centred at a distance between 5 and 10 nm (measured from the substrate), and that is why the curve corresponding to Sample TR49 is between AR10 and AR05 in Figs. 2-3 show the amount of injected charge as a function of the programming voltage pulse amplitude. Based on this figure, it is apparent that the most efficient charge tunnelling mechanism takes place in the case of AR05 (it stores very large injected charge at very low voltages).

	AR05	AR10	AR15	TR49
Thickness of bottom layer (nm)	4	10	15	52
Thickness of layer with NCs (nm)	3	3	3	
Thickness of top layer (nm)	44	37	33	

Table 1 *Layer structure of the examined samples*

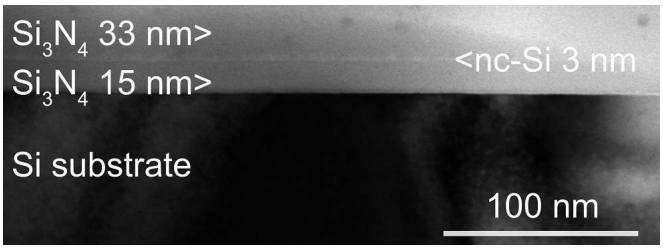

Figure 1 *Characteristic XTEM image of Sample AR15*

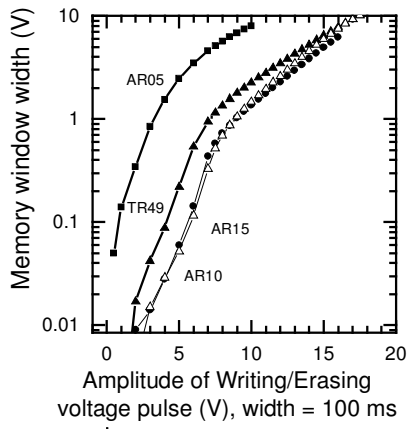

Figure 2 *Memory window width of the examined samples as a function of programming voltage pulse amplitude*

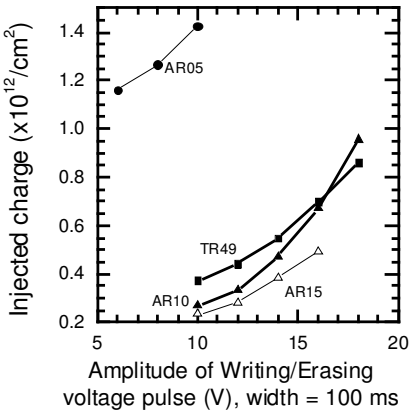

Figure 3. *Injected charge of the examined samples as a function of programming voltage pulse amplitude*

Integrated calorimetric gas sensors

M. Ádám, and P. Fürjes

Immediate detection of combustive gases and organic vapours below the Lower Explosion Limit (LEL) is essential for alarming both in public and industrial environment, where the risk of developing explosive gas mixture continuously exists. The typical concentration range to be detected is between 0.1 and 3 v% in air for different gases and vapours, however, the sensor must also be able to operate safely if the concentration exceeds the LEL value. Solid state gas sensors of various operation principles can be used in alarming systems. H_2 is detected by Pd gate FET and Pd resistor in the ppm and volume percent range respectively, while conductivity type sensors can be sensitised for detection of low concentration H_2, CH_4 or CO. Nevertheless, most of the available devices exploit the calorimetric effect by measuring the variation of heat conductivity or the heat generated by catalytic combustion.

Integral microhotplate structures with a power dissipation of 18 mW at 550 °C were formed by front side porous Si micromachining technique as presented in Fig. 1. The suspended Pt heaters embedded in low stress non-stoichiometric silicon-nitride show 2000 ppm/°C thermal coefficient, thereby providing high sensitivity of the device. Due to the low thermal mass and excellent thermal isolation the bare microhotplate can be heated up to the operation temperature within 3 ms.

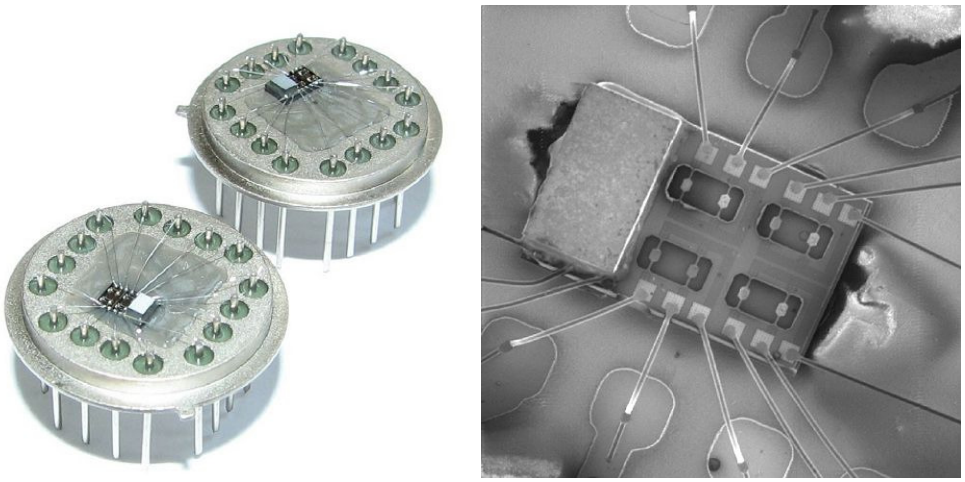

Figure 1 *Mounted chips for olfactory detection of explosives. (left) The three micropellistors are complemented with a heat conductive device. (right) Chip size: 2×3mm.*

Two of the key issues of the development of catalytic combustion type sensors were analysed: the selection and production of active catalytic particles (RuO_2, Rh, Pd, Pt,

Co_3O_4, as well as their mixtures) on the micropellistor surface as well as the realisation of a reliable thermal conduction between heater element and catalytic surface for sensing the temperature increase produced by the combustion. In order to form a reproducible heat contact on the filament, and to improve the long term stability, while maintaining a relatively large specific surface for catalyst support, a novel process sequence was implemented applying thin film deposition and electrochemical forming of the alumina porous matrix.

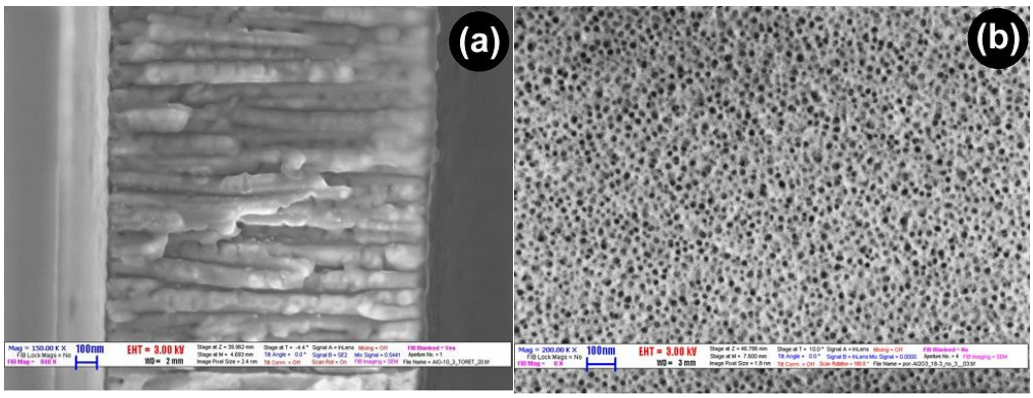

Figure 2 *Thin-film alumina porous matrix with well aligned mesopores (a), and after widening of the uniformly distributed pores by etching in phosphoric acid (b).*

IR luminescence of CdS thin films

V. Rakovics

CdS is an n-type heterojunction partner of p-type CdTe or $CuIn(Ga)Se_2$ absorber layer in polycrystalline heterostructure solar cells. The best solar cells based on $Cu(InGa)Se_2$ (CIGS) absorbers are achieved by using a very thin (50 nm) CdS buffer layer deposited by chemical bath deposition (CBD) [M.A. Contreras et al., Prog. Photovolt. 7 (1999) 311]. The conductivity of the CdS window layer has to be optimised in order to achieve high efficiency of the devices. It is well known that the conductivity of the CdS films is sensitive to heat treatment [U.S. Jadhav et al., Materials Chemistry and Physics 69 (2001) 125]. At moderate temperature the heat treatment in air increase the conductivity and photosensitivity of the layers, but above 200 °C the dark conductivity starts to decrease.

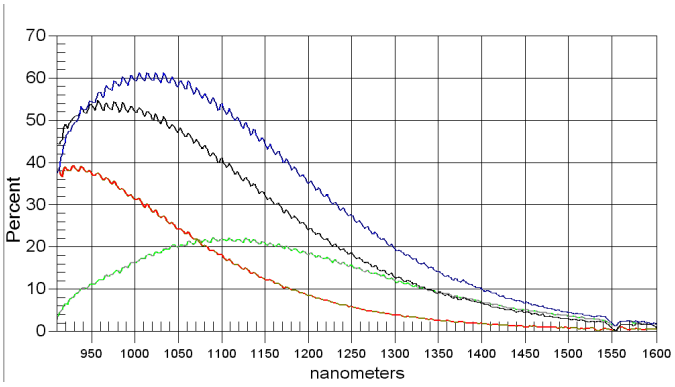

Figure 1 *IR PL spectra of CBD CdS Cu^{2+} doped samples. Peak positions shift to longer wavelengths as the doping level increases.*

Separate measurement of the conductivity of the layers in the multilayer structures is very difficult, but the change of optical absorption or photoluminescence spectra can indicate the impurity levels of the layers. High intensity infrared luminescence shows acceptor like deep levels, which compensate the electron concentration and decrease the conductivity of the n-type CdS layers.

CdS thin films prepared by chemical bath deposition have been characterised by infrared (IR) luminescence, optical transmission, and photoconductive response measurements. The conductivity of polycrystalline CdS thin films is strongly influenced by interface related defects. Broad room temperature IR luminescence peaks have been found in highly photoconductive CdS thin films. There was a strong correlation between the intensity of the IR luminescent peaks and the photoconductivity of the CdS layers. Dark conductivity of the CdS layers can be increased by heating the samples in air and decreased in forming gas. The heat treatment of Cu doped CdS films results higher photoconductivity and smaller dark conductivity. Fig. 1 shows the infrared luminescence spectra of Cu^{2+} doped and heat treated CdS films. The luminescence peak for photosensitive CdS films shifts to longer wavelengths as the doping level increases.

Optimum design of InGaAsP/InP surface emitting LEDs for application in spectroscopy

V. Rakovics, S. Püspöki, and I. Réti

The peak of emission spectra of InGaAsP/InP IR diodes can be tuned by changing the composition of InGaAsP active layer lattice matched to InP (Fig. 1).

InGaAsP/InP LED sources emitting at 920-1680 nm wavelength have high optical brightness compared to traditional lamps. Near parallel and narrow beam can be obtained by application of small lenses if the device emitting area is small.

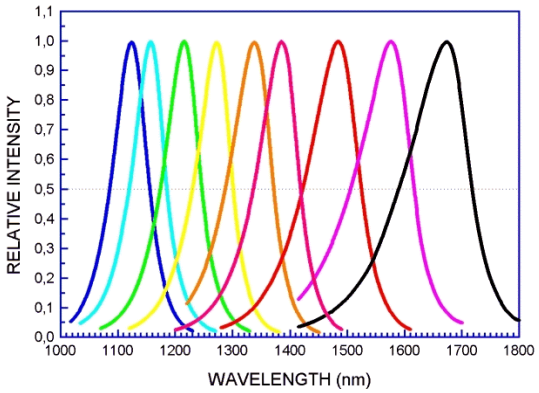

Figure 1 *Normalised intensity spectra of nine different InGaAsP/InP LEDs emitting in the 1000-1700 nm wavelength range.*

Unfortunately the efficiency and the spectrum of the devices are sensitive to the change of current density and temperature. For spectroscopic application the spectral stability of LEDs is the most important factor. Our main goal was to optimise the chip construction in order to decrease the current heating effect.

Sample preparation: InGaAsP/InP double heterostructure IR emitting diodes were prepared by Liquid Phase Epitaxy (LPE). The chip construction can be seen in Fig. 2. Surface emitting broad area and oxide defined chips were prepared after metallization of the wafers.

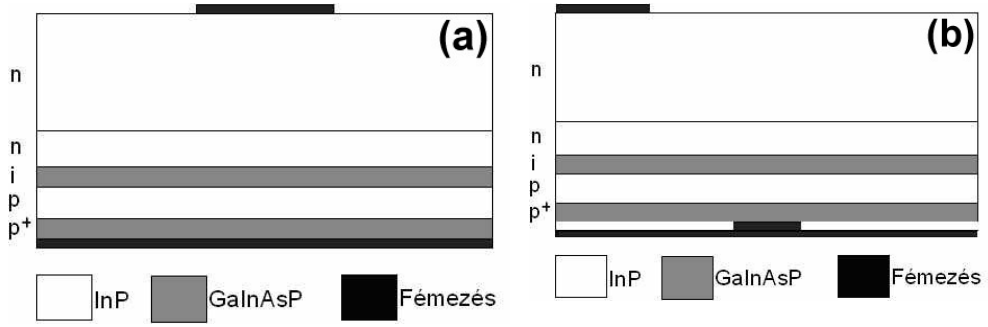

Figure 2 *Schematic cross section of InGaAsP/InP double heterostructure LEDs (a) 300 μm × 300 μm rectangular active area (b) oxide defined circular active area.*

Observations regarding the temperature sensitivity and power saturation of InGaAsP lasers and light emitting diodes (LED's) have led to extensive studies to find the responsible mechanisms [A. Sugimura, IEEE Journal of Quantum Electronics, 17 (1981) 441 – 444, and L. C. Chiu et al, IEEE Journal of Quantum Electronics QE-19 (1983) 1335-1338]. As a result of current heating, the junction temperature increase in CW operation, and the emitted power saturate at a certain current. The light-current curves are not linear even in short pulse operation.

We prepared and investigated nine different wavelength InGaAsP/InP surface emitting double heterostructure LEDs (Fig. 1). Silicon oxide defined different area diodes were prepared (Fig. 2). The doping level in the p-InP confining layer was fixed

in order to keep the magnitude of the leakage current. Optical power and spectral characteristics of the diodes were investigated as a function of driving current and case temperature. The output power saturation and the temperature sensitivity of the diodes depend on the composition of the active layer. At high driving current densities the band-to-band Auger recombination greatly affects the radiance saturation in InGaAsP/InP LED's. In pulse operation, the maximum output power of small area LED's is proportional to the volume of the active layer.
In case of broad area diodes (Figs. 3-4) the output power saturation tarts at the short wavelength side of the emission spectra. The position of intensity maximum is shifted towards longer wavelengths. The intensity at the peak wavelength is gradually decreases. The intensity in the longest wavelength region increases while the output

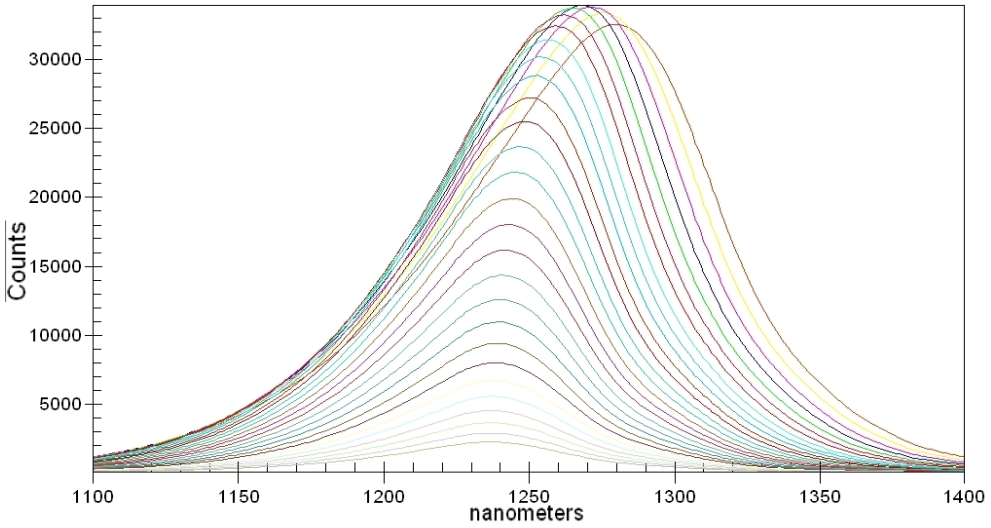

Figure 3 *Intensity spectra of a typical surface emitting LED at different operating current (20-400 mA QCW) and at fixed case temperature.*

power saturates. Realising an optimum design of current density and heat resistivity of the chip, high brightness and spectral stability can be obtained. Current heating induced red shift can be compensated by the blue shift caused by band filling at high current densities (Fig. 5).

The output power saturation is dominated by current heating in CW operation mode. Optimal chip design and packaging can help to reduce the current heating effect. Long wavelength diodes are more sensitive to current heating. Investigation of the LED spectra helps to find the optimum construction and operating conditions.

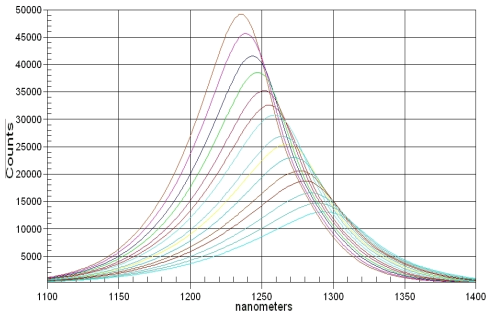

Figure 4 *Intensity spectra of a typical surface emitting LED at various temperatures (30-170 ^{o}C) and at fixed driving current.*

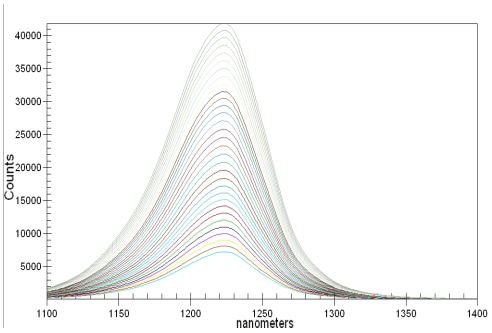

Figure 5 *LED spectra at 40-400 mA QCW driving currents. The device is optimised for use in food spectroscopy. Chip size: 500 μm x 500 μm. The circular (d= 100 μm) oxide defined active region is in the middle of the chip.*

Sensors for automotive applications

(Supported by ENIAC JU project - SE2A, No: 12009)

G. Battistig, A. Pongrácz, A. Nagy, and P. Fürjes

A large project called SE2A has started in 2009 in the frame of the European ENIAC-JU call. The main aim of the project is to develop new sensors, sensor systems, the architecture of active vehicle control systems and the corresponding technologies in order to increase the safety of the vehicle on the road, to increase the fuel efficiency and to decrease the emission of the engines of the cars of the near future.
Main objectives of the development at MFA:

- True ground speed determination by tyre integrated 3D vectorial force sensor – MEMS device development
- Full membrane force sensor – mechanical optimisation, new design
- Technology development: introduce deep reactive ion etching into MFA's MEMS technology in order to form 3D Si structures with perpendicular walls and high aspect ratio
- Device and system optimisation
- Other sensor developments for NO_x, combustible gases, pressure, contactless temperature, airflow, fuel quality, etc.
- New sensor disciplines and realizations by MEMS technology
- Investigation of the thermal properties of the packed device
- Installation of test structures, devices and systems in a test vehicle, verification of 3D force sensor and microwave based true ground speed measuring methods

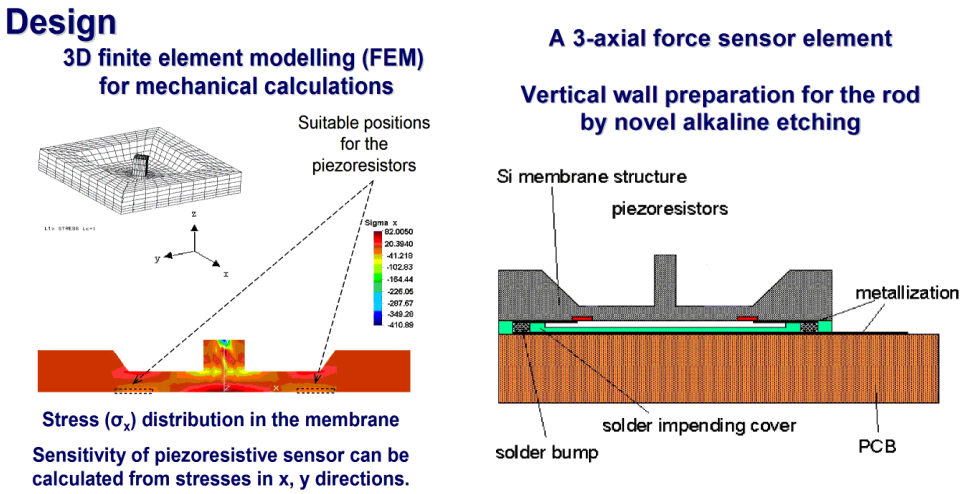

Figure 1 *The full membrane type 3D force sensor is planned to integrate into a tyre and monitor continuously the deformation of the tyre. The deformation reveals the forces acting between the tyre and the road surface.*

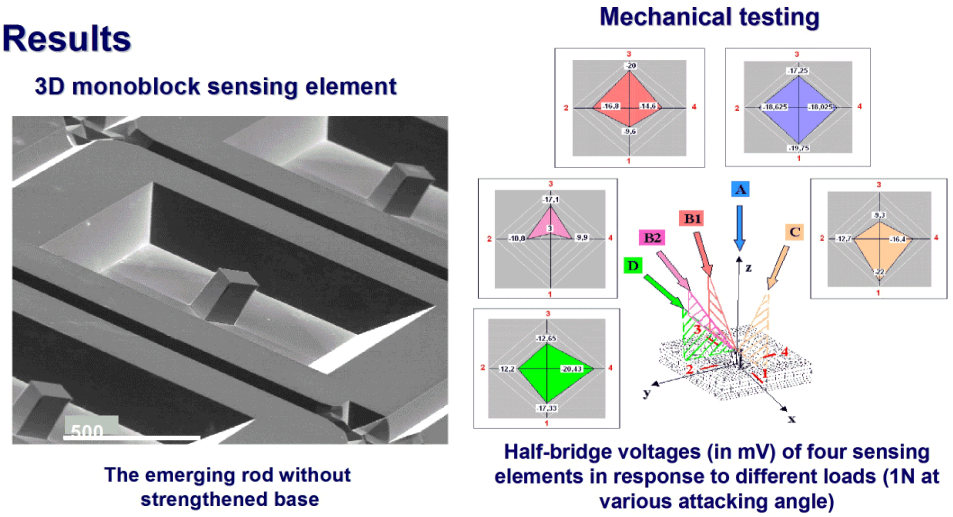

Figure 2 *The deformation revealed information is sent to the active vehicle control system where the actual vectorial velocity of the vehicle is calculated.*

The full membrane type 3D force sensor is planned to integrate into a tyre and monitor continuously the deformation of the tyre (Fig. 1). The deformation reveals the forces acting between the tyre and the road surface. This information is sent to the active vehicle control system where the actual vectorial velocity of the vehicle is calculated (Fig. 2). The vectorial force sensor is planned to integrate onto the internal wall of the tyre. A crucial question is to find the right place in the tyre wall where the

sensor should be fixed. Mechanical simulations are run in order to model the mechanical properties and the deformations of a loaded rotating tyre.

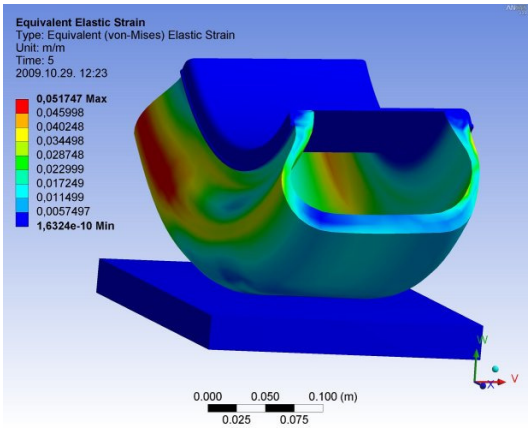

Figure 3 *Mechanical simulations of the deformations of a loaded and rotating tyre.*

A new design of the full-membrane vectorial force sensor is needed as the forces attacking the Si MEMS sensor element could be rather high. The force range of the new sensor is calculated to be 2-5 N at maximum.
The proper packaging of the sensor, the method of its integration into the tyre and the commun┬ication between the sensor element and the active vehicle control system is also considered.

Sensors for Terahertz imaging

Supported by Hungarian Scientific Fund (OTKA) CNK 77843

B. Szentpáli, P. Basa, and G. Battistig

The aim of this starting project is to develop a thin film thermopile device with structure and dimensions appropriate for high sensitivity detection of THz radiation. An array of such thermopile devices is very promising for THz imaging
As the beginning of the project a test structure is developed and manufactured with the following features:

- linear thermopiles in series
- the thermopile structure is produced from p and n dopped poly-Si thin film
- the supporting membrane is 0.5–3 μm thick Si_3N_4
- the poly-Si linewidth is 10 μm, film thickness is 0.5 μm
- the voltage generated on the structure is ~ 18 mV/K
- the resonance frequency of the structure is about 0.1 THz

After the optimisation of the structure, dimensions and materials applied, higher sensitivity and output voltage is expected at higher frequencies. For the test measurements and later for imaging a bright THz source is needed. The available sources mostly provide short but intense THz pulse triggered by a femto-second laser

shot. The power density of that THz pulse is large but the average power of such a THz source is rather low.

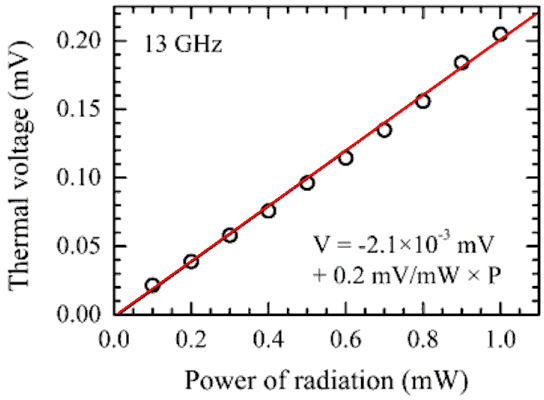

Figure 1 *The thermal voltage response of the thermopile device measured at 13 GHz is 0.2 mV/mW.*

For the test measurements and later for imaging a bright THz source is needed. The available sources mostly provide short but intense THz pulse triggered by a femto-second laser shot. The power density of that THz pulse is large but the average power of such a THz source is rather low. On the market a new source appeared recently, which provides continuous THz radiation of about n×10 mW in the 100–180 GHz frequency range with tuneable but narrow band-width. Our future experiments are based on a THz source like the mentioned one.

Effect of the structural materials on thermal behaviour of 3D tactile sensor – thermal characterisation of 3D piezoresistive tactile sensor

M. Ádám, T. Retkes, T. Weidisch, and A. Nagy

Devices among sensors, accomplishing artificial touch perception, receive increasing attention, particularly in medical applications. Tactile sensors to be implemented in robotic hands or other diagnostic apparatus demand for the development of special devices. Owing to the unique construction the piezoresistive 3D tactile sensor developed and manufactured by MFA and TactoLogic Ltd. is most suitable for those tasks. However, thermal stability of the sensor assemblies is required for integrated system application.

Various measurements were carried out in order to establish the exact thermal behaviour of the sensor including thermal imaging of the warming-up process using thermographic IR camera. The offset and sensitivity change of the device affected by the heat caused by the power supply and ambient temperature were extensively

analysed applying constant and dynamic loads. The elastic rubber covering of the sensor structure plays a crucial role in the function and protection of the device; however, it strongly affects its thermal behaviour, too. Various type of packaging was developed for different applications; some of them are shown on Fig. 1.

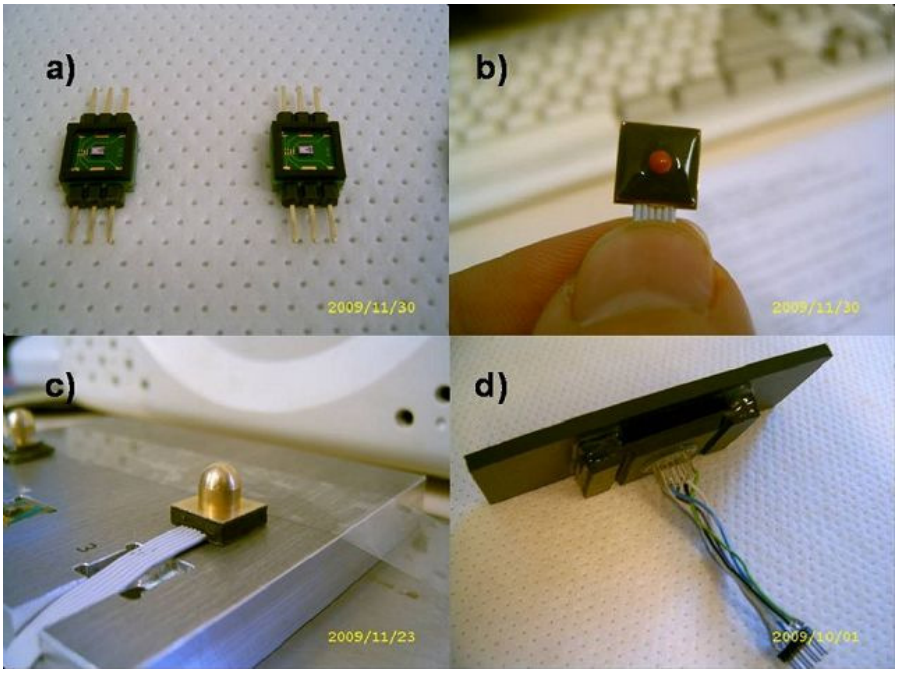

Figure 1. *Various types of 3D tactile sensor packaging: bare sensor (a), (b), (c) and tactile sensor integrated into a rubber sheet (d).*

Not only the value but also the direction of the shift in the offset voltage depends on the use of covering material. Change of the offset voltage in case of bare (a) and elastic rubber covered (b) sensor element is shown on Fig. 2. In bare sensors the reference resistors placed in the bulk Si and the sensing resistors on the bridge element are under different thermal conditions causing significant discrepancy in the resistance value, which results in offset voltage shift. It is also possible that elevated temperature generate mechanical stress which is capable to alter the resistivity of the piezoresistors. Offset shift of rubber covered chips can be caused by mechanical stress originating from the difference in thermal expansion coefficient of the silicon and the elastomer.

The side effects determined by thermal expansion and relaxation during practical operation i.e. application of mechanical force are also not negligible, remarkable drop of sensitivity can be observed over the temperature of approximately 50 °C in case of the rubber covered sensor structure.

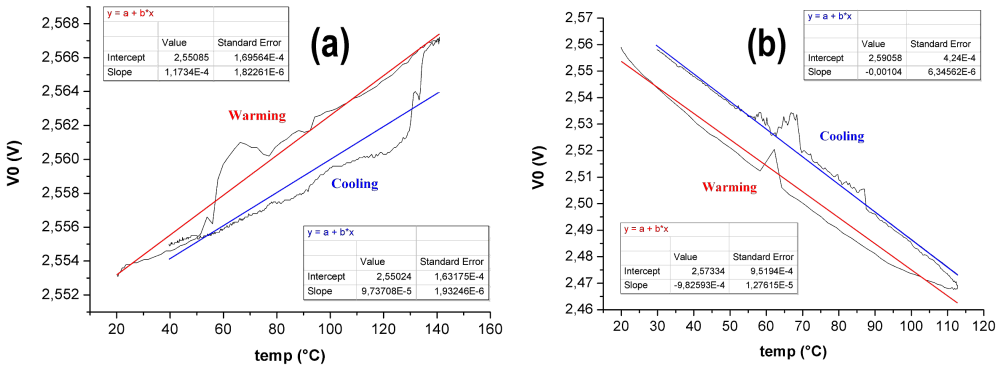

Figure 2 *Offset shift of bare (a) and elastic rubber covered (b) membrane as a function of ambient temperature. Thermographic IR camera (BME EET Thermal Lab) was used for thermal mapping.*

Capacitive pressure sensor

T. Kárpáti, A. E. Pap, M. Ádám, and P. Fürjes

A silicon based capacitance pressure sensor was developed in the co-operation of the MFA and Weszta-T Ltd. for measuring pressure range of 0-1000 mbar. The sensor was fabricated by 3D bulk silicon micromachining technology, a thin crystalline silicon membrane (thickness: 3-5µm) forms the moving top electrode of the capacitor. The static bottom electrode was realised by metal deposition and structuring on glass substrate (Fig. 1). Critical steps of the fabrication are the thin silicon membrane formation and the anodic wafer bonding, chip dicing and testing of the device.

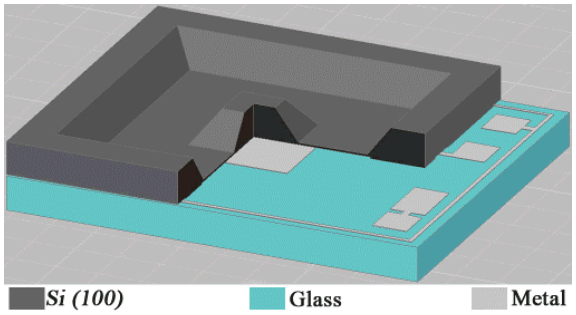

Figure 1 *Schematics of the capacitive pressure sensor.*

3D MEMS structure was manufactured by double side bulk silicon micromachining technology achieving remarkable improvement of the former membrane formation techniques. For realisation of these structured thin layers forming the moving parts of the sensor structure, a special structuring process was developed by the application of

ElectroChemical Etch Stop (ECES). The ECES process was significantly improved using the anisotropic alkaline etching for the formation of 2-4µm thick compact silicon membranes. The structure deformation and functional behaviour were analysed by FEM modelling using ANSYS. The metal electrodes were realised by aluminium evaporation and patterned by etching technique on glass substrate. The fabricated structures are presented in Figs. 2-3.
For anodic bonding a SÜSS MicroTech SB6L Wafer Bonder was applied. The 500µm thick Pyrex glass and the structured silicon wafers were bonded at low temperature (T_{max}=380 °C) anodic bonding. The bonding quality and strength were analysed by crack-opening method, optical microscopy, scanning electron microscopy (SEM) and secondary ion mass spectrometry (SIMS). For proper wafer alignment the SÜSS MicroTech MA6/BA6 mask-aligner machine was utilised. After successful wafer bonding the effects of post-annealing were investigated. The applied annealing reduced the mechanical stress generated in glass wafer during the bonding process.

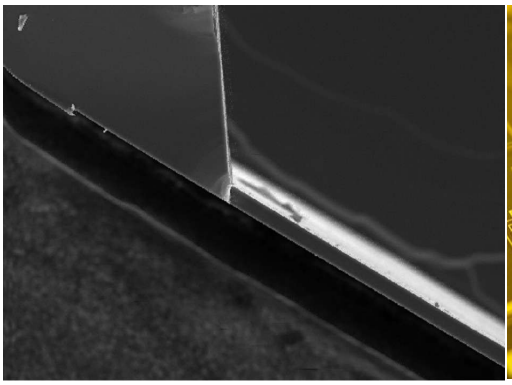

Figure 2 *The free standing silicon membrane forming the moving electrode of the capacitor fabricated by bulk micromachining.*

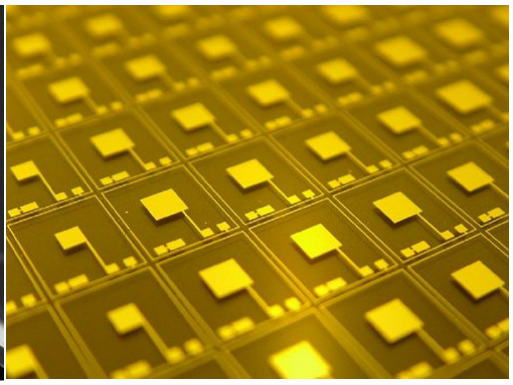

Figure 3 *Metal electrodes of the capacitive sensors realised on glass wafer.*

The fabricated and packaged capacitance pressure sensors (see Fig. 4) were functionally tested in the working pressure range. The output capacity was measured under pressure of 0 to 1000 mbar. As required the device had near linear response in the measured pressure range as in Fig. 5 presented.

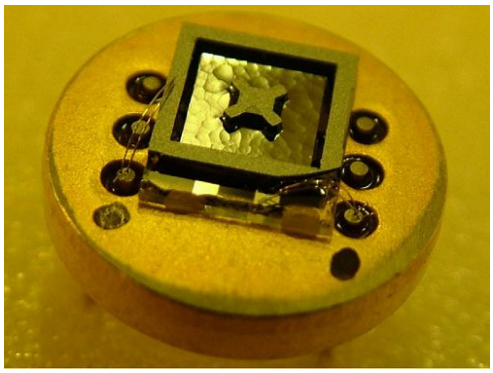

Figure 4 *Assembled and packaged capacitive pressure sensor.*

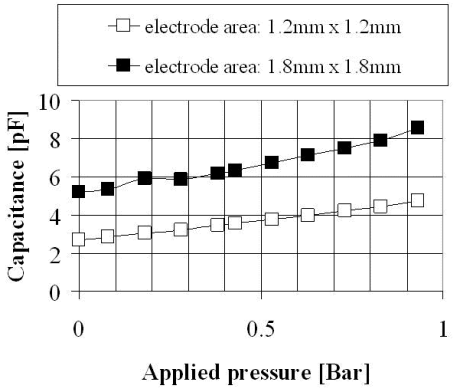

Figure 5 *Test characteristics of the pressure sensor.*

Solar cell technology related developments

(Supported by Hungarian Scientific Fund (OTKA) NK 73424)

Z. Lábadi, Á. Németh, and I. Bársony

The aim of the Solar Cell Innovation Center is to develop an R&D facility for thin film solar cells with CuInGaSe active layer. The cross-section of the solar cell structure is shown in Fig. 1.

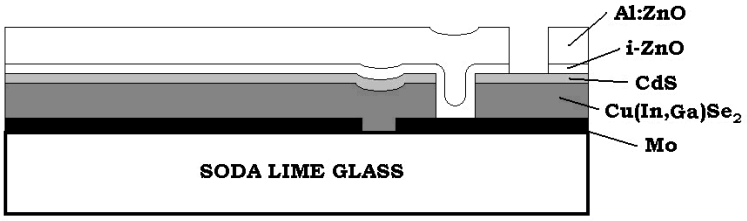

Figure 1 *Cross section of a CIGS solar cell structure.*

The multi-purpose thin film deposition and structuring facility was developed to research the above mentioned thin film solar cell structure. Several preliminary experiments were carried out in the different chambers in order to determine the optimal range of parameters for producing devices.

Experiments related to TCO ZnO deposition:
On the basis of previous experiments Al doped ZnO layers with optimal electrical and optical parameters were deposited by reactive sputtering. Table 1 summarises the parameters of the optimised TCO layer.

Parameter of the layer	Vol.
Specific resistivity [Ωcm]	7.34×10^{-4}
Variation coefficient [%]	<10
Charge carrier mobility [cm^2/Vs]	25
Concentration [cm^{-3}]	3.5×10^{20}
Thickness [nm]	180

Table 1 *parameters of the deposited TCO ZnO*

The resulted thin films were etched in order to gain optimal surface roughness for light trapping. 0.25 % HCl treatment for 5 seconds at room temperature was found to be as optimal etching conditions. Fig. 2 shows the surface of the etched layer.

Results related to the selective laser cutting of thin films:
Laser cutting experiments of ZnO:Al TCO layers were carried out in a wide range of parameters (1-25cm/s speed, 1-10 kHz pulse frequency and 200-5800 mW power, see Fig. 3) but the pulse energy was kept in a narrow range. Optical microscopy of the cuts revealed that there is a critical power for the full ablation of the layer. The evaluation of ellipsometry measurements using a Cauchy-model and a double-layer optical model structure resulted in reliable thickness values. An optimal set of laser cutting parameters (i.e. pulse frequency, ablation threshold energy and overlapping parameter as a function of layer thickness) was found, and criteria for the transparent conductive character of the layer were also established. These results offer a feasible in-line technique to set proper cutting parameters of the TCO layer.
A new technology facility at the Microtechnology Department:
A new Atomic Layer Deposition (ALD) facility was installed in the clean room of the Microtechnology Department. The reactor was bought and installed with the support of the Hungarian National Scientific Fund (OTKA NK73424).
Main technical characteristics of the new equipment are:

- Manufacturer: Picosun Oy, Finland
- Type: SUNALE™ ALD reactor with a pneumatic lift
- Substrate size: 4’ diameter wafer
- Number of sources: Total of four, including a Picosolid™ booster source

Pictures of the general layout of the machine and inside look of the reactor chamber can be seen in Figs. 4-5.

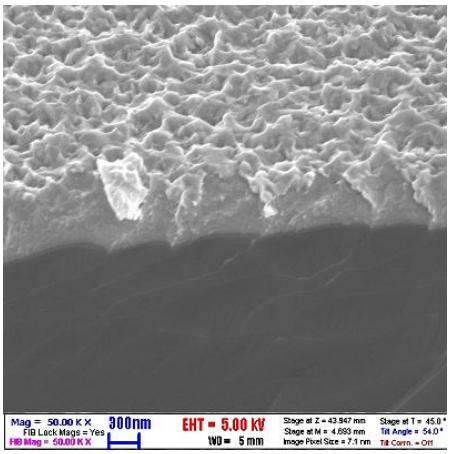

Figure 2 *Surface of TCO ZnO after etching with 0.25% HCl for 5 seconds at room temperature.*

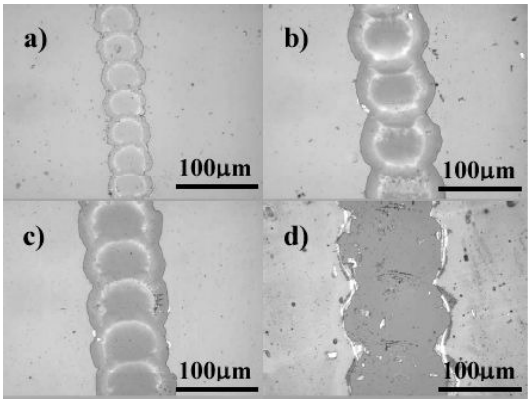

Figure 3 *Optimal laser scribes performed with a speed v, and power P on four different films with thicknesses of: (a) 163 nm (v=3.33cm/s, P=575 mW), (b) 451 nm (v=5cm/s, P=575 mW), (c) 763 nm (v=5cm/s, P=575 mW), and (d) 1304 nm (v=8.33 cm/s, P=575 mW), respectively.*

Figure 4 *SUNALE™ ALD reactor*

Figure 5 *Inside view of the reactor chamber*

The ALD method relies on alternate pulsing of the precursor gases and vapours onto the substrate surface and subsequent chemisorption or surface reaction of the precursors. The method allows controlled monolayer deposition of metal oxides, sulphides and nitrides onto different surfaces, including inside coverage of hollow surfaces. The main research goal in 2010 will be the study of the deposition of a ZnO buffer layer onto a $CuInGaSe_2$ polycrystalline surface, which allows us to replace the current wet chemical CdS deposition technology.

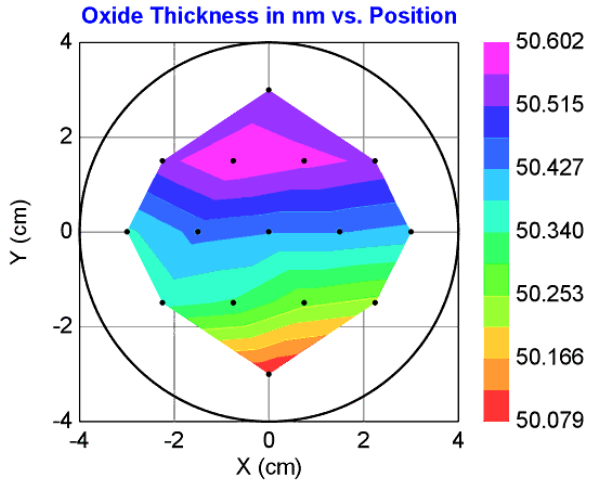

Figure 6 *Results of thickness uniformity test (50nm Al_2O_3 on silicon, the thickness is measured by ellipsometry).*

Thin Film Physics Department

Head: János L. LÁBÁR, D.Sc., scientific advisor

Research Staff

- György SÁFRÁN, C.Sc., Deputy Head of Department
- Árpád BARNA, D.Sc., Emeritus
- Péter BARNA, D.Sc., Emeritus
- György Gergely, D.Sc., Emeritus
- Miklós MENYHÁRD, D.Sc.
- Béla PÉCZ, D.Sc., Deputy Director
- György RADNÓCZI, D.Sc.
- Zsolt CZIGÁNY, Ph.D.
- László DOBOS, Ph.D.
- Olga GESZTI, M.Sc.
- Sándor GURBÁN, M.Sc.
- György Zoltán RADNÓCZI, Ph.D.
- Attila SULYOK, Ph.D.
- Péter SÜLE, Ph.D.
- Lajos TÓTH, C.Sc.
- Katalin BALÁZSI, Ph.D.**
- Viktória KOVÁCSNÉ KIS, Ph.D. **
- András KOVÁCS, Ph.D. **

Ph.D. students / Diploma workers

- Zsolt FOGARASSY, Ph.D. student
- László KÓTIS, Ph.D. student
- Fanni MISJÁK, Ph.D. student
- Marianna SZERENCSI, Ph.D. student
- Lajos SZÉKELY, Ph.D. student
- Mohamed FATHY, Ph.D. student
- Ákos Koppány KISS, diploma worker

Technical Staff

- Sándor CSEPREGHY, engineer
- Ferencné GLÁZER, lab. assistant *
- Andrea JAKAB, technician
- Andor KOVÁCS, engineer
- István KOVÁCS, engineer
- László PUSKÁS, technician *

* part time; ** on leave

The Thin Film Physics Department concentrates on major aspects of structure development of thin films and their surfaces and interfaces. Activity spans from basic research to industrial applications, from deposition of films to their characterisation by TEM, AES and by other complementary methods, including development of both preparation instrumentation and characterisation methods. The range of studied materials cover metals, semiconductors and insulators. Basic research: Both scattering of electrons and ions is studied, including their utilisation in spectroscopy, diffraction and ion mixing and the models for structure development are refined. Industrial applications include the study of materials for hard coating, low-friction coatings, semiconductor devices and their contacts, together with various applications of metallic nanoparticles and nanocomposites. The Department is experienced in different forms of co-operation as indicated by our participation in several European and National Research Projects, in education, and in fulfilling specific industrial contracts. Members of the Department regularly teach and supervise university students of different levels (starting research (TDK), B.Sc., M.Sc., and Ph.D.).
Social-professional activities of the members of the Department include participation in National and International Scientific Bodies and Committees, Boards of Societies and Journals, organising conferences and schools and chairing sessions in them.

Materials for Robust Gallium Nitride, MORGaN

(EU-FP7-NMP- 214610) 2008-2011

B. Pécz, L. Tóth, A. Barna, A. Georgakilas (FORTH), M. Alomari (Ulm), E. Kohn (Ulm)

The MORGAN team will develop GaN-based devices for power electronics with the co-ordination of THALES. Nitride layers will be grown on diamond, and polycrystalline diamond will be also used for the passivation of nitride devices.
This project will therefore try to demonstrate the advantage of innovative composite substrates and devices for use in extreme environments both in terms of electric field and thermal dissipation. MORGaN will combine the excellent thermal behaviour of polycrystalline diamond to the electrical efficiency of GaN compounds. The full potential of GaN without being limited by the thermal conductivity of SiC will be realised by the end of the project. Another goal of the project is to develop novel technologies and GaN based devices (for example sensors operating up to 1000oC) working in harsh environment. MFA performs characterisation of the wafers and layers by transmission electron microscopy. Diamond substrates, layers grown onto them directly, as well as novel metallization techniques will be characterised in this project started in November 2008.
MFA participates in several Work Packages (WP) and by now achieved results in some of them.

TEM study of GaN films grown by MBE onto single crystal diamond
The GaN layers have been grown at FORTH (The Foundation for Research and Technology – Hellas) by molecular beam epitaxy (MBE) onto single crystalline diamond platelets manufactured by Element 6. As shown in Fig 1. the AlN buffer layer is very homogeneous. Threading dislocations are also visible in the layer. The GaN layers grown by MBE at FORTH onto (001), (110) and (111) diamond substrates are in all three cases hexagonal. The orientational relationship of the GaN layer to the different diamond substrates was determined as well by electron diffraction.

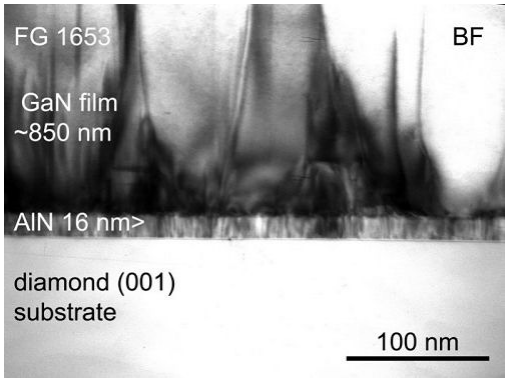

Figure 1 *Bright field overview image of the AlN buffer layer and lower region of the GaN layer.*

Thermal oxidation of InAlN layers

Concerning the grown nitride layers we have also studied a specific behaviour of InAlN, namely its thermal oxidation. We were able to determine the thickness of the oxide layer formed in the thermal process, as shown in figure 2. Getting an oxide layer via thermal oxidation instead of a new deposition step is very promising from technology point of view. These results were published in the paper: Thermal oxidation of lattice matched InAlN/GaN heterostructures by M. Alomari, A. Chuvilin, L. Toth, B. Pecz, J.-F. Carlin, N. Grandjean, C. Gaquière, M.-A. di Forte-Poisson, S. Delage, E. Kohn, Phys. Status Solidi C7, No.1, 13–16 (2010)/DOI 10.1002 /pssc.200982623

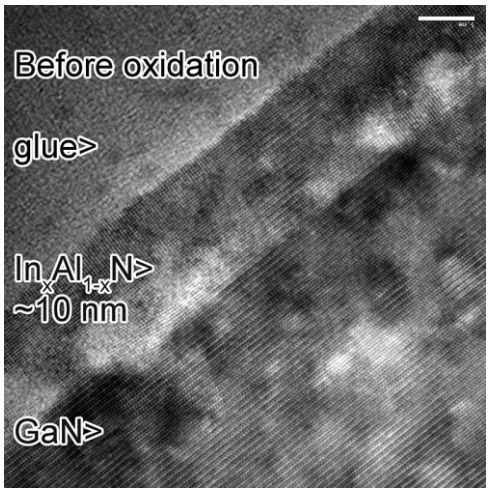

Figure 2a *HRTEM cross sections of 10 nm InAlN/GaN prior to oxidation*

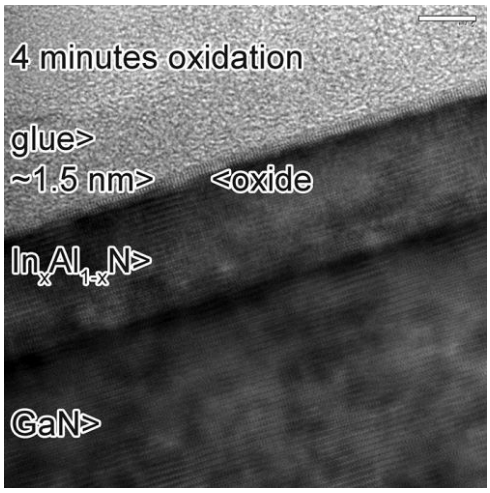

Figure 2b *Thermally oxidized at 800 °C in O_2 atmosphere for 4 minutes*

HIGH-EF: „Large grained, low stress multi-crystalline silicon thin film solar cells on glass by a novel combined diode laser and solid phase crystallisation process"

(FP7-ENERGY-2007-1-RTD 213303)

J. L. Lábár, G. Sáfrán, B. Pécz, and A. Jakab, G. Andrä (IPHT),
S. Christiansen (IPHT), F. Falk (IPHT), and J. Schneider (CSG Solar)

Utilisation of alternative energy sources is one of the major challenges of our days. Direct production of electricity from the abundantly available sunshine is an attractive and fast developing solution. Although close to 90% of the currently manufactured solar cells (SC) are wafer-based Si products, the share of thin film SCs is increasing quickly. HIGH-EF will provide the silicon thin film photovoltaic (PV) industry with a unique process allowing for high solar cell efficiencies (potential for >10%) by large, low defective grains and low stress levels in the material at competitive production costs. This process is based on a combination of melt-mediated crystallisation of an amorphous silicon (a-Si) seed layer (<500 nm thickness) and epitaxial thickening (to >2 μm) of the seed layer by a solid phase epitaxy (ESPC) process.

The HIGH-EF project reached significant mile-stones in 2009. The thickness of seed layers was reduced to 110 nm, while the thickness of absorber layers was increased to 1.6 μm. Solar cells were manufactured from these layer structures. Current research concentrates on increasing the efficiency of the SCs by pinpointing the efficiency limiting defects, their origin and the way to eliminate them.

The role of MFA in the project is structure examination ranging from the micrometer scale down to the atomic level by transmission electron microscopy (TEM), local chemical analysis, as electron induced X-ray emission spectroscopy (EDS), electron energy loss spectroscopy (EELS) and elemental mapping by energy filtered TEM (EFTEM), all performed in the TEM. These examinations are crucial for identifying both the efficiency-limiting defects and their origin. To solve these tasks two bottle-necks had to be faced: time-consuming sample preparation on the one hand and the need for the development of methods on the other hand, as elaborated below.

Preparation of TEM samples from these materials is time-consuming, since the interesting layers are deposited on glass, which is extremely sensitive to the ion beam that is regularly used for thinning the TEM samples. Usage of Ar-ion beams with reduced energy (6 kV) and reduced current (1 mA) can only be applied with grazing incidence (during the entire procedure from the very start) to avoid formation of artefacts in the samples. As a consequence, preparation of a single cross-sectional TEM sample of that kind takes 3 days on the average as compared to the traditional high-energy (10 kV), high-ion-current (2-3 mA) method that takes only 1 day per sample on the average (including the post-cleaning with low energy ions, when the fast, high-energy preparation is ready; this later post-cleaning procedure is identical for both approaches). Frequently, preparation of two TEM samples (one cross-sectional and one plan-view) from the same layer is also needed. Additionally, it is not uncommon to examine these samples in two different TEMs: one with large tilt

possibility, used for diffraction-related work and EDS and the other with low-tilt possibility for high-resolution work, EELS and EFTEM.
In year 2009 we successfully identified the role of the interface between the seed and the epitaxial layers in determining the dislocation density at the ESPC-grown absorber layer as compared to the dislocation density in the laser crystallised (LC) seed layer. The optimum method to clean the LC layer prior to the deposition of the next a-Si layer seems to be crucial.
The most characteristic and most abundant defects in all layers are stacking faults (SF) and twin boundaries. Small angle boundaries and incoherent twins are much less frequent. Figures 1 and 2 give examples of layers with different density and distribution of dislocations within grains and grain boundaries.

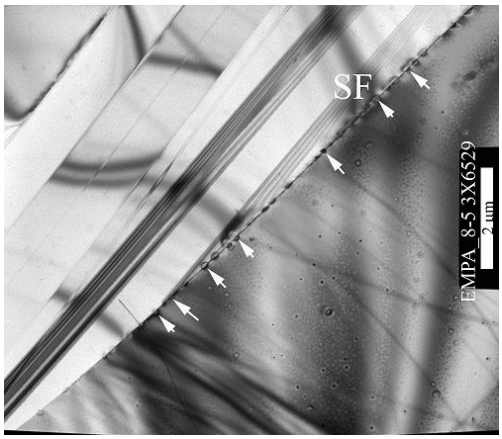

Figure 1 *Example of a Si-layer where dislocations are only seen at the grain boundary. Several stacking faults (SF) and twin lamellae are also seen in the image. Plan-view TEM sample*

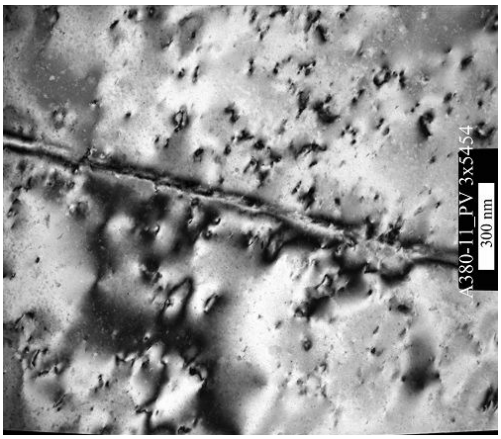

Figure 2 *Example of Si grains with dislocation density as high as $8*10^9$ cm^{-2} Plan-view TEM sample*

A further puzzle to be solved is to find the origin of the measured twist within the large grains of the seed layer, since the dislocation networks, offered theoretically for the explanation of the twist, were not observed in the TEM.
The local twist of the grains is not only measured by electron backscattering (EBSD) in the scanning electron microscope (SEM) by HIGH-EF partner EMPA in Switzerland, but was also confirmed in some TEM samples by measuring the change in orientation by convergent beam electron diffraction (CBED) using a new software module, developed during the HIGH-EF project, embedded into the popular *ProcessDiffraction* program. This procedure is based on the identification of the Kikuchi-bands and on the measurement of their intersections (the zone axes) from the direction of the straight-through beam, also taking into account their direction as compared to the static co-ordinate system of the TEM. Such feed-back to technology is also essential to reach the targeted device parameters.

Influence of HIPIMS plasma ionisation on the microstructure of TiN

(EU FP6 project, INNOVATIAL NMP3-CT-2005-515844)

A.P. Ehiasarian(SHU), A. Vetushka(SHU), Y.Aranda Gonzalvo(HA),

L. Székely, G. Sáfrán, and P. B. Barna

HIPIMS (High Power Impulse Magnetron Sputtering) discharge is a new PVD technology for the deposition of high-quality thin films. In this method, a high power density is applied at the cathode yielding a higher degree of plasma ionisation than in conventional magnetron sputtering. Correlation has been determined between the technology parameters, structure and properties of TiN films in dependence of the peak discharge current (I_d).

Fig.1a illustrates the variation of the hardness and Yong modulus, Fig.1b the variation of texture in dependence of the peak discharge current. The [111] texture changes to [200] at 30A peak discharge current. The cross-sectional microscopic investigations of films clearly show the growth morphology and also the texture of the film deposited at various peak discharge currents (Fig.2). All films have columnar morphology of zone T structure. It means that the texture evolution is related to competitive growth. The orientation changes of competition could be related to the changes of the ion/neutral ratio at the various peak discharge currents.

In the film prepared at 30A the HRTEM investigation (Fig.3) reveals very high density, pure grain boundaries.

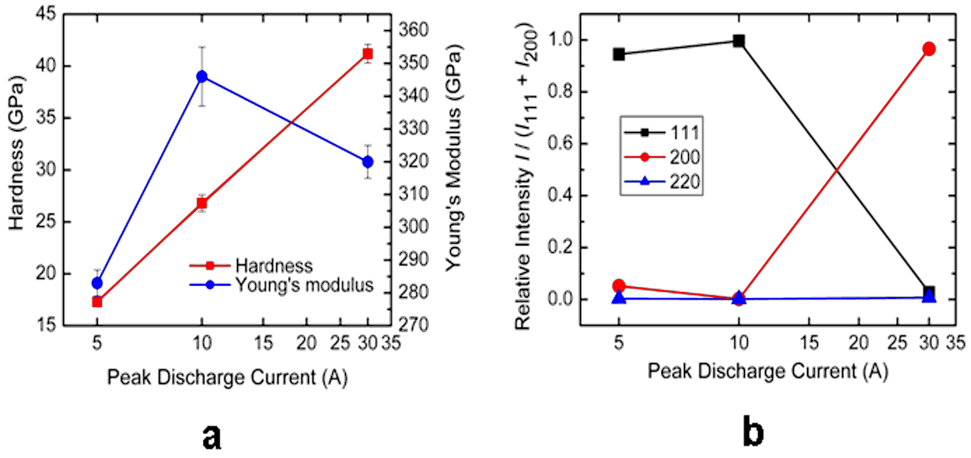

Figure 1 *Hardness and Young modulus (a) and texture (b) of TiN films deposited at various peak discharge currents*

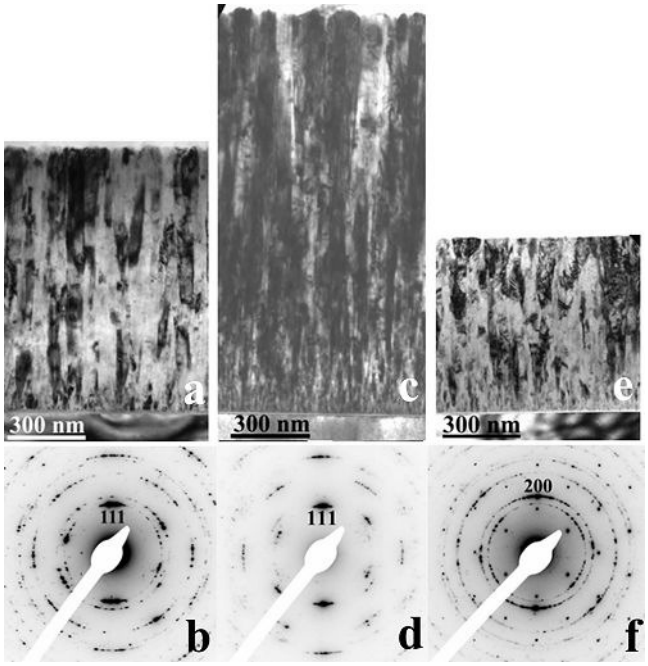

Figure 2 *Cross-sectional TEM micrographs and corresponding SAED patterns of films deposited at peak currents a) 5 A, b) 10 A, and c) 30 A.*

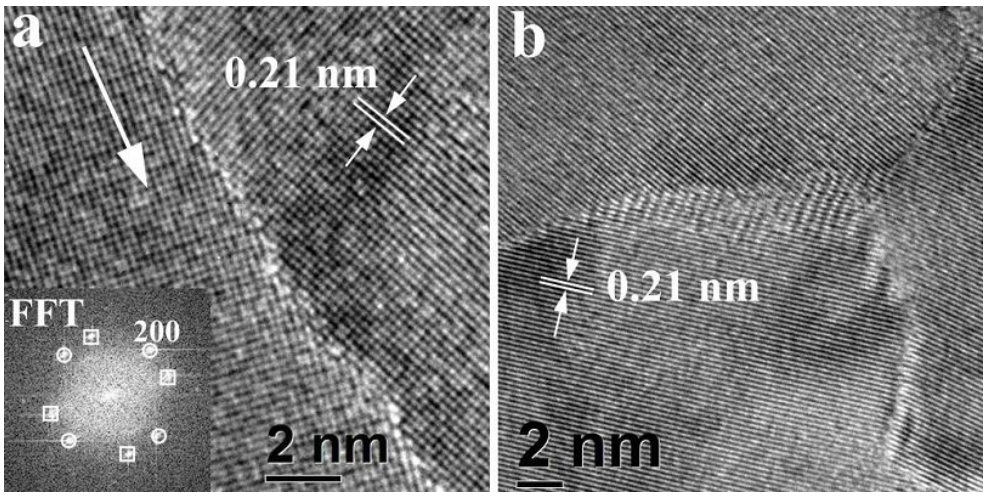

Figure 3 *High resolution cross-sectional TEM micrograph with corresponding FFT pattern (a) and plan view TEM micrograph (b) of film deposited at I_d = 30 A*

New specific columnar nanocomposite microstructure in $Ti_{0.41}Al_{0.57}Y_{0.02}N$ thin films

(EU FP6 project, INNOVATIAL NMP3-CT-2005-515844)

L. Székely , G. Sáfrán, M. Moser (MUL), P. H. Mayrhofer (MUL), and P. B. Barna

In polycrystalline thin films the columnar structure might have various morphologies depending on the preparation method and parameters (substrate temperature, incidence angle of the vapour beam, etc.) and on the layer composition, including also the co-depositing impurities. The last can modify also the phases constituting the film. The structures are generally fiber-like constituting of single- or nano-crystals, columnar of parallel walls or V-shaped constituting of single crystals or fragmented. In the present study, a new type of specific columnar structure has been discovered in $Ti_{0.41}Al_{0.57}Y_{0.02}N$ thin films. In this structure the hcp-AlN and fcc-TiN phases coexist and alternate within distances of a few nm. The alternating phases of different contrast line up along fibers so that a "pearl necklace"-like pattern is recognised by TEM (Fig. 1). The parallel fibers build up bundles and the bundles are forming columns. The two phases are strictly aligned with respect to each other exhibiting texture axis of *hcp-AlN<0002>*//fcc-TiN<111> perpendicular to the film plane.

The dark field TEM images of in-plane specimens of the thick film indicate that the nanocrystalline fibers with nearly identical in-plane orientation are grouped into domains (spotty bright regions in Fig. 2). These domains are corresponding to the individual columns. The in-plane orientation of the individual columns is random.

The HRTEM image and FFT of the cross sectional sample of $Ti_{0.41}Al_{0.57}Y_{0.02}N$ composition is presented in Fig. 3 (a) and reveal the spatial distribution of the coexisting fcc and hcp phases. The measured lattice distances and fast Fouirer transforms of the individual nanocrystals undoubtedly reveal that the nanocrystals of the hcp and fcc phases are alternately stacked on each other with a 3~5 nm period. Stacking nanocrystals of alternative phases along parallel lines will manifest the discovered pearl necklace feature.

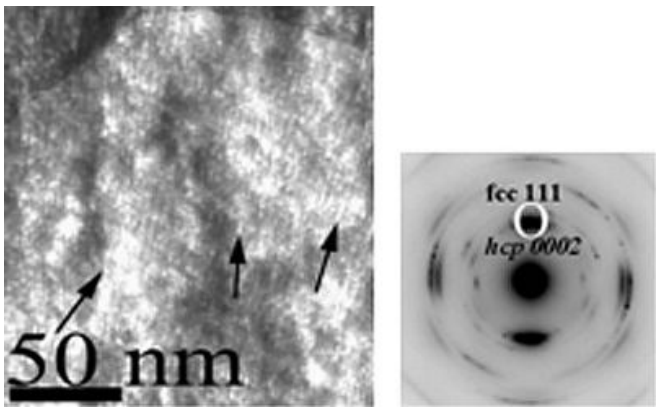

Figure 1 *The "pearlnecklace"-like fiber structure of columns and the texture in TiAlYN film. Dark field image and SAED pattern of cross-sectional sample.*

The marks in the HREM image indicate the fcc 200 and the *hcp 10-10* lattice fringes as they are stacked on top of each other. FFT of the HREM image containing of the two phases simultaneously prove the above described structure. In Figs. 3 (b, c) the HREM image with two pair of alternate stacking hcp and fcc nanocrystals and the corresponding FFT pattern are shown. Figure 3 (d) is composed only by the reflections of the hcp, while that of Figure 3 (e) with the reflections of the fcc phases. It is clearly seen that HREM images of Figs. 3 (d) and (e) are complementary, that proves the alternate stacking of hcp and fcc phases.

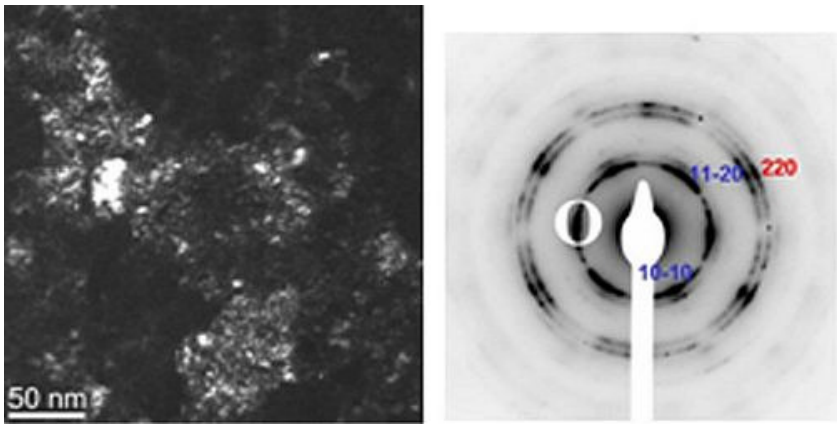

Figure 2 *Domains of the fcc-TiN and hcp-AlN crystals of nearly the same azimuthal orientation. Dark field image and SAED pattern of an in-plane sample.*

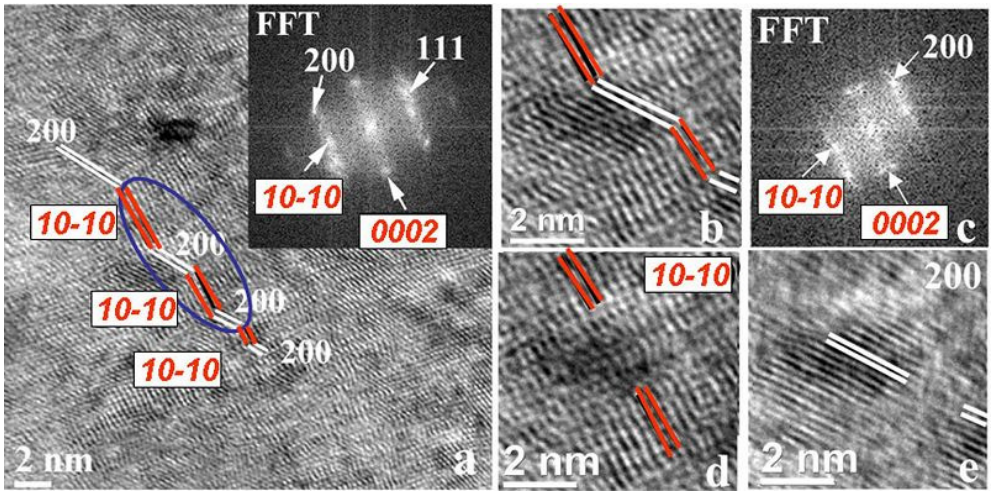

Figure 3 *The HREM image with corresponding FFT pattern (a), the HREM image with two pairs of alternate stacking hcp and fcc nanocrystals (b) and the corresponding FFT pattern (c), (d) and (e) are complementer HREM images taken with the hcp and fcc reflections, respectively.*

CORRAL: Corrosion protection with perfect Atomic Layers

(EU FP7, NMP3-SL-2008-213996)

G. Radnóczi, B. Pécz, L. Tóth, I. Kovács, Zs. Czigány, A. Jakab,
J. Kohlemainen (DIARC, Finland), S. Tervakangas (DIARC, Finland),
and E. Bergmann (HESSO, Switzerland)

The objective of this project is to develop the CORRAL concept of the perfect layer for corrosion protection, validate it through comparison with macroscopic corrosion tests and apply it to candidate coatings. The three year project started in September 2008.
MFA takes part in the structural and morphologic characterisation of the coatings and provides knowledge on the formation mechanisms of the coating and failure analysis.
Structural characterisation of the coatings is carried out mainly by transmission electron microscopy (TEM).
Examples of TEM images of CORRAL coatings are shown in Figs. 1-2.

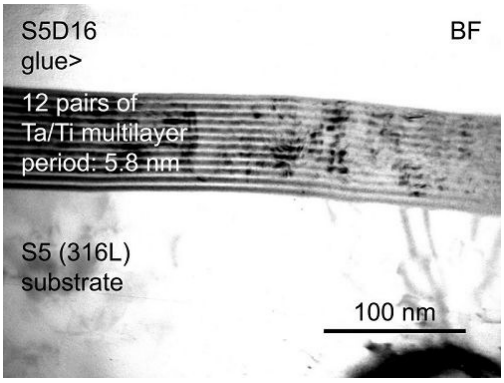

Figure 1 *TEM image of a metallic polycrystalline multilayer coating (70 nm thick) deposited onto stainless steel substrate. The crystallite size seems to be larger than the individual layer thickness suggesting local epitaxial growth of Ta and Ti on each other.*

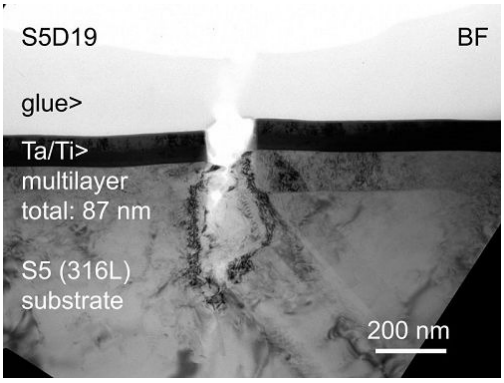

Figure 2 *Defects within coatings were also observed. In this sample the defect seems to be the result of a local damage of the substrate.*

The coatings are prepared on realistic substrates of steels and Al alloys. Metallic, oxide, nitride and other single and multilayer coatings of both amorphous and crystalline in their nature are prepared mainly by using deposition techniques having good conformal coverage on uneven and rough substrates of complicated shape (ALD, HIPIMS, FCAD). The coatings with different thickness between 10-100 nm are prepared by six partners of the consortium.

FOREMOST: fullerene based opportunities for robust engineering: making optimal surfaces for tribology

(EU FP6, integrated project IP-FP6-515840)

G. Radnóczi, K. Balázsi, Zs. Czigány, F. Misják, T. Geszti, A. Kovács, and A. Jakab

The project arrived to the stage when selection of the coatings for possible industrial application has been made. Characteristic coatings for applications in tribology and containing fullerene like layered nanostructures are the C-metal nanocomposites and nitride or plastic coatings containing with embedded fullerene-like particles, mainly WS_2 as well as CBN based coatings.

The structural characterisation of these coatings by transmission electron microscopy is carried out partly in Budapest at MFA.

Besides of the tribological and structural aspects other physical properties like galvanomagnetic properties of the coating are investigated to map and assure multifunctional application of the developed structures.

BC_xN_y thin films deposited at 250 °C by pulsed reactive magnetron sputtering of a B_4C target in an Ar/N2 plasma were studied. The composition and structural details of the major phases depend on the N_2 concentration in the plasma and have significant influence on the Young′s modulus and the elastic recovery of the BCxNy thin films.

The incorporation of WS_2 IFLM nanoparticles and their effect on tribological properties has also been studied.

In a workshop organised by the FOREMOST consortium a very successful talk has been presented on the topic of the fundamental film formation mechanisms playing also important role in the formation of coatings aimed at in the FOREMOST project.

The overall objective of the project is to provide industry with a new generation of composite coatings systems and surface engineering solutions, based on the incorporation or in situ grown in inorganic fullerene-like nanoparticles/structures into coatings and lubricants, to significantly reduce and control friction and wear in rolling and sliding contacts in order to extend operational life, reduce maintenance requirements and reduce the environmental impact of a wide range of mechanical systems.

The final application of the coatings is foreseen in industries like aerospace, automotive, machine tools, etc. Reducing friction benefits the environment by a consequential drop in CO_2 emission. The project has 31 partners and ends in 2010 (http://www.foremost-project.org/home.asp).

ROD-SOL All-inorganic nano-rod based thin-film solar cells on glass

(EU FP7, 227497)

B. Pécz, G. Z. Radnóczi, A. Jakab, and L. Tóth,
V. A. Sivakov (IPHT), Thomas Stelzner (IPHT) and S. Christiansen (IPHT)

A new EU-funded project is turning to nanotechnology in a bid to dramatically ramp up the efficiency of solar cells. The three-year project has a budget of EUR 4 million, EUR 2.9 million of which will come from the Nanosciences, nanotechnologies, materials and new production technologies (NMP) Theme of the Seventh Framework Programme (FP7).

The aim of the project is to develop new, more cost-effective nanomaterials for solar cells. In a time of rising energy prices, the race is on to develop new, cheaper ways of exploiting renewable energy sources. Photovoltaics is an important pillar of this effort, as solar energy is available in almost unlimited amounts.
The solar cells currently in use have an efficiency of around 18%. However, producing these cells requires a lot of raw materials and is an extremely energy-intensive process. In the future, thin film solar cells are expected to dominate the market, as their production costs are much lower. But the efficiency of these new cells, at around 10%, is rather low. The ROD-SOL project aims to up the efficiency of these thin film solar cells by developing and optimising the synthesis of silicon nanorods on cheaper substrates such as glass or metal foils.
According to the project partners, these minute structures are ideal for trapping light energy so that it can be transformed into electricity. A major challenge will be determining the optimal diameter of these nanorods, as the diameter influences the efficiency of the structures. The novel materials and processes developed in the project will be tested and implemented by the companies involved in ROD-SOL.

MFA contributes to the work mostly with TEM characterisation of the nanorod structures grown by research partners. The aim of this effort is to select a suitable process and optimal process parameters for producing the nanostructures for future solar cells. A wide variety of structures were characterised including nanorods grown under gold catalyst particles, nanorods etched from bulk Si and some porous structures obtained in unsuccessful experiments as well.
Nanorods (NRs) grown under gold catalyst by the vapour-liquid-solid (VLS) method exhibit in some cases unwanted kinks, twin boundaries and other defects as seen in fig.1. The surface roughness of the NR is also an issue. NRs grown this way are not always epitaxial, as revealed by electron diffraction analysis. In addition the gold contamination seems to result in disadvantageous electrical properties according to research partners. On the other hand this process seems the most straight forward one for growing NRs on a wide variety of substrates.

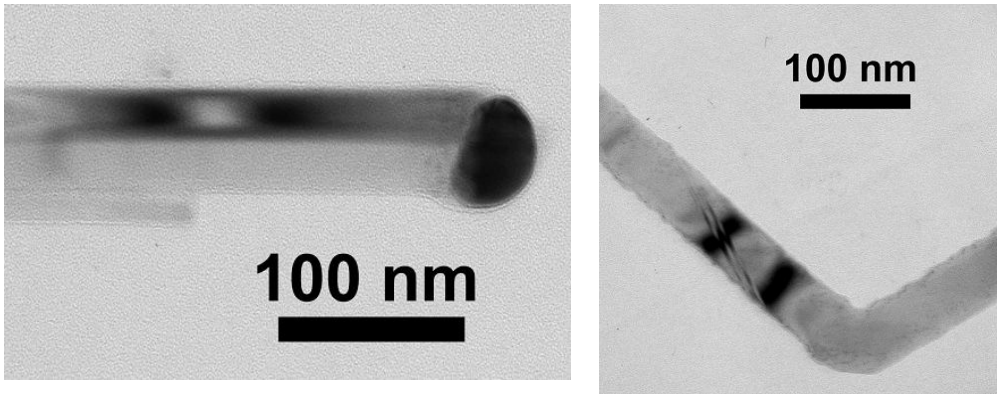

Figure 1 Examples of nanorods grown by VLS process. A nanorod tip is seen on the left with the gold catalyst particle on it. On the right a kink is shown on a NR.

NRs obtained by downward etching into the single crystalline Si wafers are of better crystalline quality, however, the control of the rod diameter seems more difficult in this process. An example of such a structure is shown in fig 2.
In this process NR are obtained by wet etching enhanced by Ag catalyst particles. This way a perfect crytallinity is inherited from the Si wafer as revealed in TEM, however, the cross section of the NRs depends on the arrangement of the catalyst particles sinking into the wafer. Experiments on accurate control of the etching process are still going on. Even control of etching direction was achieved resulting in zig-zag structures. The results of these experiments are under publication in The Journal of Physical Chemistry.

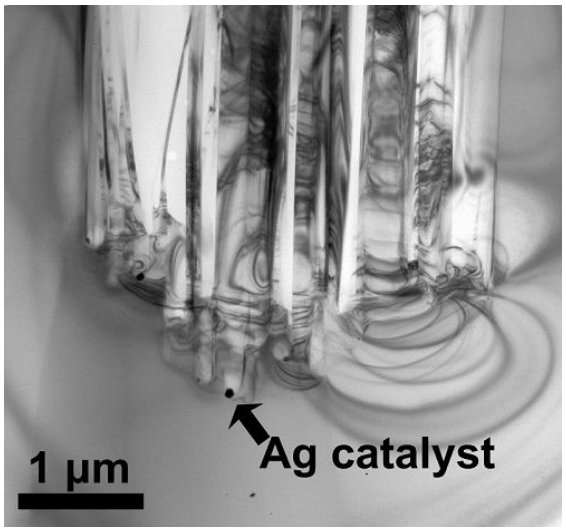

Figure 2 *NRs of different diameter obtained by etching. Ag catalyst particles left after the process are visible at the bottom of some etching channels*

Microscopy of forsterite samples implanted by energetic ions

G. Szenes (ELTE), V. K. Kovács, B. Pécz, and V. Skuratov (Dubna)

Interstellar dust contains a considerable amount of silicates, forsterite and enstatite. The crystallinity is about 11-18% of the total silicate mass in the ejecta of supergiants. Then the grains are gradually amorphized during the evolution of dust and a mean crystallinity of only about 0.2-0.4% has been reported in the diffuse interstellar medium (ISM). Any new information on the amorphization mechanism is of high value, as interstellar dust plays a key role in the formation of galaxies and evolution of the Universe. It was proposed by Bringa et al. (Astrophysical Journal, 662, 2007, 372) that crystalline silicates may be amorphized by cosmic ray (CR) particles. It is well-known, that energetic ions induce a transient melt in insulators and, usually, the amorphous structure is preserved after solidification due to the rapid cooling. Individual amorphous cylinders are formed along the trajectory of projectiles and the overlapping of these cylinders leads to the amorphization. Bringa et al. performed experiments with irradiation of Mg_2SiO_4 forsterite crystals by 10 MeV Xe ions. They concluded that the density and energy of CR Fe ions are suitable to amorphize crystalline silicates in quantitative agreement with the experimental data.

To check if it was reliable to extrapolate the results of MeV Xe irradiation to the effect of energetic CR, systematic experiments were done by irradiating TEM samples using Ar, Fe, Kr and Xe beams of 1-1,2 MeV/nucleon energy in JINR Dubna. Tracks with a mean radius R_e=1.36 nm were observed after irradiation by 56 MeV Fe ions while no tracks were induced by a 48 MeV Ar beam. An amorphous track that is formed due to the high energy Xe irradiation is shown in Fig. 1. Regarding the low temperature of the interstellar dust, the variation of the flux of CR Fe ions and of the inelastic energy deposition by the ion energy, we concluded that 13400 Myr would be required for the complete amorphization of crystalline forsterite grains. This is too long compared to the lifetime of silicates in the ISM (400 Myr). Although CRs are not responsible for the amorphization they contribute to the steady state concentration of crystalline silicates by ion-induced crystallisation of amorphous silicates. Our estimates show that the probability of such an effect is about 10^5 times higher compared to that of complete amorphization of silicate grains.

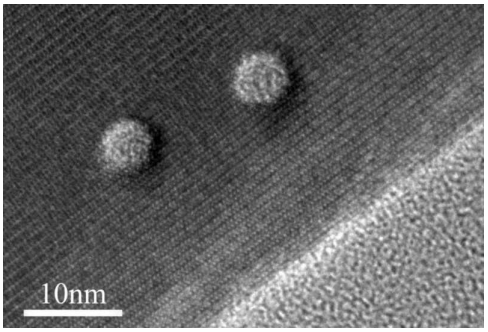

Figure 1 *High-resolution electron microscope image of a forsterite sample irradiated by 130 MeV Xe ions; the (0 1 0) lattice planes with the distance 1.02 nm are visible. (Reproduced by the permission of the AAS.)*

"Ab-inito" simulation of AES depth profile

(PL-15 Project between the Polish and Hungarian Academy of Sciences)

L. Kotis, Gy. Safrán, M. Menyhárd, A. Jablonski, and L. Zommer

The initial structure of a sample is generally not visible in the as-measured AES depth profiles, because of the finite inelastic mean free path of Auger electrons, backscattering effect and ion- bombardment-induced specimen alteration. Thus, an extended reconstruction of "real" initial structure from measured AES depth profile is needed. For a case study the C (23.3 nm) / Ta (26.5 nm) / C (22.7 nm) layer system was studied XTEM determined the initial structure of the sample. The XTEM measurement showed that interfaces are sharp (< 1 nm). The layer system was AES depth profiled with applying Ar^+ ion bombardment of 1keV at angles of incidence: 72°, 78° and 82°. The as-recorded AES depth profiles (Fig. 1) show that the layer transitions C1/Ta and Ta/C2 have different widths and the apparent thickness of the layers depends on the sputtering conditions, however. Elaborate evaluation procedure is thus necessary to remove all these artifacts from the measured depth profiles. For the reconstruction of initial structure of sample, we simulate the whole AES depth profile using calculated backscattering factors, electron attenuation lengths (from the NIST database) and TRIDYN simulation for describing the sample alteration at the C2/Ta interface and a trial-and-error procedure at the Ta/C1 interface. Fig. 2 shows the measured (Ar, 1keV, 72°) and simulated AES depth profiles. The simulated AES depth profile agreed well with the measured profile, thus demonstrating the validity of our approach.

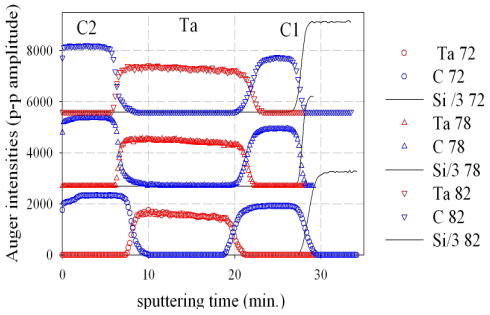

Figure 1 *As measured AES depth profiles. Sputtering conditions: Ar^+, 1 keV, angles of incidence 72°, 78° and 82° (see legends).*

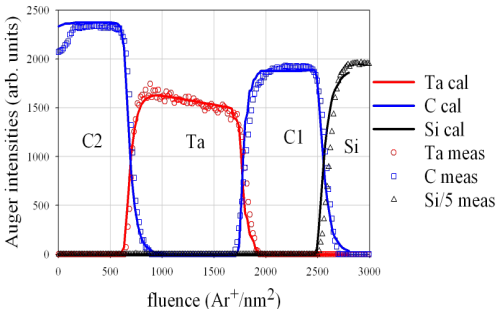

Figure 2 *Measured and reconstructed by simulation AES depth profile of the C/Ta/C/[Si substrate] structure.*

Layer growth by ion mixing

(SI-3/2008 Bilateral contact between Slovenia and Hungary)

A. Barna, L. Kotis, J. L. Lábár, A. Sulyok, M. Menyhárd, A. L. Tóth, L. Illes, A. Zalar (JSI), and P. Panjan (JSI)

Ion-irradiation-induced ion mixing generally produces a Gaussian type of concentration distribution. In the last year, we have shown that Ga ion irradiation of C/Ni interface produces a Ni_3C-rich mixed layer. This layer, however, had sharp interfaces in contrast to the general expectation. For better understanding the process, we have replaced Ga with Ni, using the medium energy ion implantation facility of Dresden-Rossendorf AIM. C/Ni samples of various thicknesses were irradiated by Ni^+ ions of 20 and 30 keV. XTEM image of the irradiated sample is shown in the Fig. 1. It shows that the average Ni penetration depth is less than the thickness of the C layer, and that the interface mixing probably are caused by low energy Ni^+ ions, and the mixed layer is separated from the pure Ni and C layers by sharp interfaces. The layer growth scales with the square root of fluence. This dependence is shown in Fig. 2, which summarises the results measured on various samples with carbon thickness of 21 and 40 nm and irradiated by 20 and 30 keV Ni^+, respectively.

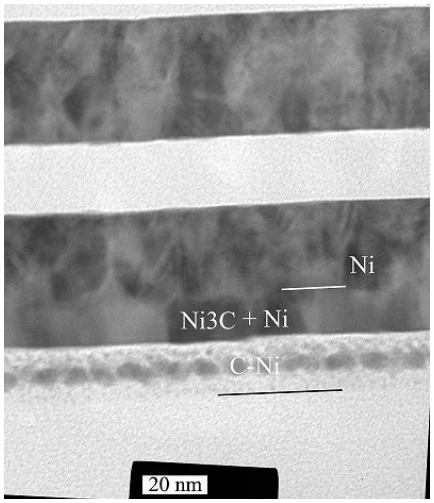

Figure 1 *The XTEM image of the C/Ni sample irradiated by Ni+ ions of 20 keV with fluence of 200 Ni^+/nm^2.*

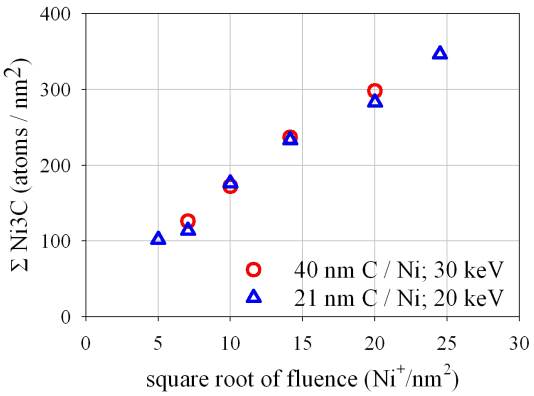

Figure 2 *The amount of Ni_3C formed as a function of various ion irradiation of C/Ni sample of various layer thicknesses.*

The slopes are the same for the two cases, which are explained by the similar deposited energy in the two irradiation experiments. The layer growth behaviour is thus the same as in the case of Ga irradiation. It follows the layer growth phenomenon is not connected to the "strange " behaviour of Ga.

Electron diffraction patterns of carbon based fullerene-like nanostructures.

(FOREMOST EU-FP6)

Zs. Czigány, and L. Hultman (IFM)

Carbon based thin films with fullerene-like nanostructure were deposited by reactive DC magnetron sputtering. The short range order in amorphous and fullerene-like carbon compounds has been characterised by selected area electron diffraction patterns (SAED) and compared with simulations of electron scattering by model nanoclusters. Broad rings in SAED pattern from fullerene-like CN_x (Figure 1.) at ~1.2 Å, ~2 Å, and ~3.5 Å indicate a short-range order similar to graphite, but peak shifts indicate sheet curvature in agreement with high-resolution transmission electron microscopy images. Fullerene-like CP_x (Figure 2.) exhibits rings at ~1.6 Å and 2.6 Å that can be explained if it consists of fragments with short-range order and high curvature similar to that of C_{20} molecule.

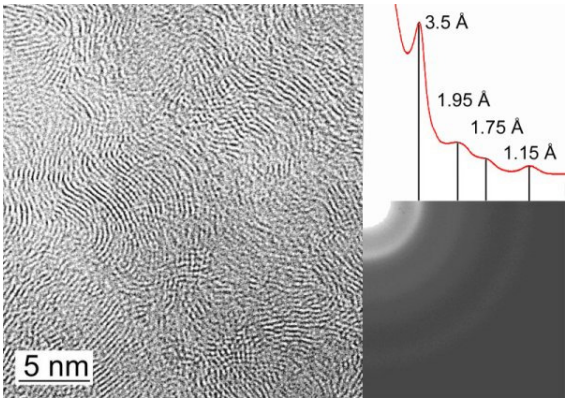

Figure 1 *HRTEM micrograph and electron diffraction pattern of fullerene like CN_x*

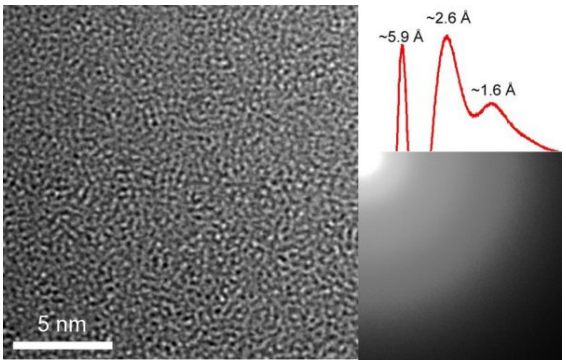

Figure 2 *HRTEM micrograph and electron diffraction pattern of fullerene like CP_x*

Conversion of AREPES (angular resolved elastic peak) experimental spectra measured in arbitrary units to absolute units

(PL-15 Project between the Polish and Hungarian Academy of Science)

G. Gergely, S. Gurban, M. Menyhard, A. Jablonski, L. Zommer, and K. Goto

Electron spectra (AES, XPS, EPES, etc.) are generally measured in arbitrary units. On the other hand Goto succeeded to measure the elastic peak spectra (EPES) in absolute units using his special CMA. From the measured elastic current, the elastic backscattering probability can be deduced. Zemek et al. published AREPES experimental spectra - measured with a small CMA with variable angle detection of α_d, and a small conic angle of acceptance with α_d axis and 4.1° semi-angles - in arbitrary units. We transformed these results into absolute units, by fitting the experimental data of Goto at 42° CMA angle to the experimental points of Zemek. Additionally these spectra (already in absolute units) were corrected for surface excitation losses (SEP) using the SEP parameters of Werner and Jablonski and Chen (corrected by us). The average differences, between the SEP corrected experimental data (in absolute units) and MC simulation, determine the quality factor of SEP correction. SEP parameter of Werner for Si and Ni resulted in the best quality factors.

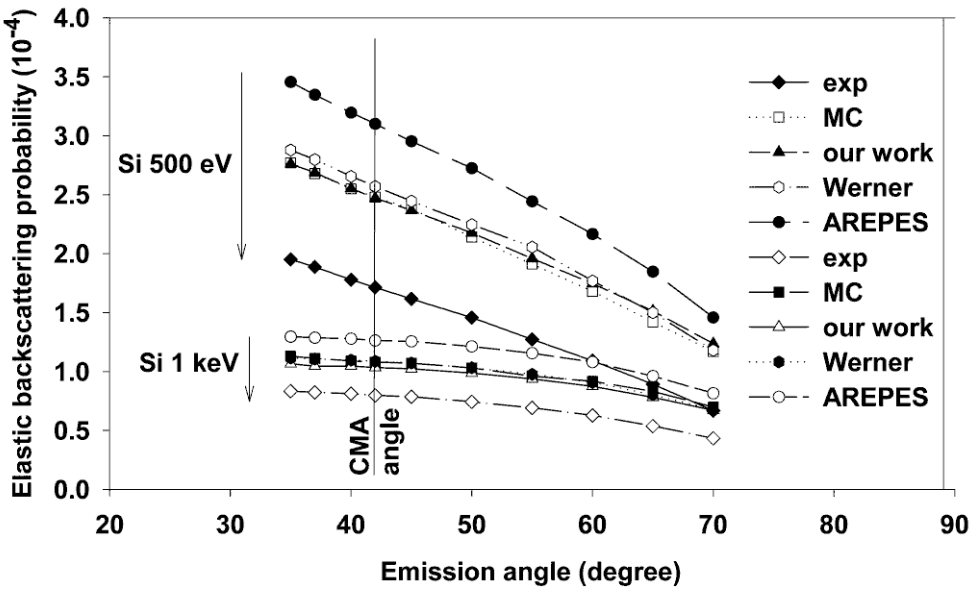

Figure 1 *The backscattering probabilities derived from experiments (exp), SEP corrected (our work, Werner and AREPES by Jablonski and Zemek) and MC simulation are plotted vs α_d emission angle at 0.5 and 1 ke V*

The molecular dynamics simulation of ion-induced ripple growth

(supported by bilateral German-Hungarian exchange program DAAD-MÖB and by OTKA K-68312)

P. Süle, and K.-H. Heinig

Ion-bombardment induced nanopatterning driven by self-organisation process has become a powerful tool for bottom-up nano-fabrication in the last decade. Among them, one of the most important is the atomistic computational simulation of nanopattern evolution. Until now no real time, nanoscale simulation is available for pattern growth in the nanoscale. The reason is the huge methodological and computational difficulties occur during simulations. In particular, thin film growth in general and also nanopatterning require multiscaling approaches. However, the implementation of such methods remains still challenging. To overcome this situation we developed a much simpler approach, in which we show that the growth of ripples (wavy nanoscale periodic features) could be simulated by the serial impact of energetic ions if the simulations are started from pre-patterned surfaces.

In Fig 1 the schematic model of the assumed process is shown. First few tens of a monolayers are sputtered away and a roughened wavy surface develops upon F1 fluence. Further ion fluence (F2), which is much smaller, than F1, turns the system into rippled state. Our central idea is to model the latter step only using a pre-patterned initial state, hence the computationally challenging first step with F1 fluence can be bypassed. In Fig 2 the pre-patterned rippled stripe and the ion-sputtered one are shown. In Fig 3 the cross-sectional view of the ion-sputtered 50 nm ripple is shown. The presented results are in accordance with available experimental results. The growth rate of the ripples peaks at ~50 nm wavelength in agreement with experiment. The evolution of the interface width as a function of the ion fluence is also shown in Fig 4. Below 35 nm wavelength ion erosion rules the development of the morphology, while above 35 nm growth takes place again in accordance with experiment.

To sum up, we present a new and efficient computational scheme for nanoscale pattern growth under highly non-equilibrium conditions. Nanopatterning could be modelled and simulated until now by much simpler approaches (like kinetic Monte Carlo and phenomenological methods). These approaches involve many assumptions and predetermined mechanisms. Moreover they deal with artificial structures (e.g. fcc lattice) and complex atomic interactions are excluded. Molecular dynamics simulations when combined with the serial addition approach is a powerful tool for generating nanopatterns.

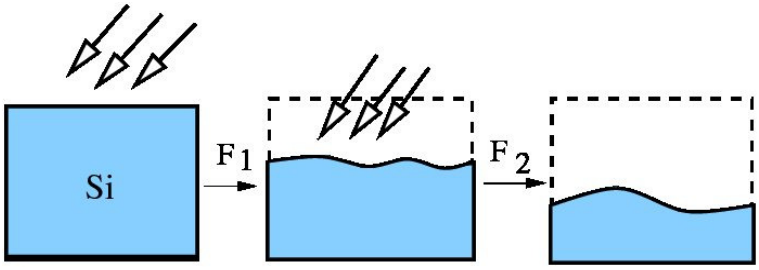

Figure 1 *The schematics of the sputtering induced surface patterning process First few nms of top layers are eroded and sputtered with ion fluence F_1. During this process the surface becomes somewhat roughened and wavy, although smoothening effects are strong. In the next step, ripples develop under the effect of fluence F_2. The assumption F_1 >> F_2 allows the simplification of simulated sputtering. The total fluence is F_1+F_2.*

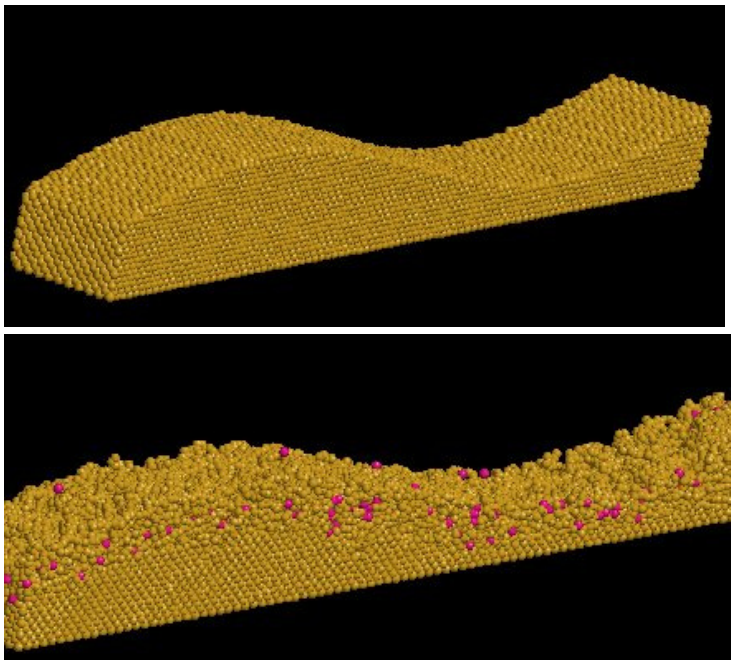

Figure 2 *The snapshot of a pre-patterned wavy surface of striped Si(110) with 50 nm wavelength before ion-bombardments. The lower snapshot shows the ion-bombarded surface of the pre-patterned Si rippled stripe after 1000 ions impact.*

Contacts to III-nitride semiconductors

(OTKA K77331)

L. Dobos, B. Pécz, L. Tóth, Zs. J. Horváth, Z. E. Horváth, and P. Basa

The goal of the project is to form and characterise MAX phases [M. W. Barsoum and T. El-Raghy, American Scientist 89, 334 (2001)] in GaN. No one has done I know of MAX phase in III-nitride, only the special literature mentions the existence of MAX phases in III-nitride (Ti_2GaN, Cr_2GaN, V_2GaN).

In recent years, the ternary compounds $M_{N+1}AX_N$, where N=1 to 3, M is an early transition metal, A is an A-group element (IIIA or IVA), and X is either C and/or N, attract increasing interest owing to their unique properties. MAX phases represent a new class of nitrides and carbides and can be best described as nanolaminates. They combine some of the best properties of metals and ceramics.

The obtained results are the following: in the case of annealed n-GaN/Ti(40nm)/Au(120nm) samples the high resolution study of the interface showed the formation of some phases [Fig. 1(a)]. The HRTEM insert [Fig. 1(b)] shows the characteristic stacking of two Ti–N layers separated by Ga layers. It was found that the distance of Ga layers is about 7 Å and the lattice plane spacing of Ti_2GaN MAX phases is about 1.34 nm. The small nitrogen atoms are not resolved in the micrograph. In these (211) type compounds every third layer is an A-group element, in our case a Ga layer. The "nanolayered" crystal structure of the ternary nitride is clearly revealed, the contrast is changed in every third layer in Fig. 1(b). The (006) lattice planes of the ternary phase are parallel to the interface. In our series of experiments no such a MAX phase was observed in samples containing only a single Ti layer (annealed at 900 °C). This predicts the conclusion that both Au and Ti plays a role in the formation of the above intermetallic phase and Au grains were also found on GaN after annealing [see Fig. 1(a)] as well as Au diffused into topmost part of n-GaN.

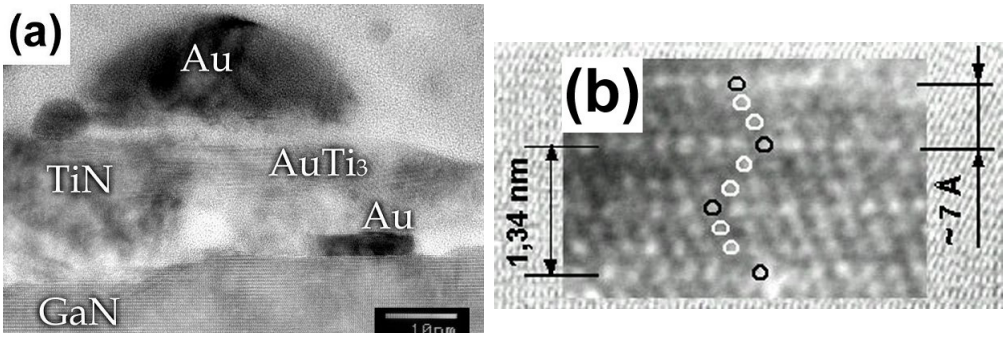

Figure 1 *(a) HRTEM micrograph of the n-GaN/Ti/Au interface after annealing at 900 °C. (b) Insert shows the layer sequ-ence in the Ti_2GaN – MAX phase – grain*

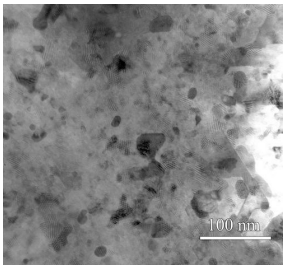

Figure 2 *Plan view image of 900 °C annealed n-GaN/Ti/Au sample after removal of unreacted metallic layers.*

The results of XRD, EDS and SAED examinations were confirmed by the analysis of HRTEM pictures. Namely, Ti_2GaN MAX phases as well as Au grains were found at the vicinity of Au/Ti/n-GaN interface in the sample annealed at 900 °C.
A plan view TEM image in Fig. 2 shows dark grains indicating Au containing crystals in the 900 °C annealed GaN semiconductor. These grains grown into the GaN could be made visible after the removal of the metallic contact layers by chemical etching. EDS analysis of these crystallites indicate the presence of both Au and Ti.
The formation of new phases (ternary MAX phase) led to near ohmic behaviour and increased series resistance at 900 °C.

Analytical electron microscopical study of the competitive adsorption of heavy metals in soils

(OTKA PF 63973)

P. Sipos (GKKI), T. Németh (GKKI), V. Kovács Kis, and I. Mohai (KK)

Soil mineral phases play a significant role in controlling heavy metal mobility in soils. The effective study of their relation needs the integrated use of several analytical methods. In this study, analytical electron microscopy analyses were combined with sequential chemical extractions on soils spiked with Cu, Zn and Pb. Our aims were to study the metal sorption capacity of soil mineral phases and the effect of presence of iron oxide and carbonate on this property of soil minerals.
Sorption characteristics of bulk soil samples and discrete soil mineral constituents were studied by Cu, Zn and Pb batch sorption experiments and analytical electron microscopy analyses. Copper and zinc sorbed mostly on soil mineral constituents, while lead was associated mainly to soil organic matter. Additionally, the competitive situation resulted in increase of the role of iron oxides in Pb sorption. Close association of iron oxides and silicates resulted in significant change in their sorption capacities for all the studied metals. The alkaline conditions due to the calcite content in one of the studied soil samples resulted in both increased role of precipitation for Pb and Cu and elevated sorption capacity for Cu by discrete mineral particles. Using the analytical electron microscopy analyses the sorption characteristics of metals were supported by particular data. When the methods used in this study are combined, they become an extremely powerful means of getting a deeper insight into the soil–metal interaction.

NTPCRASH

(TECH_08-A2/2-2008-0104)

M. Menyhard, A. Sulyok, S. Gurban, A. Toth, L. Illes, C. Balazsi, A. Petrik, V. Varga, and F. Wéber

Consumption and weight reduction induce a demand for new materials in car production. Two types of reinforced plastic (composite) have been investigated here:
-disordered composite of polypropylen (PP) with 50% and 75% short cellulose fiber.
-ordered composite of epoxy resin with textile of carbon fiber.

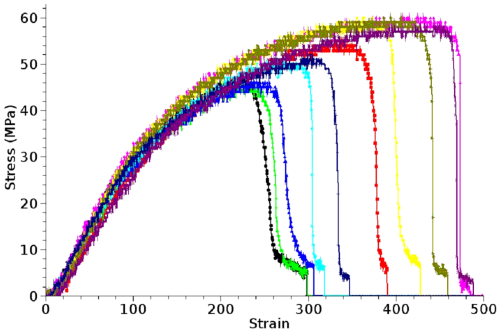

Figure 1 *Stress-strain curve of PP-cellulose composite with high variance of strain*

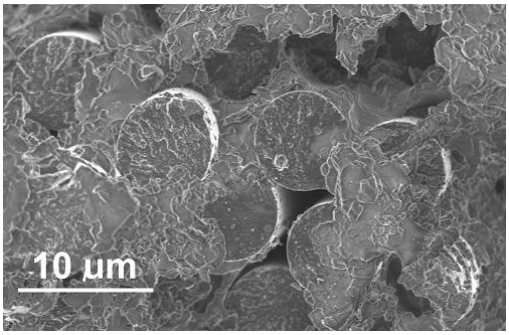

Figure 2 *SEM image on fractured surface of epoxy-carbon composite with resin-free void*

Mechanical investigation of PP-cellulose composite showed that 75% fiber content doubles the level of strain tolerated before fracture compared to the other one. The benefit of this improved strain is limited because the variance of the tolerated strain is also increased tremendously (see Fig. 1). The strain variance was minimal on composite with lower cellulose content (not shown). Scanning Electron Microscopy (SEM) images taken on fractured surfaces showed local failures of good dispersion (file of fibers) more often with larger cellulose content.
Epoxy-carbon composite provided a magnitude higher stress level, however, with a lower strain. The fractured surface investigated by SEM showed clear brittle fracture of the carbon fibers and resin with good adhesion to that. The images revealed some resin-free voids extending to the fractured surface (see Fig. 2), showing that the procedure filling the carbon textile with epoxy resin was not perfect.

Metanano: „Development of noble metal based innovative products for applications in environment protection, cosmetics, sensors and catalysts”

(NKFP-07-A2-METANANO-0-0710120730)

J. L. Lábár, O. Geszti, Zs. Fogarassy, A. Jakab, G. Pető, A. Csanády (BayATI), H. Hargitai (BayATI), A. Bajáki (Metal Art), and S. Bánki (Metal Art)

The aim of the Metanano project is to develop high quality products: dry powders, layers, suspensions and these on solid substrates for pharmaceutical, cosmetic, sensor and catalyst applications. Both public and military applications are targeted. The role of MFA was two-fold in year 2009. On the one hand complex examination of nano-materials was carried out. On the other hand the examinations were supported by mathematical-physical simulations (Fig. 1).

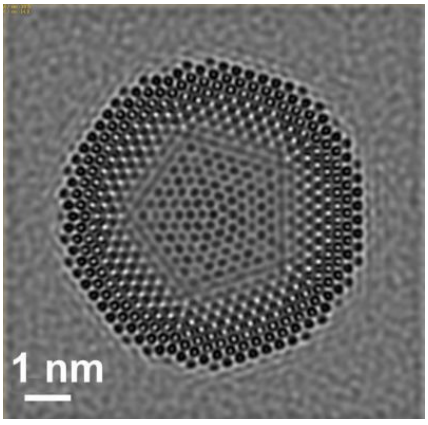

Figure 1 *Simulated HRTEM image of a 5-fold twinned Au-nanoparticle on amorphous Carbon support.Defocus=-38.5 nm*

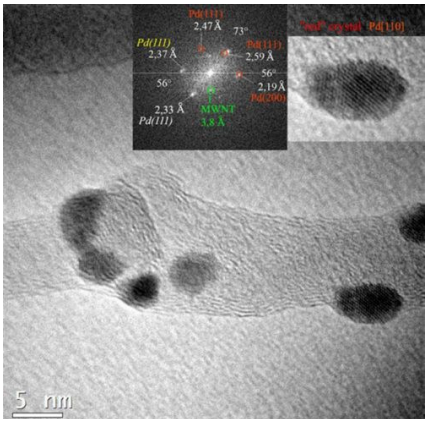

Figure 2 *Pd nanoparticles attached to multiple walled Carbon nanotubes (WCNT)*

In year 2009 nanoparticles were successfully produced in sol form both by chemical reduction and electrochemical methods. Deposition of nanoparticles directly on substrates was also successful (Fig. 2). Size distribution of nanoparticles was measured by different methods (TEM, Zeta-sizer) and both the role and the limits of these methods were determined. The smallest size-fraction can only be properly measured by TEM, while larger sized particles are better seen with the Zeta-sizer. The main difference is the different weighing (by orders of magnitude) if we measure “number-fraction” or “volume-fraction” or we simply measure “intensity ratios (Fig. 3). Stability of the nanoparticles was also investigated. Ag nanoparticles are shown in Fig. 4 as an example. The air in Budapest contains considerable amount of

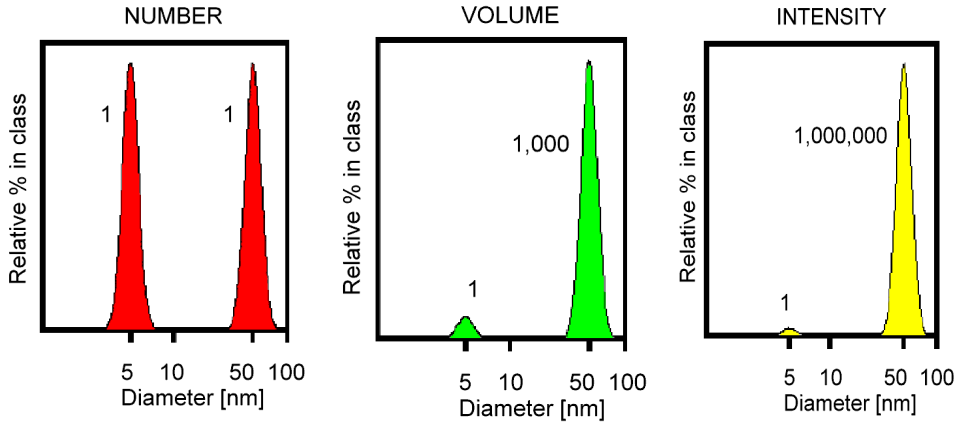

Figure 3 *Different representations of the same sample (=equal number of 5 nm sized and 50 nm sized particles)*
Link: http://www.malvern.co.uk/

Sulphur, which is also responsible for the degradation of buildings and sculptures. This Sulphur also attacks some nanoparticles even in the sol form. Our investigation shows that the smallest fraction of the nanoparticles is resistant against this attack (=remains stable), while larger particles are prone to formation of Ag-Sulphide. Composition was confirmed by EDS. We offer an explanation for this observation: the smallest size remained small in the sol, because its stabiliser shell is the most perfect, prevented these particles from growth in the sol. The same perfect shell must have also protected the small particles from being corroded by S.

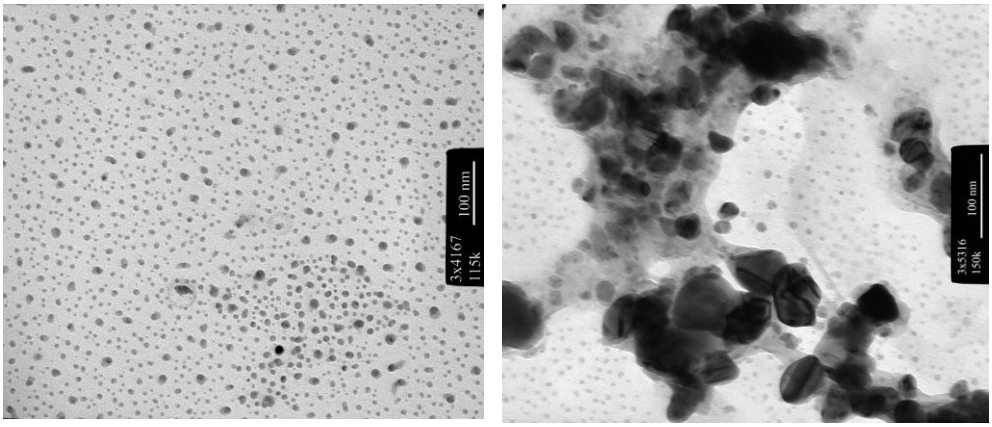

Figure 4 *Ag sol stored in S-contaning air for 70 days. The smallest sized fraction remained intack (stable), while larger sized fraction formed large Sulphide particles (confirmed by EDS).*

Ceramics and Nanocomposites Department

Head: Csaba BALÁZSI, Ph.D.,

Research Staff

- János VOLK, Ph.D.
  Deputy Head of Department

- Péter ARATÓ D.Sc.
- László BARTHA, D.Sc., Professor Emeritus
- Csaba Sándor DARÓCZI, dr. Univ.
- András DEÁK, Ph.D.
- István GAÁL, C.Sc.
- Gréta GERGELY, Ph.D.
- Ngyuyen Quoc KHANH, Ph.D.
- István Endre LUKÁCS, Ph.D.
- Judit PFEIFER, C.Sc.
- Attila L. TÓTH, Ph.D.
- László URAY, C.Sc.

Ph.D. students / Diploma workers

- Orsolya KOSZOR, Ph.D. student
- Eszter FÜLÖP, Ph.D. student
- Róbert ERDÉLYI, Ph.D. student

- Gyula BABÓCS, Diploma worker
- Viktória HALÁSZ, Diploma worker
- Viktória KONRÁD, Diploma worker
- Áron NAGY, Diploma worker
- Zoltán SZABÓ, Diploma worker
- Valentin SÓTI, Diploma worker
- Mihály TÓTH, Diploma worker

Technical Staff

- Levente ILLÉS, B.Sc., engineer
- Ferenc WÉBER, M.Sc., engineer
- Viktor VARGA, technician
- Attila PETRIK, technician

The main task of the department is to study the relationships between processing parameters, micro- and nanostructures and properties of ceramics and their nanocomposites.

In the year 2009 our research activity have been focused on the development of novel nanocomposites with original structural designs in order to provide new functions to ceramic matrices:

- investigation of mechanical, electrical, thermal, sensorical and biological properties of ceramics,
- development of carbon nanotube silicon nitride nanocomposites,
- 1D, 2D and 3D semiconductor oxides (e.g. ZnO, WO_3) for sensor devices,
- hydroxyapatite biocomposites for medical and enviromental uses, outcome of advanced preparing methods, and
- a pilot scale production of silicon nitride tools and parts exists as well.

Silicon Nitride-Based Ceramics and Nanocomposites

(Supported by SVEDNANO, OTKA K63609, MTA-RAS)

Cs. Balázsi, P. Arató, O. Koszor, G. Gergely, J. Pfeifer, and F. Wéber

A world-wide interest on ceramic nanocomposites with novel structure and function may be observed. High level of synergism of mechanical, thermal and physical properties is foreseen. Our team elaborated firstly a processing method for composites with silicon nitride matrix and carbon nanotube (CNT) reinforcing phase. In this year we continued the investigation of relationships between processing parameters, micro- and nano-structures and properties of CNT, carbon black, graphite, graphene/silicon nitride composites. The silicon nitride nanocomposites systems retained the mechanical robustness of the original systems. Bending strength high as 700-800 MPa was maintained and an electrical conductivity of 18 S/m was achieved in the case of 3 wt% CNT addition. Electrically conductive silicon nitride ceramics have also been realised by carbon black (in order of 1000 S/m) and graphite additions in comparison. These data mean that the percolation trough the CNTs network is providing conductivity, while the ceramics are bonded each to the neighbouring particles providing the mechanical strength. New carbon polymorphs like graphene were introduced to ceramic matrices. A large amount of direct structural observation was carried out by scanning electron microscope (SEM) and transmission electron microscope (TEM). Bright field TEM and SEM images show the graphene located between α-Si_3N_4 grains (Fig. 1) and β-Si_3N_4 grains after sintering (Fig. 2).

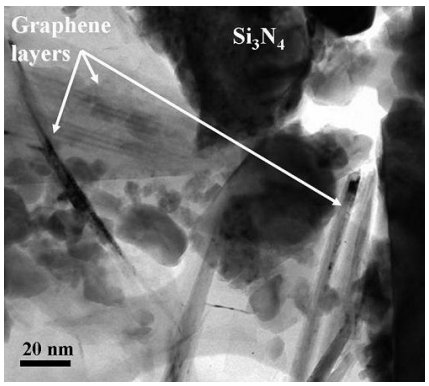

Figure 1 *TEM image of graphene/Si_3N_4 powder mixture prepared by attrition milling.*

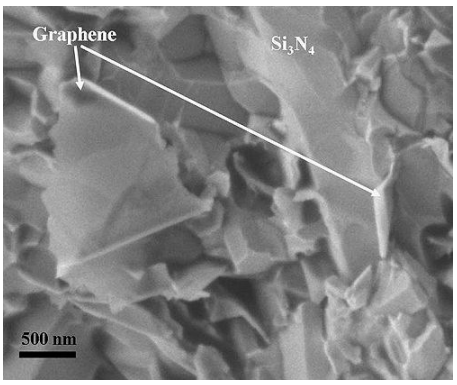

Figure 2 *SEM image shows fracture surface of the sintered graphene/Si_3N_4 composite.*

It is obvious that a composite which is wear resistant, refractory and conductive will be used in a wide region. As an extension of previous investigations tribology tests were conducted to explore the effects of microstructure, the type and quantity of carbon additives and the preparation routes on the behaviour. The new micro tribometer of Thin Films Department was used, Gy Sáfrán and V Zsigmond participated in the measurements. Examined nanocomposites consisted of Si_3N_4 and

C in the proportions of 1 – 10 wt % carbon nanotube (CNT), or carbon black (CB), or graphite, or graphene. The specimens were produced by hot isostatic pressing. Unlubricated ball-on-disk tribology tests with silicon nitride counterface were carried out at room-temperature in ambient atmosphere. The diameter of Si_3N_4 balls was 4,80 mm, the load 5 N, the linear speed 5 cm s^{-1} . Contact profilometer was used to profile the wear tracks. The friction coefficients of the pure Si_3N_4 and Si_3N_4 samples with 3 wt% CNT were about 0,77-0,81. Addition of 10% graphite and 3% CB to Si_3N_4 resulted in friction coefficients about 0,83 and 0,72 respectively (Fig. 3). Si_3N_4 samples with 3% graphene showed distinct lower friction levels of about 0,52 and smaller scatter in measured values. The wear track study (Fig. 4) revealed that high graphite content in the Si_3N_4 matrix caused relatively big wear particles and an uneven wear track. The course of the friction coefficient vs. time/lap plots was found to provide data on some heterogeneity in the surface layer of the ceramic body originating probably from sample processing. Friction values measured at different places on a disk sample were found to converge with increasing number of laps.

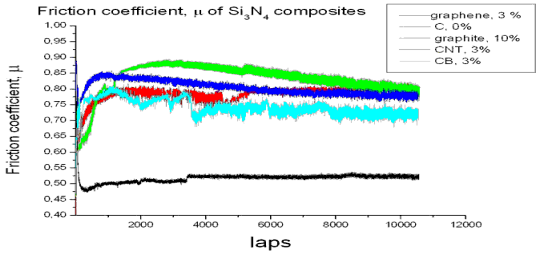

Figure 3 Friction coefficients of Si_3N_4/C composites

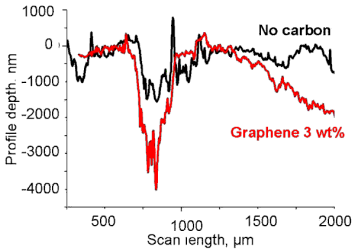

Figure 4 Wear tracks

In order to understand the plots in Fig. 3 and 4 note that the composition of the Si_3N_4 composite component (90% Si_3N_4, 4% Al_2O_3, 6% Y_2O_3) was not varied, consequently the character of the skeleton of the structure also remained and the added carbon phases affected only the kinetics of the densification. This composition is characterised by a structure containing rod-like silicon nitride particles and an oxide phase in the space between them provides the highest strength. This structure has a serious disadvantage, the large pressure during HIP treatment squeezes carbon nanotubes from their positions between ceramic particles, their continuity is disrupted. Consequently all of the carbon phases but for graphene behave similarly at the friction coefficient vs. time/lap experiments. Graphene addition even in smaller amounts was found to have a significant effect on friction and wear properties of Si_3N_4. The shape of graphene sheets and their properties significantly differ from the other carbonaceous material, their application in ceramic matrix composites promises novel set of properties. Our preliminary experiments suggested that the conductivity of graphene containing material is strongly depending on the open porosity, this effect is not characteristic for composites having other additives. This result and the mentioned difference between tribological behaviours suggest that graphene is able to form a second skeleton in ceramic matrices.

Nano hydroxyapatite (HAp) and polymer based bio-compatible nanocomposites

(Supported by OTKA BIOCER, OTKA-NSF-MTA)

Cs. Balázsi, G. Gergely, F. Wéber, I. Lukács, A. L. Tóth., L. Illés, and Zs. E. Horváth

Hydroxyapatite, $Ca_{10}(PO_4)_6(OH)_2$ is chemically similar to the mineral component of bones and teeth. HAp is among of the few materials that are classified as bioactive, meaning that it will support bone in growth and osteointegration when used in orthopaedic, dental and maxillofacial applications. Coatings of hydroxyapatite are often applied to metallic implants, especially stainless steels and titanium alloys to improve the surface properties. HAp can be produced from biogenic materials like coral, seashell, eggshell (Fig. 1), body fluids and some synthetic methods: various techniques were developed for the synthesis of hydroxyapatites, based on solid state reactions, chemical precipitation reactions, hydrothermal reactions, sol-gel methods and mechano-chemical methods using different calcium and phosphorus containing starting materials.

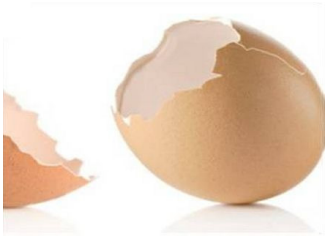

Figure 1 Macroscopic view of eggshell

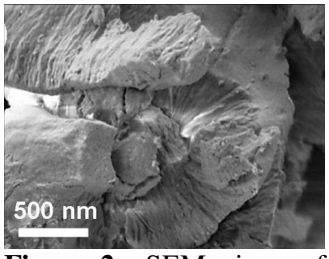

Figure 2 SEM views of eggshell

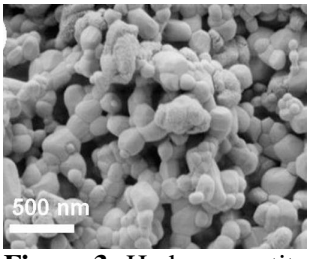

Figure 3 Hydroxyapatite product

Hydroxyapatite may be employed in forms such as powders, porous blocks or beads to fill bone defects or voids. These may arise when large sections of bone have had to be removed (e.g. bone cancers) or when bone augmentations are required (e.g maxillofacial reconstruction or dental applications). The bone filler will provide a scaffold and encourage the rapid filling of the void by naturally forming bone and provides an alternative to bone grafts. It will also become part of the bone structure and will reduce healing times compared to the situation, if no bone filler was used. Coatings of hydroxyapatite are often applied to metallic implants (most commonly titanium/titanium alloys and stainless steels) to alter the surface properties. In this manner the body sees hydroxyapatite-type material which it is easy to accept. Without the coating the body would see a foreign body and work in such a way as to isolate it from surrounding tissues. In our department, hydroxyapatite nanopowders have been produced by using eggshell (Fig. 2) and seashell derived raw materials and phosphoric acid. To synthesise calcium phosphate powders, shells were crushed and milled in a ball milling and an attritor milling set up. The ball milling process resulted in micrometer sized coagulated coarse grains with smooth surface, whereas attrition milled samples are characterised by the nanometer size grains, homogeneous HAp

resulted even after milling. This characteristic morphology is being preserved even after firing at high temperature (Fig. 3).

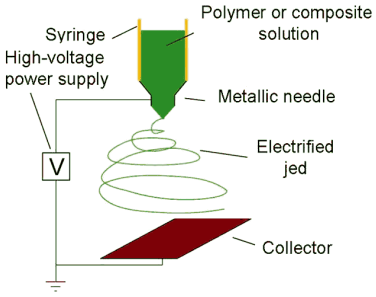

Figure 4 *Schematics of electrospinning*

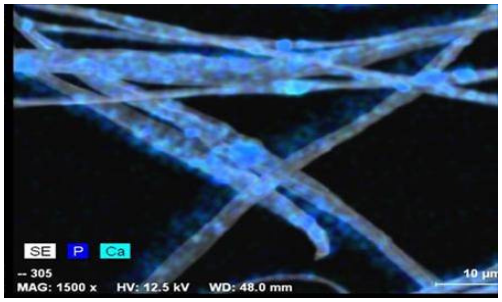

Figure 5 *EDS map of homogeneous distributed HAp particles*

Elaboration processes of the HAP has been developed and applications by electrospinning. Our laboratory started to study various type of ceramic-polymer composites with the relative newly set up purchased by Ceramics and Nanocomposites Department (Fig. 4). Electrospinning gave a three dimensional arrangement of polymer micron and nano fibers. In composites prepared in our laboratories HAP nanoparticles were dispersed in a polymer matrix. Used different type of suspensions by electrospinning technique, biopolymer mats with different structures were produced. Small diameter fibers with big HAp agglomerates were fabricated using acetone and acetic acid. Mats with a bigger diameter size and homogeneous distributed HAp particles were produced by applying acetone and isopropanol (Fig. 5). In vivo experiments (Fig. 6) have been undertaken using rats and rabbit calvaria in the framework of intensive co-operations with Semmelweis University and Hallym University, Korea. MicroCT (micro computer tomography, Fig. 7) results show that nano-hydroxyapatite powders are acting as excellent bone fillers in explicit manner in only 3 weeks.

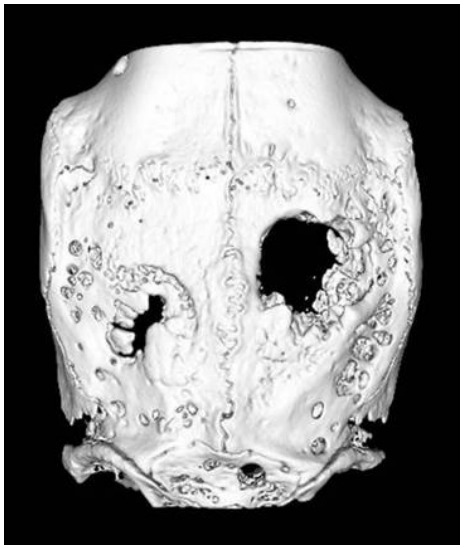

Figure 6 *(LEFT image) Filled areas with nanohydroxy-apatite showing bene-ficial healing (left part) and un-changed reference black hole area (right part).*

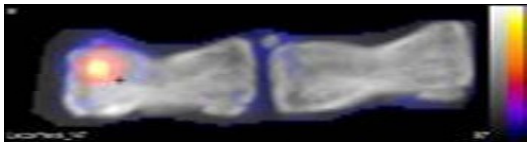

Figure 7 *MicroCT of hydroxy-apatite incorporated in rats (red area).*

Tungsten oxide functional ceramics

(MTA-OTKA-NSF)

Cs. Balázsi, J. Pfeifer, I. Lukács, Z. E. Horváth, and A. L. Tóth

The excellent gas sensing properties of the tungsten oxides have been manifested first of all in nanostructure and 1D, and 2D open structured forms. For optimal performance the sensing layer substrates should be of large specific surface. In this paper we report on electrospinning – a candidate for fabrication of large specific surface tungsten oxide nanofibers. By electrospinning we mean a process to produce nanofibrous material. A solution of polymer (cellulose-acetate) and inorganic addition is put in a syringe, which is controlled by a stepper motor. The solution leaves the needle, and flies to the target (a metal plate) driven by the high voltage switched between the target and the needle. While in the air, the solvent evaporates, and the dry matter forms tissue or dust depending on the recipe. Tungstic acid hydrate (H_2WO_4 H_2O) and the tungsten oxide hydrate ($WO_3.1/3H_2O$) have been added to the polymeric precursor. We analysed the structure of the samples with X-ray diffraction (XRD, Fig. 1) and mapped their morphology with scanning electron microscope (SEM, Fig. 2). The tungsten content of certain fibers was monitored by energy dispersive spectroscopy (EDS, Fig. 3).

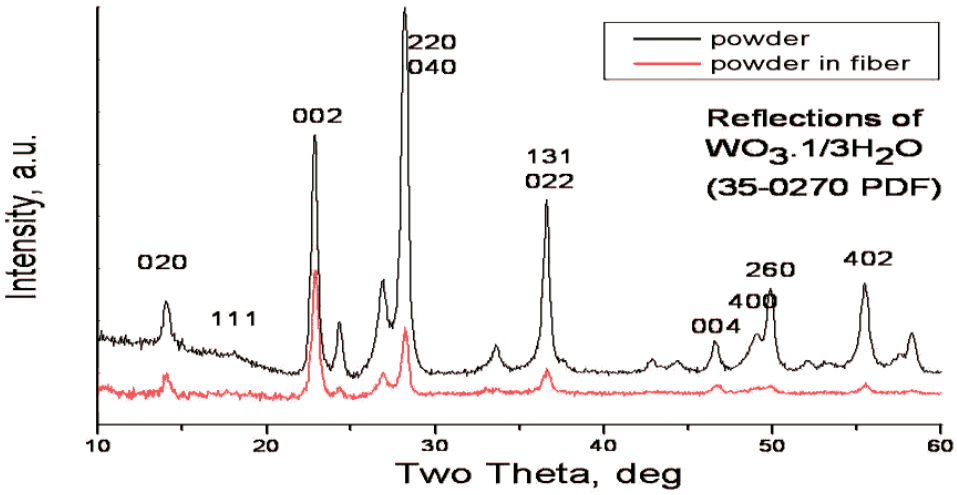

Figure 1 *XRD of CA tissue doped by $WO_3.1/3H_2O$*

A solution of acetone, propanol, cellulose-acetate (CA) and various proportions of tungsten oxide-hydrates were used. The ratio used for the preparation of the shown samples is as follows; acetone: propanol: CA: tungsten oxide hydrate: = 8g:2g:2g:0,5g. In Fig. 2, 3 the tissue contains $WO_3 1/3H_2O$ prepared according to the method suggested in this laboratory.

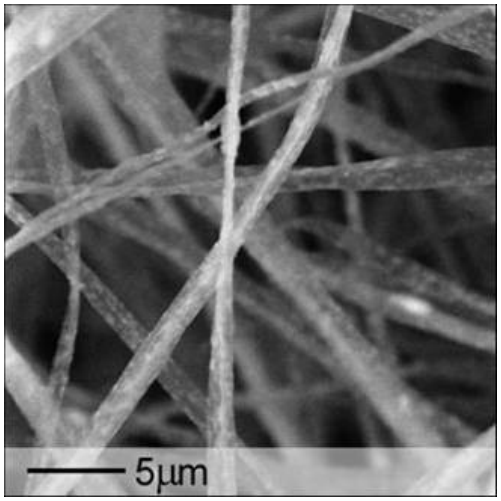

Figure 2 *SEM image of CA tissue doped by $WO_3.1/3H_2O$*

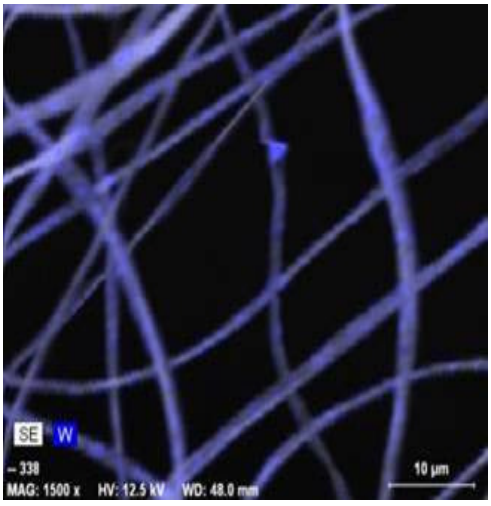

Figure 3 *EDS map of CA tissue doped by $WO_3.1/3H_2O$*

The preparation conditions for the maximal WO_3 content of the CA tissue were found. Due to the WO_3 content the fibers became thinner and rougher. Singular WO_3 particles (of mostly sub micrometer size) are visible in the SEM images. The phase of the WO_3–containing compound is preserved after electrospinning. The EDS maps show the distribution of W in the fibers.
We produced nanofibrous tissues containing reasonable amounts of tungsten oxide by the electrospinning method. With the help of XRD and SEM it was shown that both tungstic acid hydrate and $WO_31/3H_2O$ essentially preserved their original crystal structure and morphology. EDS also proved a satisfactory dispersion of the element W in the fibers.

In this field even an international symposium was organised by our department:

EMRS FALL MEETING Symposium:
Novel bio&chemosensing materials for Health, Safety and Security Applications

The effect of solution concentration on nanowire morphology grown by wet chemical technique

(OTKA K76287)

N. Q. Khánh, J. Volk, I. Lukács, A. Deák, Gy. Sáfrán, and R. Erdélyi

ZnO as a biocompatible, wide band gap semiconductor is a very promising candidate material for biosensor application. One of its advantages is the ability of ZnO nanostructures to grow by such a simple, low temperature, economical method like a wet chemical technique. As for biosensor application thin ZnO nanowires with high aspect ratio are preferable to improve the sensitivity of the sensor via increasing of the surface to volume ratio. Our present work focuses on the investigation of the effect of the solution concentration on the morphology of the wet chemically grown nanostructures, and hence development an effective route for growth of thin ZnO nanowires with extremely high aspect ratio.

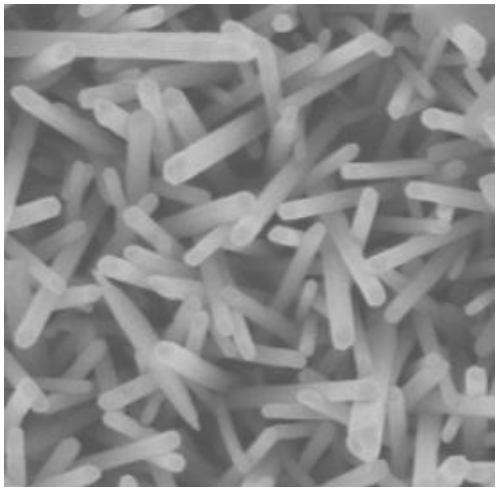

Figure 1 *Plan-view FESEM image of ZnO nanorods grown in 20 mM aqueous zinc nitrate/(HMT) solution at 95 °C for 13.5 h (2x2 μm² image)*

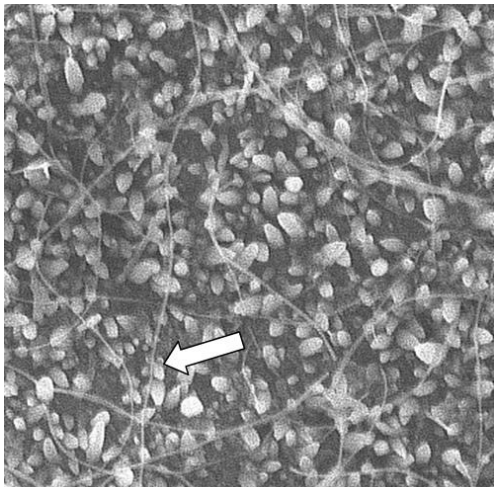

Figure 2 *Plan-view FESEM image of ZnO nanowires grown in 1 mM aqueous zinc nitrate/(HMT) solution at 95 °C for 13.5 h (2x2 μm² image)*

Using zinc nitrate and hexamethylen-tetramine (HMT) equimolar aqueous solution at 95 °C for 13 hour growth with RF sputtered ZnO substrates, relatively high concentration (20 mM) resulted in quasi vertical ZnO nanorods measuring 70-80 nm in diameter and about 2 μm in length (Fig. 1). The top of these rods are rather flat and has a hexagonal shape indicating that the growth took place in direction of *c*-axis (0002 plane). The flatness of the top is missing, when the concentration of precursors decreased to 5 mM. Instead, nanorods with average diameter of 60 nm and 800 nm length are pointed at their tip. At low concentration (1 mM) only very short rods

could grow (Fig. 2). Their average diameter and length are around 50 nm and 170 nm, respectively. Besides, many long nanowires laying randomly on the surface of

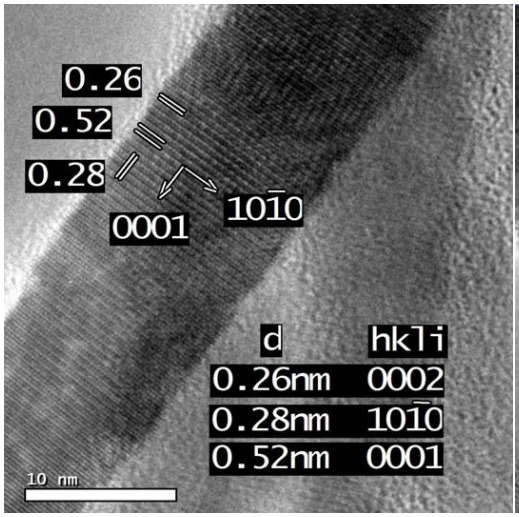

Figure 3 *HRTEM image of ZnO nanowire grown in 1 mM aqueous zinc nitrate/(HMT) solution at 95 ^{o}C for 13.5 h.*

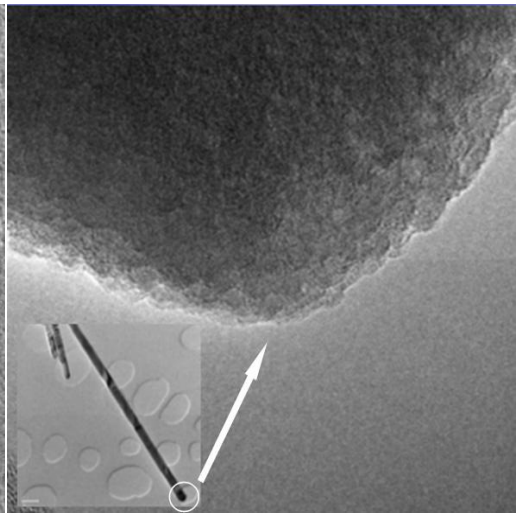

Figure 4 *HRTEM image of ZnO nanorod grown in 20 mM aqueous zinc nitrate/(HMT) solution at 95 ^{o}C for 13.5 h. Low resolution TEM image shown by the inset*

the substrate can be observed. The wire shown by the arrow in Fig. 2 has 16 nm diameter and 3 μm in length giving the aspect ratio ~ 200. The sample grown at 0.2 mM (not shown here) reveals the same character like the 1 mM one, but the density of the nanowires is less. On the high resolution TEM image of the nanowire (Fig. 3) the lattice fringes can be clearly seen. The lattice spacing of 0.52 nm perpendicular to the longitudinal axis of the wires confirms the growth in *c*-axis. The same character was found for the rods (Fig. 4).

Electromechanical characterisation of vertically grown ZnO nanorods

(OTKA PD77578)

J. Volk, R. Erdélyi, and I. E. Lukács

ZnO nanowires and nanorods (NW/NR) attract a great interest not only for photonic applications but also for electromechanical sensors and for energy converters. Wang et al., for instance, demonstrated a nanogenerator that draws energy from the ambient environment and produces DC current. They ascribed the origin of the operation to the internal electric field which is built up between the compressed and tensed sides of the bent piezoelectric nanowire (Fig. 1). However, their explanation is still under debate. In the used model the significant conductivity of the nanowires (ρ=0.01-1 S/cm), as well as the weak rectifying property of the top contact is ignored.

Our work, which is supported by OTKA foundation and started in April 2009, aims to make a systematic mechanical, electrical, and coupled electromechanical investigation on ZnO NR/NW. The main goal of 2009 was to establish in house all the necessary techniques for the fabrication, simulation, and characterisation of ZnO nanorods.

The highly ordered vertical NR arrays were grown by using a direct writing lithographic method and low temperature (T=85 °C) aqueous chemical growth. Due to the dose optimisation, carried out on our electron beam lithography system the homogeneity of the arrays (Fig. 2) is now comparable with that of the earlier ones fabricated by J. Volk on state-of-the-art facilities in Japan between 2006-2007.

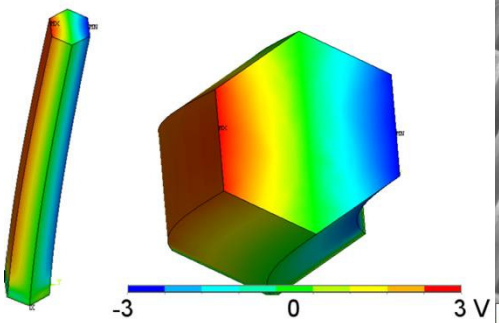

Figure 1 *Electric potential distribution in a curved ZnO nanowire calculated by finite element analysis*

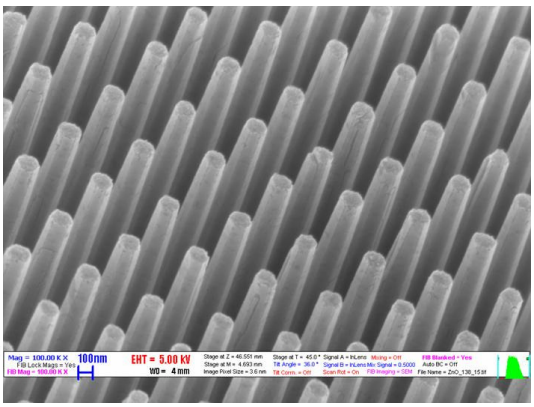

Figure 2 *Scanning electron micrograph on highly ordered ZnO nanowire array*

The mechanical test, which was carried out by a nanomanipulator arm mounted in a scanning electron microscope revealed that the epitaxial nanorods are surprisingly robust. The quantitative mechanical analysis is still in progress. The electrical characterisation on vertically standing NRs was carried out by conductive AFM technique (Smart SPM 1010), where the probe-tip was coated with Cr/Au conductive bilayer. The results show Schottky-type characteristics on Au/ZnO substrate as well as on Au/ZnO NR interface, the calculated resistivity of the NR is about 70 Ωcm (Fig. 3). In order to obtain a more robust and Ohmic-type top contact in some cases the NR arrays were at first embedded in a spin-coated polymer layer and partially etched back by oxygen plasma. The NRs protruded 100-300 nm from the polymer top-surface were contacted by thermally evaporated Cr/Au bilayer. The obtained structures show indeed linear I-V curves. Another method to determine the electrical behaviour of the single NWs/NRs is illustrated in Fig. 4. There, the NW is transferred from its origin to an insulating surface and is contacted with two or four Cr/Au wires to extended contact pads by using e-beam lithography and subsequent metal deposition step. The contacted nanocrystals show surprisingly high electrical resistance, which may be ascribed to an insulating interfacial layer between the metallization and the ZnO NW.

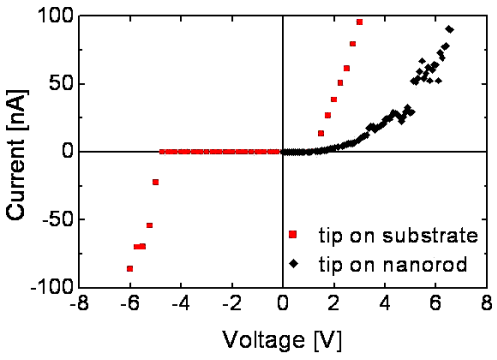

Figure 3 *Current-voltage curves taken by a conductive AFM tip on ZnO substrate and on ZnO nanorod*

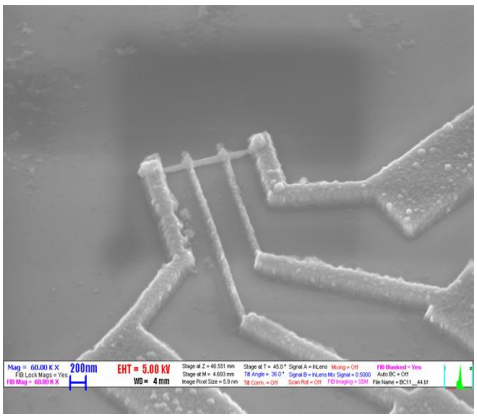

Figure 4 *Contacted lateral ZnO nanowire fabricated by e-beam lithography*

In 2010 the participants intend to continue the described methods and make systematic mechanical and electrical measurements on several NWs/NRs. The wet-chemically grown nanocrystals will be compared to nanorods which are produced by vapour-liquid-solid (VLS) or vapour-solid (VS) type dry process.

TEM lamella preparation by FIB

A. L. Tóth, L. Illés, Gy. Sáfrán, and G. Z. Radnóczi

The transmission electron microscopy (TEM) is one of the most versatile methods of the visualisation and investigation of micro- and nanosized structures. The nanoparticles naturally are thin enough to be transparent for TEM observation, but due to the strong electron-solid interaction the bulk materials have to be thinned. Aiming to reach this submicrometer thickness several methods have been developed during the decades.
The MFA successfully applied the TEM for thin film research, not only using, but inventing ion beam thinning methods to obtain foils of different structures with a quality second to none.

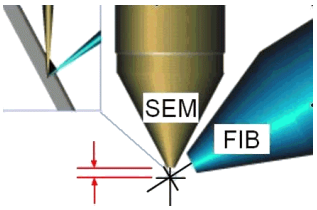

Figure 1 *Scheme of the LEO 1540XB cross beam system*

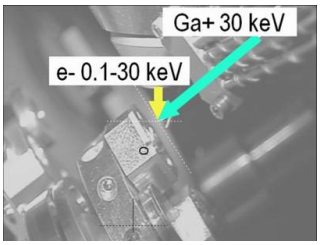

Figure 2 *View of the specimen chamber with the beam paths*

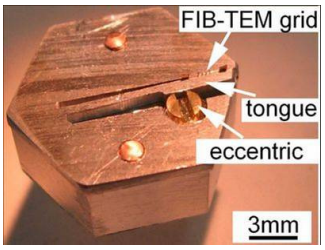

Figure 3 *TEM grid sample holder of the LEO1540XB (5)*

As the nanoresearch reached the technology in the nineties, it became more and more important to cut cross sectional TEM samples from a given place of a larger structure – as a specific transistor of an IC, or GB of a nanostructured bulk material.
In spite of the impressive number of methods, practically only one of these methods, namely the FIB allows to localise the area to be thinned with micrometer accuracy on the macrosized sample surface. In the FIB a high energy Ga ion beam of 10-100 nm diameter is used for local sputtering. Using programmable raster scanning, it is relatively easy to cut the characteristic butterfly shaped pits of the TEM lamella preparation (Fig. 4).
Even more flexible approach is the cross beam system (Fig. 1-3) where the thinning process of FIB can be positioned and even monitored by a high resolution FEG-SEM avoiding even the minimal etching of the low intensity ion beam, used in single column FIB instrument. Installing a LEO 1540XB in the MFA, the need of TEM lamella preparation became more and more reasonable. However the rough FIB shaping (cutting the holes with a 2 um thick lamella under the protective Pt layer, as shown in Fig. 4), the fine milling (below 500 nm, - Fig. 5) and the cut out of the lamella are only the first half of the preparation. It has to be lifted out and fixed onto TEM grid inside the SEM chamber. However these, seemingly primitive steps require nanomanipulators, special glue and lot of practice (Fig. 6-7). The final thinning can be made on the TEM grid (Fig. 8). After these requisites came up in 2009 the arsenal

of our TEM sample preparation has got a new method, as the TEM image of Fig. 9 illustrates.

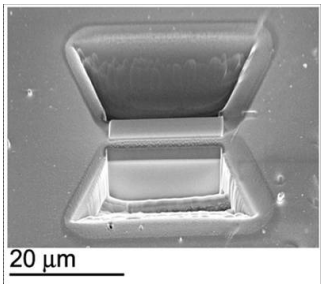

Figure 4 *Rough shaping of TEM lamella with protective Pt deposition in the middle*

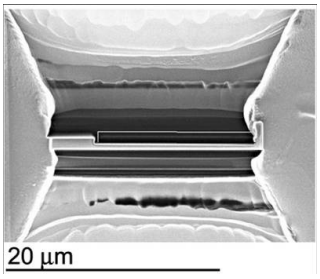

Figure 5 *Fine milling from ı um to 500 nm*

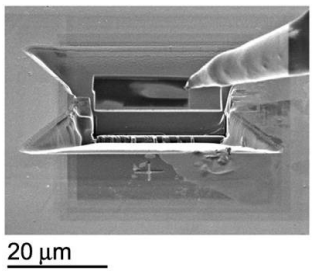

Figure 6 *Liftout the lamella using nanomanipulator and SEM*

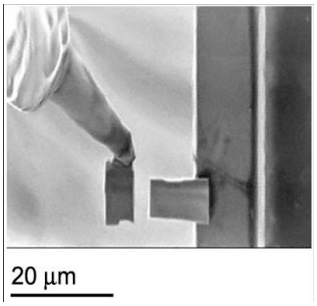

Figure 7 *Fixing to the grid and cut from the tip*

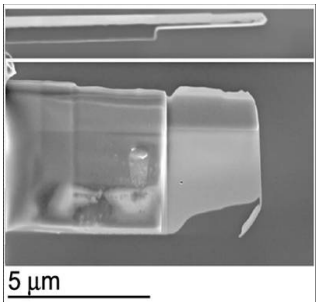

Figure 8 *Final thinning on the grid to 100 nm thickness*

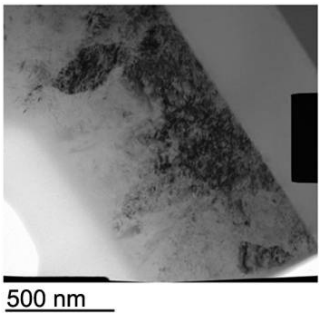

Figure 9 *TEM result*

The availability of the different ion beam techniques ensures, that the well known thick amorphized layer of the 30 keV Ga^+ FIB can be reduced to around 2 nm using subsequent low (100-300 eV) energy Ar^+ bombardment, illustrating how can the different techniques help each another aiming the visualisation of previously unseen phenomena.

Complex Systems Department

Head: György SZABÓ, D.Sc., scientific advisor

Research Staff

- István BORSOS
- Imre EÖRDÖGH, dr. Univ.
- Zoltán JUHÁSZ, Ph.D.
- Levente MOLDVAI, engineer
- Géza ÓDOR, D.Sc., scientific advisor
- Károly SZÁSZ, engineer
- Attila SZOLNOKI, Ph.D.

Ph.D. students / Diploma workers

- Jeromos VUKOV, Ph.D. student
- Lívia HANUSOVSZKY, B.Sc. student

The main scientific activity is focused on the statistical physics of different non-equilibrium systems. In collaboration with Heinig and Liedke (FZD, Rossendorf) Géza Ódor developed a driven lattice gas model of oriented dimers to study surface growth processes. This research will be continued within the framework of a two-year DAAD/MÖB project. Besides it, in collaboration with Dickman (Belo Horizonte, Brazil) Ódor investigated the main features of a phase transition to an absorbing state on one-dimensional systems when triplets of particles can create additional particles on the analogy of the contact process. The traditional contact process is also studied with Juhász (SzFKI, Budapest) on a set of small world networks.

Utilising the concepts and tools of non-equilibrium statistical physics the main scientific efforts of this group are concentrated on the investigation of evolutionary games. Many aspects of social dilemmas are studied by Szabó, Szolnoki, and Borsos in collaboration with Perc (Maribor, Slovenia), Vukov (Lisbon, Portugal), Droz (University of Geneva), Szwabinski (University of Geneva), Stark (ETH, Zürich), and Helbing (ETH, Zürich). In these mathematical models players are distributed on the sites of a lattice (or graph) and following one of the possible strategies (e.g., co-operation or defection) their income comes from games with the neighbours. For the evolutionary games the players are allowed to modify their strategy according to a dynamical rule (e.g., by imitating one of their better neighbours). We studied what happens if the players are different in the efficiency of strategy transfer (convincing capability). It is found that the motion of influential players can increase the frequency of co-operators even for their low densities on a two-dimensional lattice via a mechanism described first on scale-free graphs. The co-evolution of reputation (teaching or convincing activity) proved to be another possibility to support co-operation in the society of selfish players. The investigations of the evolving reputation showed the relevance of some dynamical details promoting the co-operative behaviour. Besides it, the co-evolutionary games were extended by

allowing the players to adopt both the strategy and noisy dynamical rule from one of their better neighbours. In agreement with our expectation this co-evolutionary rule drives the system towards a stationary state where all the players follow the same dynamical rule providing an approximately optimum frequency of co-operators under the given conditions including strategies, payoffs, connectivity structure, etc. Systematic simulations and analytical treatments were performed to clarify the effect of punishment (quantified by its cost and fine on defecting individuals) for spatial public goods games. Very recently we have begun to study a new version of evolutionary games where small groups of players choose new strategies in a co-ordinated way to maximise the group's income. This evolutionary rule extended significantly the territory of co-operation on the plane of payoff parameters for the social dilemmas.

In collaboration with Tomé and de Oliveira (University of Sao Paulo) Borsos and Szabó studied the structure of probability currents between possible configurations on a small cluster of sites for non-equilibrium two-state lattice systems. In addition an algorithm is suggested to estimate the specific entropy production characterising the deviation from the detailed balance.

Juhász and Sipos (Institute for Musicology, Budapest) developed a computer algorithm for the motive identification in large folk song corpora. This method is based on a dynamic time warping algorithm by determining inherent repeated elements of the melodies and on a self-organising map that learns (and recognises) the most typical motive contours. Using this system the typical motive collections of 22 national music cultures in Eurasia were determined. The analysis of the overlaps for the national melodies on the common map allowed us to draw a graph of connections exhibiting two distinct groups in agreement with the expectations based on geographical distribution (and history). Recently this method is applied to quantify the connections between languages.

Within this department a small group of engineers (Eördögh, Szász, and Moldvai) developed a new image processing algorithm for detecting porosity in ceramic materials. This development included the application of a high resolution line scan camera, software implementation, and test of accuracy and reproducibility on different GE (General Electric) ceramic tubes and accessories. This knowledge was utilised in the checking and reparation of quantitative microscopy equipment for the quality control of filter papers in the primary circle installed at Atomic Power Plant Paks. Continuing the previous developments the parameters of their 3D motion control software module was improved and technological experiments were performed for designing flexible calibration cables (within an R&D project in the factory Axon).

The above scientific results were published in international journals. Besides it the members of this research group held 9 invited and 3 poster lectures on conferences and 6 seminars at different universities. The international echo to the previous results of this group is characterised by the 900 citations received during the last two years. The senior researchers wrote 76 Referee Reports on scientific papers and reviewed 3 DSc and 4 PhD theses in this year.

Evolution of adoption rules in spatial social dilemmas

(Hungarian Scientific Research Fund under Grant No K-73449)

G. Szabó, A. Szolnoki, I. Borsos, and J. Vukov

Most of the games represent simplified real-life situations and help us to find an optimum action. Due to the simplifications the players have only a few options to choose and the corresponding incomes are quantified by a payoff matrix allowing us to apply the tools of mathematics. The theory of games has been used successfully both in economics and political decisions. Subsequently the concept of payoff matrix is adopted by biologists to quantify the effect of species interactions on their fitness in the mathematical models of Darwinian evolution. Nowadays the evolutionary game theory provides a general mathematical framework for the investigation of multi-agent systems used widely in economy and other social sciences. The application of the concepts and tools of non-equilibrium statistical physics gave a relevant boost in the systematic investigations of these systems.

In the simplest spatial models players are distributed on the sites of a square lattice and their income comes from games played with the neighbours. Within the context of social dilemmas the players can follow only one of the two strategies called co-operation C and defection D and their payoff depend on their strategies. During the evolutionary imitation process a randomly chosen player x can adopt the strategy from one of the neighbours (y) with a probability $W=1/(1+\exp(P_x-P_y)/K_x)$ dependent on the payoff difference (P_x-P_y) and a noise parameter K_x characterising the stochasticity in the imitation process. In the previous models all the players used the same dynamical rule in their strategy adoption. Now this model is extended by allowing the players to use different adoption rules quantified by a set of possible K_x values and this personal feature can also be adopted on the analogy of strategy imitation with the same payoff-dependent probability. Our analysis is focused on those cases when the mutual co-operation (defection) yields unit (zero) payoffs for the equivalent players while the defector receives b again a co-operator who gets nothing. For b>1 this game represents a weak Prisoner's dilemma where the intelligent (selfish) players are enforced to choose D providing the lowest total payoff for them. In this case the individual interest is in conflict with the common one and the selfish individual behaviour drives the well-mixed community into a state (called "tragedy of the community") where the players try to exploit each other.

Initially the players use either C or D strategy and one of the possible adoption rules quantified by the possible K_x values. Due to the co-evolutionary process the system evolves into a final stationary state characterised by the portion of co-operators and a distribution of K_x values. It turned out that the C and D strategies coexist and all the players use the same adoption rule in the final state for most of the cases. Figure 1 shows the time-dependent portion of players who use one of the five possible

dynamical rules. The corresponding K_X values are indicated by coloured circles within the *b*-*K* phase diagram (see the inset) where the solid line separates the region of *C*+*D* coexistence and territory of homogeneous defection (*D*).

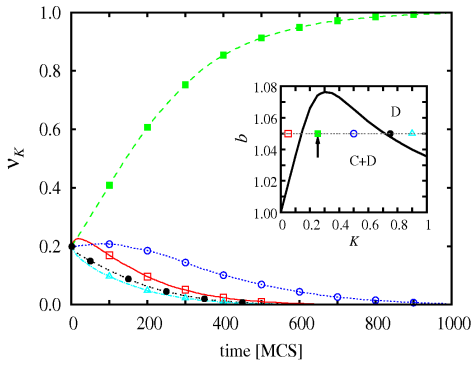

Figure 1 *Time-dependent frequency of players using one of the five possible rules for b=1.05 allowing the coexistence of C and D strategies.*

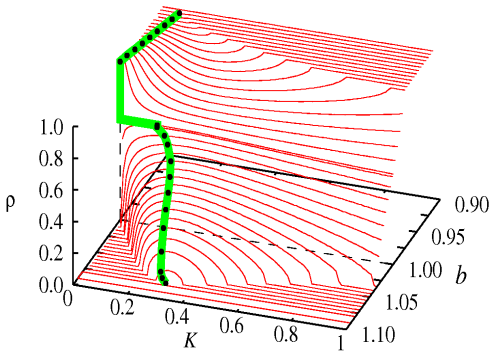

Figure 2 *The black bullets indicates the favored rule (K) and the corresponding frequency of cooperators selected by the coevolutionary rule for different values of temptation b.*

In Figure 2 the red lines denote the portion of co-operators when varying the value of noise level *K* for different values of temptation *b* in a society where all the players use the same evolutionary rule characterised by *K*. Notice that in this co-evolutionary game the Darwinian selection favours those noise levels that optimise approximately the frequency of co-operators in the region of Prisoner's Dilemma. For the case of Stag Hunt game the Darwinian selection favours the minimal noise level appearing within the region of coexistence of *C* and *D* strategies. The analytical techniques of non-equilibrium statistical physics were capable to reproduce the above numerical results with an adequate accuracy.

The application of the above idea of co-evolutionary games seems to be a suitable tool to find those region of model parameters (including connectivity structures, payoffs, evolutionary rules, strategy set, etc.) which play distinguished role in the real systems. At the same time these investigations raise many questions about the model features favouring homogeneous or inhomogeneous characteristics for the players.

Motive identification in 22 folksong corpora using dynamic time warping and self organising maps

(Hungarian Scientific Research Fund under Grant No K-63312)

Z. Juhász

A system for automatic motive identification of large folksong corpora is described in this article. We want to find the most frequently appearing motive types in a well defined melody corpus, with the assumption that each motive type may have several variants. However, the repetition inside a melody can also be considered as an indication of a motive. Therefore, we suppose two possible detection modes of the motives. In addition to the "culture-defined" motive identification, based on the frequent appearance in different songs, we also suppose the existence of the "melody-defined" identification which is based on the repetitions inside the melodies.

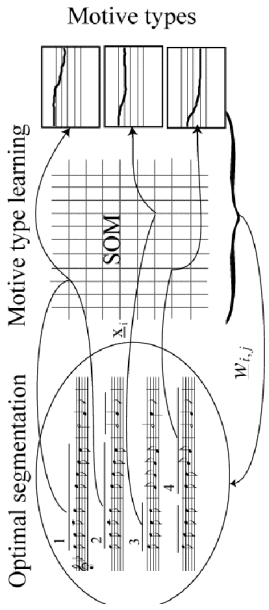

Figure 1 *The learning system for motive identification.*

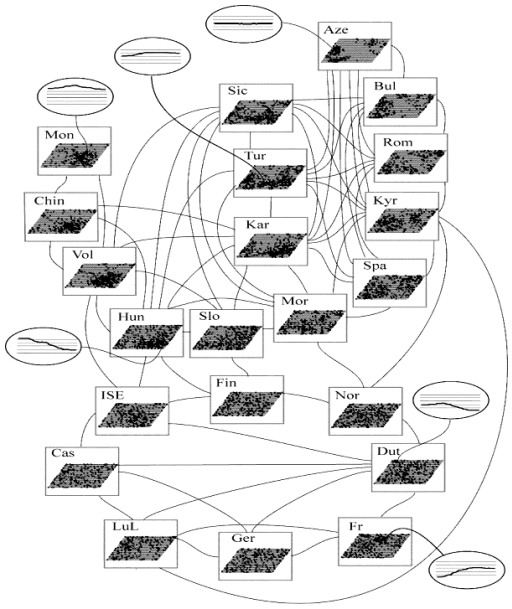

Figure 2 *The graph of deterministic relations of 22 musical cultures in Eurasia.*

The learning unit of the system described in this paper is a self organising map (SOM), trained by the contour functions of the motives. The motive identification in a given melody is accomplished in two steps. Firstly we determine the repeating elements of the melody by an algorithm based on dynamic time warping. After that, the remaining melody parts are analysed using a self organising map, which learns and identifies the most frequently appearing patterns as "culture-defined" motives. The system operation is demonstrated in Fig. 1.

Our current possibilities allowed us to set up 22 folksong corpora, each of them consisting of 600-2400 melodies, representing Hungarian, Slovak, Moravian, Chinese, Mongolian, Kyrgyz, Mari-Chuvash-Tatar, Karachay-Balkar, Anatolian Turkish, Azeri, Sicilian, Spanish, Rumanian, Bulgarian, Polish - Cassubian, Finnish, Norwegian, German, Luxembourgian-Lotharingian, French, Dutch and Irish-Scottish-English musical traditions. To construct the national/areal motive type sets, we first had to deduce the characteristic motive contour type collections for each of the 22, by training 22 SOM-s of size 20*20 lattice points separately. After determining the 22 national/areal motive contour type collections, a new large self organising map of size 30*30 was trained by the united set of them, in order to determine the set of all possible motive contour types appearing anywhere in the 22 cultures.

This common SOM allows us to classify all motive types of a given national/areal collection on it. We call this process "excitation of the common map by a culture". These excitations activate different patterns on the common SOM, and the analysis of the overlaps lead to a comprehensive picture of the cross contact of our 22 melody corpora. The graph of the system of closest relationships is summarised in Figure 2, where a connection line indicates the deterministic contacts between musical cultures. The nodes of the graph show the excited area of the common SOM by the 22 national/areal motive collections. Some typical motive types belonging to the most important parts of the map are also indicated in round windows.

This analysis clarified that "Eastern" cultures prefer motives in high regions of the melody, generally moving between the octave and the fifth as well as fourth, while the "Western" melodies prefer motives connecting the tonic to a fifth or a fourth beyond the tonic. The combined analysis of the contact probabilities and the overlaps of the national/areal patterns indicated several distinguishable branches among the Eastern cultures. The Mongolian-Chinese-Volga branch highly prefers motives in high, while the Sicilian-Turkish-Karachay branch evaluates a balance between these high motives and those of an explicitly low ambit. The close contacts of Hungarian, Slovak and Moravian cultures to these two distinguishable branches are based mainly on the high motive types. At the same time, the high motive types gradually disappear in the Spanish-Kyrgyz-Romanian-Bulgarian-Azeri branch, while the dominance of motives of low ambit connects them to the Sicilian-Turkish-Karachay branch.

Not forgetting the simplifications made during the application of our technique, we can state that the motive analysis allowed us to draw a rather perspicuous picture of the cross-cultural connections of different folksong cultures. We hope that these results may demonstrate the feasibility of an extended research of "musical linguistics", and suggest an efficient and quantitative tool for "melody mining", using artificial intelligence and other mathematical tools.

ACTIVITIES

MFA Seminar Talks

14 January 2009 **Vlado LAZAROV**
(University of Oxford, Oxford, UK): "*Structure and properties of Iron-Oxide films grown by MBE*"

21 January 2009 **Géza ÓDOR**
(MTA MFA, Budapest, Hungary): "*Mapping of surface growth onto two-dimensional driven lattice gas model*"

23 January 2009 **Spas D. KOLEV**
(University of Melbourne , Melbourne, Australia): "*Application of polymer inclusion membranes in the industrial and analytical separation of metal ions*"

11 February 2009 **Valeriu CHIRITA**
(Linköping University, Sweden): "*A formula for increased strength in TiN-based ternary and quaternary compounds*"

18 February 2009 **Péter PETRIK**
(MTA MFA, Budapest, Hungary): "*The new Woollam M-2000DI spectroscopic ellipsometer: properties and applications*"

26 February 2009 **Ágoston NÉMETH**
(MTA MFA, Budapest, Hungary): "*Investigation of ZnO thin layer structures*"

15 April 2009 **Jean Pol VIGNERON**
(Facultés Universitaires Notre-Dame de la Paix, Namur, Belgium): "*Photonic crystal reflectors in living organisms*"

22 April 2009 **György SÁFRÁN**
(MTA MFA, Budapest, Hungary): "*The tribology laboratory at MFA, first experiences with the CSM microtribometer*"

13 May 2009 **Fanni MISJÁK**
(MTA MFA, Budapest, Hungary): "*Structure formation in multiphase thin films*"

20 May 2009 **Krisztián KERTÉSZ**
(MTA MFA, Budapest, Hungary): "*Investigation of photonic crystal type structures of biological origin*"

17 June 2009	**Enikő HORVÁTH** (MTA MFA, Budapest, Hungary): "*Nanofabrication using electron and ion beam-assisted deposition techniques and characterisation with microanalytical and microelectrical methods*"
24 June 2009	**Cesare FRIGERI** (CNR-IMEM, Parma, Italy): "*Structural instability of hydrogenated a-Si/a-Ge multilayers prepared by sputtering*"
01 July 2009	**Krisztián PALOTÁS** (Budapest Univ. of Technology and Economics, Hungary): "*Detection of giant magnetic contrast on Co nano-islands using spin-polarised STM: the effect of the chemical nature of the tip*"
04 August 2009	**A. SUBRAHMANYAN** (Indian Institute of Technology, Madras, India): "*Results on high efficient tungsten oxide based electrochromics*"
26 August 2009	**Anita PONGRÁCZ** (MTA MFA, Budapest, Hungary): "*Silicon carbide nanocrystals on silicon*"
02 September 2009	**Ján DUSZA** (Institute of Materials Research, Kosice, Slovakia): "*Silicon nitride and aluminum oxide based nanocomposites*"
23 September 2009	**Wolfgang REHM** (Technische Hochschule, Munich, Germany): "*Aging behaviour of PV-modules of a 1 MW PV-plant*"
28 October 2009	**Ferenc BELEZNAY** (MTA MFA, Budapest, Hungary): "*The Nobel Prize in physics 2009*"
11 November 2009	**György KÁDÁR** (MTA MFA, Budapest, Hungary): "*The Casimir effect and NEMS*"
25 November 2009	**János VOLK** (MTA MFA, Budapest, Hungary): "*Application of new nanofabrication tools at MFA presented on ZnO nanowires*"
09 December 2009	**Géza MÁRK** (MTA MFA, Budapest, Hungary): "*Short range and long range order in photonic crystal type nanoarchitectures of biological origin: relationship between the structure and colours*"

Research and Development Partners

ALVES, Eduardo *(Instituto Technológico e Nuclear, Sacavém, Portugal)*

ARIAKE, Jun *(Akita Research Institute of Advanced Technology (AIT), Akita, Japan)*

BACAKOVA, Lucie *(Institute of Physiology, Prague, Czech Republic)*

BARABAS, Reka *(Babes-Bolyai University, Cluj Napoca, Romania)*

CALDERON-MORENO, Jose *(Univ. Politecnica de Catalunya UPC, Barcelona, Spain)*

CHANG-HOON, Chae *(Clinical Dentistry, Hallym University, Seoul, Korea)*

COLLINS, Robert W. *(University of Toledo, USA)*

DICKMAN, Ronald *(Departamento de Fisica and National Institute of Science and Technology of Complex Systems, ICEx, Universidade Federal de Minas Gerais, Belo Horizonte-Minas Gerais, Brazil)*

DUB, Sergei *(Institute of Superhard Materials (UAS), Kiev, Ukraine)*

FILIZ, Cinar *(Prof. Adnan Tekin High Tech. Cer. and Comp. Res. Center, Istanbul, Turkey)*

GOLDSTEIN, Robert *(Goldstein, Institute of Problems in Mechanics, Moscow, Russia)*

GOUMA, Pelagia-Irene *(Stony Brook State University - SUNY, Stony Brook, NY, USA)*

GULBINSKY, Witold *(Koszalin University of Technology, Institute of Mechatronics, Nanotechnology and Vacuum Technique, Koszalin, Poland)*

GYEKENYESSI, John *(NASA Glenn Research Center, Cleveland, USA)*

HEINIG, Karl-Heinz *(FZD, Rossendorf, Germany)*

HERRMANN, Mathias *(Fraunhofer IKTS Fraunhofer-Institut für Keramische Technologien (IKTS), Dresden, Germany)*

HULTMAN, Lars *(Thin Film Physics department of Linköping University, Sweden)*

IMRE, Alexandra *(Argonne National Laboratory, Argonne, USA)*

JABLONSKI, Alex *(Institute of Chemical Physics, Polish Academy of Sciences, Warsawa, Poland)*

KOLITSCH, Andreas *(Istitute of Ion Beam Physics and Materials Research, Dresden-Rossendorf, Germany)*

KOVACS, Janez *(Jozef Stefan Institute, Ljubljana, Slovenia)*

LIEDTKE, Volker *(Austrian Research Centers, Seibersdorf, Austria)*

MALHERBE, Johan *(University of Pretoria, Pretoria, Republic of South Africa)*

NUTSCH, Andreas *(Fraunhofer Institut für Integrierte Systeme – Bauelementetechnologie IISB, Erlangen, Germany)*

ONURALP, Yucel *(Prof. Adnan Tekin High Tech. Cer. and Comp. Res. Center, Istanbul, Turkey)*

OSSI, Paolo, M *(Politecnico di Milano, Department of Energy, Milano, Italy)*

OZKAN ZAYIM, Esra *(Physics Department, Istanbul Technical Univ., Istanbul, Turkey)*

PADTURE, Nitin *(Ohio State University, Columbus, USA)*

PARK, Jun-Woo *(Department of Oral and Maxillofacial Surgery, Sacred Heart Hospital, Hallym University, Seoul, Korea)*

PAULEAU, Yves *(National Polytechnic Institute of Grenoble, CNRS-LEMD, France)*

PERC, Matjaz *(University of Maribor, Maribor, Slovenia)*

PIETRALUNGA, Silvia *(CoreCom, Milano, Italy)*

PISCHOW, Kaj *(Savcor Ltd., Mikkeli, Finland)*

SHIKIMAKA, Olga *(Institute of Applied Physics (MAS), Kisinev, Moldavia)*

SIPOS, János *(Institute for Musicology, Budapest, Hungary)*

SKORUPA, Wolfgang *(Forschungszentrum Dresden-Rossendorf, Dresden, Germany)*

STOEMENOS, John *(Aristotle University of Thessaloniki, Thessaloniki, Greece)*

STUART, Hampshire *(Materials Ireland Research Institute, Limerick, Ireland)*

SYLVESTRE, Alain *(National Polytechnic Institute of Grenoble, CNRS-LEMD, France)*

SZEKERES, Anna *(Institute of Solid State Physics, Sofia, Bulgaria)*

TOU, Teck Yong *(Faculty of Engineering, Multimedia University, Selangor, Malaysia)*

TRUSSO, Sebastiano *(Istituto per i Processi Chimico-Fisici – del Consiglio Nazionale delle Ricerche, Messina, Italy)*

VÁVRA, Ivo *(Department of Superlattice, Institute of Electrical Engineering Slovak Academy of Sciences, Bratislava, Slovak Republik)*

WAKAYAMA, Yutaka *(National Institute for Materials Science, Tsukuba, Japan)*

ZHIJAN, Shen *(Arrhenius Laboratory, Stockholm, Sweden)*

ZHURAVLEV, K.S. *(Russian Academy of Sciences Novosibirsk, Institute of Semiconductor Physics, Novosibirsk, Russia)*

Visitors

CAMPELJ, Stanislav *(Josef Stefan Institute, Ljubljana, Slovenia)*

CENIGA, Ladislav *(Institute of Materials Research (IMR), Kosice, Slovakia)*

DUSZA, Jan *(Institute of Materials Research (IMR), Kosice, Slovakia)*

FORTUNIER, Pascal *(Centre National Detudes Spatiales (CNES), Courcouronnes, France)*

HEGEDUSOVA, Lucia *(Institute of Materials Research (IMR), Kosice, Slovakia)*

HEINIG, Kerl-Heinz *(FZD, Rossendorf, Germany)*

IMRE, Alexandra *(Argonne National Laboratory , Chicago, USA)*

LIEDKE, Bartosz *(FZD, Rossendorf, Germany)*

NUTSCH, Andreas *(Fraunhofer Institut für Integrierte Systeme – Bauelementetechnologie)*

OVTAR, Simona *(Josef Stefan Institute, Ljubljana, Slovenia)*

PECHEVA, Emilia *(Institute of Solid State Physics, Sofia, Bulgaria)*

PERC, Matjaz *(University of Maribor, Maribor, Slovenia)*

PRAMATOROVA, Lyliana *(Institute of Solid State Physics, Sofia, Bulgaria)*

PRIMC, Darinka *(Josef Stefan Institute, Ljubljana, Slovenia)*

SZEKERES, Anna *(Institute of Solid State Physics, Sofia, Bulgaria)*

WAKAYAMA, Yutaka *(National Institute for Materials Science (NIMS), Tsukuba, Japan)*

Patents & Technology Transfers

Submitted applications for patent protection:

In year 2009 four applications were submitted for patent protection. All of them were started as national application. The details are the following:

P0900115 :

Priority date:	26th February, 2009
Title:	"*Measuring arrangement and method for detecting floating pollution on surface of liquid essentially for monitoring wells*"
Applicants	MFA (90%), ENVICOM 2000 Ltd. (10%)
Inventors	Miklós RÁCZ: (35%), István BÁRSONY (10%), András HÁMORI (15%), János HIDASI (10%), János MAKAI (15%), Miklós SERÉNYI (15%)

P0900401 :

Priority date:	26th June, 2009
Title:	"*Apparatus and method for manufacturing logic gates with electrical and optical inputs and electrical output*"
Applicants	MFA (100%)
Inventors	Zsolt József HORVÁTH (100%)

P0900530 :

Priority date:	27th August, 2009
Title:	"*Method of forming a mask on surface of a body having general shape, and method of producing surface structure on a medical implant using the mask*"
Applicants	MFA (100%)
Inventors	Norbert NAGY (55%), András DEÁK (25%), Zoltán HÓRVÖLGYI - BMGE (10%), István BÁRSONY (10%)

P0900774 :

Priority date:	10th December, 2009
Title:	"*CMOS compatible fabrication process of crystalline silicon based extracellular electrodes realised by chemical wet etching, and provided with parallel side walls and rounded edges*"
Applicants	MFA (85%), MTA PK (7,5%), PPKE ITK (7,5%)
Inventors	Gábor BATTISTIG (5%), László GRAND (20%), György KARMOS (5%), Károlyné PAYER (15%), Anita PONGRÁCZ (20%), István ULBERT (5%), Éva VÁZSONYI (30%).

One of our patent applications has been granted the European Patent by the European Patent Office in 2009:

EP2027058 :

Priority date:	13th June, 2006 HU0600488, PCT/HU2007/000053, WO2007/144677
Title:	"*Monolithically integrated monocrystalline micromechanical elements*"
Applicants	MFA (100%)
Inventors	Antalné ÁDÁM (16%), István BÁRSONY (16%), Csaba DÜCSŐ (16%), Magdolna ERŐS (10%), Tibor MOHÁCSY (16%), Károlyné PAYER (10%), Éva VÁZSONYI (16%).

MFA Publications in 2009

1. **Aggarwal N**, Lawson K, Kershaw M, Horvath R, Ramsden JJ: "Protein adsorption on heterogeneous surfaces", *Applied Physics Letters, 94,083110-(2009)*
2. **Alves E**, Marques C, Sáfrán G, McHargue CJ: "Temperature behavior of damage in Sapphire implanted with light ions", *Nuclear Instruments and Methods in Physics Research B: Beam Interactions with Materials and Atoms, 267, pp.1464-1467 (2009)*
3. **Alves E**, Marques C, Sáfrán G, McHargue CJ: "The Structure of Sapphire Implanted with Carbon at Room Temperature and 1000 ºC", in *Application of Accelerators in Research and Industry, Book Series: AIP Conference Proceedings, volume: 1099, pp.376-379 (2009)*
4. **Aref A**, Horvath R, McColl J, Ramsden JJ: "Optical monitoring of stem-cell substratum interactions", *Journal of Biomedical Optics Letters, 14(1),010501-(2009)*
5. **Attolini G**, Watts BE, Bosi M, Rossi F, Riesz F: "A comparative study of the morphology of 3C-SiC grown at different C/Si ratios", *Materials Science Forum, 615-617, pp.153-156 (2009)*
6. **Attolini G**, Watts BE, Bosi M, Rossi F, Riesz F: "A study of the morphology of 3C-SiC layers grown at different C/Si ratios", *ECS Transactions, 25(3), pp.397-401 (2009)*
7. **Balazsi C**, Bishop A, Yang JHC, Balázsi K, Wéber F, Gouma P: "Biopolymer-hydroxyapatite scaffolds for advanced prosthetics", *Composite Interfaces, 16(2-3), pp.191-200 (2009)*
8. **Balázsi C**, Koszor O, Fényi B, Balázsi K: "Novel structural concepts of ceramics based composites: towards enhanced functionality in Global Roadmap of Cermaics", *2nd International Congress on Ceramics, Verona, 7-14 (2008)*
9. **Balázsi C**, Koszor O, Fényi B, Balázsi K: "Novel structural concepts of ceramics based composites: towards enhanced functionality in Global Roadmap of Cermaics", *2nd International Congress on Ceramics, Verona, IT,7-14 (2008)*
10. **Balázsi C**, Sedlácková K, Pfeifer J, Tóth AL: "Synthesis and Examination of hexagonal tungsten oxide nanocrystals for electrochromic and sensing applications in Sensors for Environment", *Health and Security, Advanced Materials and Technologies (Baraton MI), Springer (ISBN978-4020- 9010-3), pp.77-89 (2009)*
11. **Bálint Z**, Moser A, Kertész K, Biró LP, Parker AR: "A supposition: structural colours resulting from both natural and sexual selection on an individual wing in the butterfly genus Cyanophrys (Lepidoptera: Lycaenidae)*", Annales Historico-Naturales Musei Nationalis Hungarici, 101, pp.63-79 (2009)*
12. **Balogh J**, Bujdosó L, Kaptás D, Kemény T, Vincze I, Kovács A, Tóth L: "Interfaces in sequence permutated Fe-B-Ag multilayers", *Journal of Applied Physics, 105, 104303-08 (2009)*
13. **Barna A**, Kótis L, Lábár JL, Osváth Z, Tóth AL, Menyhárd M, Zalar A, Panjan P: "Producing metastable nanophase with sharp interface by means of focused ion beam irradiation", *Journal of Applied Physics, 105(4), 044305 (2009)*

14. **Bársony I**, Ádám M, Fürjes P, Lucklum R, Hirschfelder M, Kulinyi S, Dücső C: "Efficient catalytic combustion in integrated micropellistors", *Measurement Science and Technology, 20,124009 (2009)*

15. **Bársony I**, Dücső C, Fürjes P: "Thermometric Gas Sensing in Solid State Gas Sensing" *(Comini E), Springer Science, DOI: 10.1007/978-0-387-09665-0_7 (2009)*

16. **Bartók A**, Csík A, Vad K, Molnár G, Tóth-Kádár E, Péter L: "Application of Surface Roughness Data for the Evaluation of Depth Profile Measurements of Nanoscale Multilayers", *Journal of The Electrochemical Society, 156(7), D253-D260 (2009)*

17. **Beresna M**, Tomasiu R, Volk J, Kádár G: "Picosecond reflectance recovery dynamics of porous silicon multilayer", *Journal of Optical Society of America B, 26, pp.249-253 (2009)*

18. **Berlind T**, Furlan A, Czigany Z, Neidhardt J, Hultman L, Arwin H: "Spectroscopis ellipsomerty characterisation of amorphous carbon and amorphous, graphitic and fullerene-like carbon nitride thin films", *Thin Solid Films, 517(24), pp.6652-6658 (2009)*

19. **Blum I**, Portavoce A, Mangelinck D, Daineche R, Hoummada K, Lábár JL, Carron V, Bernardini J: "Measurement of As diffusivity in Ni2Si thin films", *Microelectronic Engineering, Art. no.: doi:10.1016/j.mee.2009.05.020 (2009)*

20. **Borysiewicz MA**, Pécz B, Tóth L, Kaminska E, Piotrowska A, Pasternak I, Jakiela R, Dynowska E: "Formation of a Ti_2AlN layer on GaN for contact applications", in *MC 2009, Microscopy Conference (Eds.: Grogger W, Hofer F, Pölt P), Vol.3: Materials Science, pp.43-44 (2009)*

21. **Broitman E**, Furlan A, Gueorguiev GK, Czigány Z, Tarditi AM, Gellman AJ, Stafström S, Hultman L: "Water Adsorption on Phosphorous-Carbide Thin Films", *Surface and Coatings Technology, 204(6-7), pp.1035-1039 (2009)*

22. **Buzas A**, Geretovszky Z, Nemeth A, Labadi Z, Juhasz, Major C, Barsony I: "Selective Laser Cutting of ZnO: Al Contact Layers", *in 24th European Photovoltaic Solar Energy Conference, 3004-3006, 2009*

23. **Cavellin CD**, Trimaille I, Ganem JJ, D'Angelo M, Vickridge I, Pongracz A, Battistig G: "An ^{18}O study of the interaction between carbon monoxide and dry thermal SiO2 at 1100 ^{o}C", *Journal of Applied Physics, 105, 033501 (2009)*

24. **Csákó T**, Berkesi O, Kovács I, Radnóczi G, Szörényi T: "Si-doped carbon nanostructured films by pulsed laser deposition from a liquid target", *Solid State Sciences, 11(10), pp.1783-1787 (2009)*

25. **Csanády A**, Lábár JL: "A transzmissziós elektronmikroszkópia és lehetőségei a nanoszerkezetű anyagok kutatásában", *Bevezetés a nanoszerkezetű anyagok világába (Szerk.: Csanády A, Kálmán E, Konczos G), ISBN9789632840536, ELTE Eötvös Kiadó, Budapest, pp.124-143 (2009)*

26. **Csik A**, Serényi M, Erdelyi Z, Nemcsics Á, Cserhati C, Langer GA, Beke DL, Frigeri C, Simon A: "Investigation of thermal stability of hydrogenated amorphous Si/Gemultilayers", *Vacuum, 84(1), pp.137-140 (2009)*

27. **Csíkvári P**, Fürjes P, Dücső C, Bársony I: "Micro-Hotplates for Thermal Characterisation of Structural Materials of MEMS", *Microelectronics Journal, 40(9), pp.1393-1397 (2009)*

28. **Daróczi CsS**: "Élmény és Tudomány", *Természet Világa, 140 (5), XXX (2009)*

29. **Daróczi CsS**: "Kulcsok a fizikához", *Fizikai szemle, LIX., pp.184-187 (2009)*

30. **De Vico Fallani F**, Astolfi L, Cincotti F, Mattia D, la Rocca D, Maksuti E, Salinari S, Babiloni F, Vegso B, Kozmann G, Nagy Z: "Evaluation of the brain network organization from EEG signals: a preliminary evidence in stroke patient", *Anatomical Record-Advances in Integrative Anatomy and Evolutionary Biology, 292 (12), pp.2023-2031 (2009)*

31. **Detrich A**, Deák A, Hild E, Kovács A, Hórvölgyi Z: "Langmuir and Langmuir-Blodgett Films of Bidisperse Silica Nanoparticles", *Langmuir, Art.no.:DOI: 10.1021/LA9027207 (2009)*

32. **Dmitruk N**, Dózsa L, Mamykin S, Kondratenko O, Molnár G: "Effect of annealing on optical properties of thin films with β-$FeSi_2$ quantum dots*", Vacuum, 84, pp.238-242 (2009)*

33. **Dobos L**, Pécz B, Tóth L, Horváth ZE, Tóth AL, Beaumont B, Bougrioua Z: "Contacts to heavily doped n-type GaN", in *First Joint Meeting of Dreiländertagung, Multinational Congress on Microscopy (Ed.:Grogger W, Hofer F, Pölt P) MC2009, Vol. 3: Materials Science, pp.29-30 (2009)*

34. **Dobos L**, Pécz B, Tóth L, Horváth ZJ, Horváth ZE, Horváth E, Tóth AL, Beaumont B, Bougrioua Z: "Al and Ti/Al contacts on n-GaN", *Vacuum, 84(1), pp.228-230 (2009)*

35. **Droz M**, Szwabisnki J, Szabó G: "Motion of influential players can support cooperation in Prisoner's Dilemma", *European Physical Journal B,71, pp.579-585 (2009)*

36. **El Kamel F**, Gonon P, Radnóczi G: "Electrical properties of Cu/a-$BaTiO_3$/Cu capacitors studied in dc and ac regimes", *Journal of Applied Physics, 105, 074104 (2009)*

37. **Eppeldauer GP**, Brown SW, Larason TC, Rácz M, Lykke KR: "Realization of a spectral radiance responsivity scale with a laser-based source and Si radiance meters", in *Optical Radiation Measurements Based on Detector Standards (Eds.: Eppeldauer GP), Gaithersburg, pp.123-133 (2009)*

38. **Eppeldauer GP**, Racz M, Hanssen L: "Spectral responsivity determination of a transfer standard pyroelectric radiometer", in *Optical Radiation Measurements Based on Detector Standards (Eds.: Eppeldauer GP), Gaithersburg, NIST Technical Note 1621, pp.78-86 (2009)*

39. **Eppeldauer GP**, Rácz M, Larason T: "Optical characterization of diffuser-input standard irradiance meters", in *Optical Radiation Measurements Based on Detector Standards (Eds.: Eppeldauer GP), Gaithersburg, pp.34-38 (2009)*

40. **Eppeldauer GP**, Rácz M: "Design and characterization of a photometer/colorimeter standard", in *Optical Radiation Measurements Based on Detector Standards (Eds.: Eppeldauer GP), Gaithersburg, NIST Technical Note 1621, pp.181-191 (2009)*

41. **Eppeldauer GP**, Rácz M: "Spectral Power and Irradiance Responsivity Calibration of InSb Working-Standard Radiometers", in *Optical Radiation Measurements Based on Detector Standards (Eds.: Eppeldauer GP), Gaithersburg, pp.68-77 (2009)*

42. **Eppeldauer GP**, Yoon HW, Zong Y, Larason TC, Smith A, Racz M: "Radiometer standard for absolute responsivity calibrations from 950 nm to 1650 nm with 0.05% (k=2) uncertainty", in *Optical Radiation Measurements Based on Detector Standards (Eds.: Eppeldauer GP), Gaithersburg, NIST Technical Note 1621, pp.21-33 (2009)*

43. **Fekete Z**, Fürjes P: "A félvezetőgyártás ábrakialakítási módszerei", *Egyetemi jegyzetek Fizikai, kémiai- és nanotechnológiák laborhoz (könyvfejezet), kiadó: BMGE, Budapest, 14 (2009)*
44. **Fekete Z**, Fürjes P: "Szilícium alapú mikrofluidikai eszközök technológiája", *Egyetemi jegyzetek Fizikai, kémiai- és nanotechnológiák laborhoz (könyvfejezet), kiadó: BMGE, Budapest, 12 (2009)*
45. **Fényi B**, Hegman N, Szemmelveisz K, Balázsi C: "Impedance changes and carbon stability during the heat treatment of Si_3N_4 - carbon composites", *Key Engineering Materials, 409, pp.365-368 (2009)*
46. **Fried M**, Juhász G, Major C, Petrik P, Battistig G: "Homogeneity check of ion implantation in silicon by wide-angle ellipsometry", in *17th IEEE International Conference on Advanced Thermal Processing of Semiconductors – RTP 2009, ISBN 978-1-4244-3815-0/09 IEEE ,147 (2009)*
47. **Frigeri C**, Serényi M, Csik A, Erdélyi Z, Beke DL, Nasi L: "AFM and TEM study of hydrogenated sputtered Si/Ge multilayers", *Superlattices and Microstructures, 45, pp.475-481 (2009)*
48. **Gaal I**, Bartha L: "Mechanisms of Fracture in Commercial Lamp Grade Tungsten at the Ambient", *Powder Metallurgy Progress, 8(3), pp.230-240 (2008)*
49. **Galkin NG**, Goroshko DL, Polyarni VO, Chusovitin EA, Korobtsov VV, Balashev VV, Khang Y, Dózsa L, Gutakovsky AK, Latyshev AV, Shamirzaev TS, Zhuravlev KS: "Investigation of multilayer silicon structures with buried iron silicide nanocrystallites: Groth, structure, and properties", *Journal of Nanoscience and Nanotechnology, 8, pp.527-534 (2008)*
50. **Garcia G**, Lopeandía AF, Bernardi A, Alonso MI, Goñi AR, Lábár JL, Rodríguez-Viejo J: "Crystallisation of Amorphous Germanium Thin Films", *Journal of Nanoscience and Nanotechnology, 9, pp.3013-3019 (2009)*
51. **García López J**, Morilla Y, Cheang-Wong JC, Battistig G, Zolnai Z, Cantin JL: "Dynamic annealing study of SiC epilayers implanted with Ni ions at different temperatures", *Nuclear Instruments and Methods in Physics Research, Section B: Beam Interactions with Materials and Atoms, 267(7), pp.1097-1100 (2009)*
52. **Gergely G**, Gurban S, Menyhard M, Jablonski A, Zommer L, Goto K: "The inelastic mean free path of electrons. Past and present research", *Vacuum, 84(1), pp.134-136 (2009)*
53. **Gergely GK**, Makszimus A, Pázmán J, Gácsi Z: "Különleges anyagok és korszerű technológiák", *Bányászati és Kohászati Lapok, 142(4), 31-36 (2009)*
54. **Giubertoni D**, Pepponi G, Beckhoff B, Hoenicke P, Gennaro S, Meirer F, Ingerle D, Steinhauser G, Fried M, Petrik P: "Multi-technique characterization of arsenic ultra shallow junctions in silicon within the ANNA consortium", in *Proceedings of the Frontiers of Characterization and Metrology for Nanoelectronics, Albany, U.S.A.: 2009, 45 (2009)*
55. **Gubicza J**, Chinh NQ, Lábár JL, Dobatkin S, Hegedűs Z, Langdon TG: "Correlation between microstructure and mechanical properties of severely deformed metals", *Journal of Alloys and Compounds, 483(1-2), pp.271-274 (2009)*
56. **Gubicza J**, Chinh NQ, Lábár JL, Hegedus Z, Langdon T: "Twinning and dislocation activity in silver processed by severe plastic deformation", *Journal of Materials Science, 44(6), pp.1656-1660 (2009)*

57. **Gubicza J**, Chinh NQ, Lábár JL, Tichy G, Hegedűs Z, Xu C, Langdon TG: "Stability of microstructure in silver processed by severe plastic deformation", *International Journal of Materials Research, 100(6), pp.884-887 (2009)*

58. **Guczi L**, Beck A, Horváth A, Frey K, Stefler G, Pető G, Pászti Z, Geszti O: "The Effect of Oxide Morphology on Au/SiO2 in Catalysis as Scientific – Technical Discipline in Social Progress", *Science and Education, New Challenges in Catalysis V (Ed.:Putanov P) ISBN, 978-86-81125-70-0, pp.29-37 (2009)*

59. **Győrffy N**, Bakos I, Szabó S, Tóth L, Wild U, Schlögl R, Paál Z: "Preparation, characterization and catalytic testing of GePt catalysts", *Journal of Catalysis, 263(2), pp.372-379 (2009)*

60. **Hannus I**, Búza M, Beck A, Guczi L, Sáfrán G: "Hydrodechlorination catalytic activity of gold nanoparticles supported on TiO_2 modified SBA-15 investigated by IR spectroscopy", *Journal of Molecular Structure, 924-926, pp.355-357 (2009)*

61. **Höglund C**, Bareno J, Birch J, Alling B, Czigány Z, Hultman L: "Cubic $Sc_{1-x}Al_xN$ solid solution thin films deposited by reactive magnetron sputter epitaxy onto ScN (111)", *Journal of Applied Physics, 105, 113517 (2009)*

62. **Holec D**, Rovere F, Mayrhofer PH, Barna PB: "Pressure dependent stability of cubic and wurtzite phases within the TiN-AlN and CrN-AlN systems", *Scripta Materialia Art. no.: doi:10.1016/j.scriptamat.2009.10.040 (2009)*

63. **Horopantis EE**, Perentzis G, Beck A, Guczi L, Pető G, Papadimitriou L: "Identification of the presence of crystalline phase in lithiated boron oxide ionic glass conductors", *Materials Science and Engineering B, 165, pp.156-159 (2009)*

64. **Horváth ZJ**, Basa P: "Nanocrystal non-volatile memory devices", *Materials Science Forum, 609, pp.1-9 (2009)*

65. **Horváth ZJ**, Basa: "New trends in non-volatile semiconductor memories", in *Towards Intelligent Engineering and Information Technology (Ed.:Rudas IJ, Fodor J, Kacprzyk J),Springer, pp.323-333 (2009)*

66. **Horvát-Karajz K**, Balogh Z, Kovács V, Hámori A, Sréter L, Uher F: "In Vitro Effect of Carboplatin, Cytarabine, Paclitaxel, Vincristine, and Low-Power Laser Irradiation on Murine Mesenchymal Stem Cells", *Lasers in Surgery and Medicine, 41, pp.463-469 (2009)*

67. **Iablokov V**, Frey K, Geszti O, Kruse N: "High Catalytic Activity in CO Oxidation over MnOx Nanocrystals", *Catalysis Letters, DOI 10.1007/s10562-009-0244-0 (2009)*

68. **Juhász R**, Ódor G: "Scaling behavior of the contact process in networks with long-range connections", *Physical Review E, 80, 041123 (2009)*

69. **Juhász Z**, Sipos J: "A comparative analysis of Eurasian folksong corpora, using self organising maps", *Journal of Interdisciplinary Music Studies,Art. no.: doi: 10.4407/jims. (2009)*

70. **Juhász Z**: "Automatic Segmentation and Comparative Study of Motives in 11 Folk song Collections using self organising maps and multidimensional mapping", *Journal of new music research, 38(1), pp.71-85 (2009)*

71. **Juhász Z**: "Motive Identification in 22 folksong corpora using dynamic time warping and self organising maps", in *Proc. of the 10th Internapional Society for Music Information retrieval Conference, Kobe, (Eds.:Hirata K, Tzanetakis G)(ISMIR 2009),171-176 (2009)*

72. **Kádár G**: “A ferromágneses hiszterézis”, *Fizikai Szemle, LIX(5), pp.163-169 (2009)*

73. **Khánh NQ**, Berneschi S, Bányász I, Brenci M, Fried M, Nunzi Conti G, Pászti F, Pelli S, Righini GC, Watterich A: “Fabrication of channel waveguides in Er^{3+}-doped tellurite glass via N^{+} ion implantation”, *Nuclear Instruments and Methods in Physics Research section B-Beam Interactions with Materials and Atoms, 267, pp.2327-2330 (2009)*

74. **Koszor O**, Balázsi C: “The milling time effect on sintering kinetics of silicon nitride based composites”, *Key Engineering Materials, 409, pp.369-372 (2009)*

75. **Koszor O**, Horváth A, Weber F, Balázsi K, Gillemot F, Horvath M, Fényi B, Balázsi C: “The effect of neutron irradiation on the mechanical properties of advanced silicon nitride nanocomposites”, *Key Engineering Materials, 409, pp.237-243 (2009)*

76. **Koszor O**, Lindemann A, Davin F, Balázsi C: “Observation of thermophysical and tribological properties of CNT reinforced Si_3N_4”, *Key Engineering Materials, 409, pp.354-357 (2009)*

77. **Koszor O**, Wéber F, Arató P, Balázsi C: “Characterization of silicon nitride based composites with different type of carbon additions in Global Roadmap of Cermaics”, *2nd International Congress on Ceramics, Verona, IT, pp.1-7 (2008)*

78. **Kótis L**, Menyhárd M, Sulyok A, Sáfrán G, Zalar A, Kovac J, Panjan P: “Determination of the relative sputtering yield of carbon to tantalum by means of Auger electron spectroscopy depth profiling”, *Surface and Interface Analysis, 41, pp.799-803 (2009)*

79. **Kovács A**, Sato K, Lazarov VK, Galindo PL, Konno TJ, Hirotsu Y: “Direct observation of a surface induced disordering process in magnetic nanoparticles”, *Physical Review Letters, 103, 115703 (2009)*

80. **Kozma P**, Hamori A, Cottier K, Kurunczi S, Horvath R: “Grating coupled interferometry for optical sensing”, *Applied Physics B – Lasers and Optics, (DOI 10.1007/s00340-009-3719-1),97(1), 5-8 (2009*

81. **Krause M**, Bedel L, Taupeau A, Kreissig U, Munnik F, Abrasonis G, Kolitsch A, Radnóczi G, Czigány Z, Vanhulsel A: “Structural and mechanical characterization of BCxNy thin films deposited by pulsed reactive magnetron sputtering”, *Thin Solid Films, 518(1), pp.77-83 (2009)*

82. **Kurunczi S**, Horváth R, Yeh YP, Muskotál A, Sebestyén A, Vonderviszt F, Ramsden JJ: “Self-assembly of rodlike receptors from bulk solution”, *Journal of Chemical Physics,130, 011101 (2009)*

83. **Lábár JL**, Geszti O, Sáfrán G, Barna PB, Székely L, Misják F, Radnóczi G: “Process Diffraction: a SAED-based method to analyze phases and texture in nano-crystalline thin films in the TEM”, in *MC 2009 Vol.3: Materials Science, Microscopy Conference (Eds. Grogger W, Hofer F, Pölt P), Graz, AT, pp.279-280 (2009)*

84. **Lábár JL**: “Electron Diffraction Based Analysis of Phase Fractions and Texture”, in *Nanocrystalline Thin Films, Part II: Implementation, Microscopy and Microanalysis 15(1), pp.20-29 (2009)*

85. **Lábár JL**: “Nanokristályos anyagok elektrondiffrakciós vizsgálata (Process Diffraction)”, *Bevezetés a nanoszerkezetű anyagok világába (Szerk.:Csanády A, Kálmán E, Konczos G), ELTE Eötvös Kiadó, Budapest, ISBN9789632840536, pp.144-147 (2009)*

86. **Lendvai J**, Gubicza J, Lábár JL, Kuli Z: "Effect of crystallization on the deformation behavior of a Zr-based bulk metallic glass", *International Journal of Materials Research, 100(3), pp.439-442 (2009)*

87. **Lohner T**, Szekeres A, Nikolova T, Vlaikova E, Petrik P, Huhn G, Havancsak K, Lisovskyy I, Zlobin S, Indutnyy ZI, Shepeliavyi PE: "Optical models for ellipsometric characterization of high temperature annealed nanostructured SiO_2 films", *Journal of Optoelectronics and Advanced Materials, 11, pp.1288-1291 (2009)*

88. **Lugomer S**, Maksimovech A, Petõ G, Karacs A, Frenkel AI: "Fluid flow instability and microstructure evolution in the inclined laser processing of metal surface comprising impuririte", *International Journal of Pure and Applied Mathematics, 49, pp.37-44 (2008)*

89. **Luu AT**, Kajcsos Z, Thanh ND, Dung TQ, Nhon MV, Lázár K, Havancsák K, Huhn G, Horváth ZE, Tap TD, Son LT, Phuc PT: "Multi-wall carbon nanotubes investigated by positron annihilation techniques and microscopies for further production handling", *Physica Status Solidi C, 6(11),DOI 10.1002/pssc.200982105 (2009)*

90. **Major C**, Juhasz G, Petrik P, Horvath Z, Polgar O, Fried M: "Application of wide angle beam spectroscopic ellipsometry for quality control in solar cell production", *Vacuum, 84, pp.119-122 (2009)*

91. **Major C**, Nemeth A, Radnoczi G, Czigany Z, Fried M, Labadi Z, Barsony I: "Optical and electrical characterization of aluminium doped ZnO layers", *Applied Surface Science, 255, pp.8907-8912 (2009)*

92. **Malicsko L**, Pogany L, Toth AL, Horvath V, Beregi E: "Microscopic studies on imperfections in selected YAB single crystals", Crystal Research and Technology, 44(4), pp.425-432 (2009)

93. **Márk GI**, Vértesy Z, Kertész K, Bálint Z, Biró LP: "Order-disorder effects in structure and color relation of photonic-crystal-type nanostructures in butterfly wing scales", *Physical Review E, 80, 051903-1 (2009)*

94. **Maros MB**, Helmeczi NK, Arató P, Balázsi C: "Mechanical and fractographic analyses of monolithic Si_3N_4 ceramics during impact testing", *Key Engineering Materials, 409, pp.338-341 (2009)*

95. **Matuchova M**, Zdansky K, Zavadil J, Danilewsky A, Riesz F, Hassan MAS, Alexiew D, Kral R: "Study of the influence of the rare-earth elements on the properties of lead iodide", *Journal of Crystal Growth, 311(14), pp.3557-3562 (2009)*

96. **McColl J**, Horvath R, Aref A, Larcombe L, Morgan S, Chianella I, Yakubov G, Ramsden JJ: "Polyphenol restoration of cell spreading inhibition on glycoprotein substrates", *Journal of Biomaterials Science-Polymer Edition, 20(5-6), pp.841-851 (2009)*

97. **Mészáros S**, Gergely G, Ádám J: "A hazai TV képcső története", *Hiradástechnika, LXIV (9-10), pp.7-10 (2009)*

98. **Mikhaylushkin AS**, Höglund C, Birch J, Czigány Z, Hultman L, Simak SL, Alling B, Tasnadi F, Abrikosov IA: "Stability of ternary perovskites Sc_3EN (E = B, AL, Ga, In) from first principles", *Physical Review B, 79(13), 134107 (2009)*

99. **Misják F**, Barna PB, Szerencsi M, Radnóczi G: "Morphologies, due to growth process induced segregation in two component thin films", in *MC 2009 (Eds.:Grogger W, Hoffer F, Pölt P), Graz,AT, pp.473-474 (2009)*

100. **Misják F**, Horváth ZE, Barna PB, Radnóczi G: "Development of texture and morphology in Cu-Ag thin nanocomposite films on Si", *Journal of Physics Conference Series, 100, 082008-(2008)*

101. **Mitterer C**, Lechthaler M, Gassner G, Fontalvo GA, Tóth L, Pécz B, Raible M, Maier K, Bergmann E: "Self-lubricating chromium carbide/amorphous hydrogenated carbon nanocomposite coatings: a new alternative to tungsten carbide/amorphous hydrogenated carbon", *Tribology, 223(J5), pp.751-757 (2009)*

102. **Naganuma H**, Kovacs A, Harima T, Shima H, Okamura S, Hirotsu Y: "Structural analysis of interfacial strained epitaxial $BiMnO_3$ films fabricated by chemical solution deposition", *Journal of Applied Physics, 105,07D915 (2009)*

103. **Nagata T**, Volk J, Yamashita Y, Yoshikawa H, Haemori M, Hayakawa R, Yoshitake M, Ueda S, Kobayashi K, Chikyow T: "Interface structure and the chemical states of Pt film on polar-ZnO single crystal", *Applied Physics Letters, 94, 221904 (2009)*

104. **Neidhardt J**, Czigány Z, Sartory B, Tessadri R, Mitterer C: "Wear-resistant Ti–B–N nanocomposite coatings synthesized by reactive cathodic arc evaporation", *International Journal of Refractory Metals and hard Materials, 28(1), pp.23-31 (2009)*

105. **Nemcsics A**, Heyn C, Stemmann A, Schramm A, Welsh H, Hansen W: "The RHEED tracking of the dropletepitexal grown quantum dot and ring structures", *Material Science Engineering B,165, pp.118-121 (2009)*

106. **Nemcsics Á**, Nagy S, Mojzes I, Schwedhelm R, Woedtke S, Adelung R, Kipp L: "Investigation of the surface morphology on epitaxially grown fullerene structures", *Vaccuum, 84, pp.150-154 (2009)*

107. **Nemcsics Á**, Nagy S, Mojzes I, Turmezei P: "Fractal and structural entropy calculations on the epitaxially grown fulleren structures with the help of image processing", in *Proc. of 7th Int. Symp. on Intelligent Systems and Informatics, Subotica, pp.65-67 (2009)*

108. **Nemcsics Á**, Schuszter M, Dobos L, Turmezei P: "Investigation of Electrochemically Etched GaAs(001) Surface with the Help of Image Processing", *Acta Polytechnica Hungarica, 6, pp.95-102 (2009)*

109. **Nemcsics Á**: "In-Situ Investigation of the Growrh of Low-Dimensional Structures", *Towards Intelligent Engineering and Information Technology (Eds.:Rudas I, Fodor J, Kacprzyk J), Springer Verlag, Heidelberg, pp.557-572 (2009)*

110. **Nemes–Incze P**, Tapasztó L, Darabont A, Lambin P, Biró LP: "Scanning tunneling microscopy observation of circular electronic superstructures on multiwalled carbon nanotubes functionalised by nitric acid", *Carbon, 47, pp.764-768 (2009)*

111. **Németh A**, Lábadi Z, Tóth L: "Oscillations and power-dependent hysteresis in reactive ZnO plasma", *Vacuum, 84(1), pp.218-220, 2009*

112. **Ódor G**, Dickman R: "On the absorbing-state phase transition in the one-dimensional triplet creation model", *Journal of Statistical Mechanics-Theory and Experiment, 2009, P08024 (2009)*

113. **Ódor G**, Liedke B, Heinig KH: "Mapping of (2+1)-dimensional Kardar-Parisi-Zhang growth onto a driven lattice", *Physical Review E, 79, 021125 (2009)*

114. **Ódor G**: "Univerzalitási osztályok és fázisátalakulások komplex, nemegyensúlyi rendszerekben", *Fizikai szemle, 4, pp.136-140 (2009)*

115. **Oroszi L**, Der A, Kirei H, Rakovics V, Ormos P: "Manipulation of microfluidic flow pattern by optically controlled electroosmosis", *Microfluidics and Nanofluidics, 6(4), pp.565-569 (2009)*

116. **Osán J**, Reinhardt F, Beckhoff B, Pap AE, Török S: "Probing Patterned Wafer Structures by Means of Grazing Incidence X-ray Fluorescence Analysis", *ECS Transactions, 25, pp.441-451 (2009)*

117. **Pecz B**, Stoemenos J, Voelskow M, Skorupa W, Dobos L, Pongracz A, Battistig G: "Epitaxial 3C-SiC nanocrystal formation at the SiO_2/Si interface by combined carbon implantation and annealing in CO atmosphere", *Journal of Applied Physics, 105(8), 083508 (2009)*

118. **Perc M**, Szolnoki A: "Coevolutionary games - a mini review", *BioSystems, DOI:10.1016/j.biosystems.2009.10.003 (2009)*

119. **Petrik P**, Fried M, Vazsonyi E, Basa P, Lohner T, Kozma P, Makkai Z: "Nanocrystal characterization by ellipsometry in porous silicon using model dielectric function", *Journal of Applied Physics, 105, 024908-(2009)*

120. **Petrik P**, Fried M, Zolnai Z, Khánh NQ, Li J, Collins RW, Lohner T: "Dielectric Function and Defect Structure of CdTe Implanted by 350-keV Bi Ions", *Materials Research Society Symposium Proceedings, 1123, 1123-P05-01-(2009)*

121. **Petrik P**, Lohner T, Polgar O, Fried M: "Ellipsometric characterization of disorder created by ion-implantation ellipsometry", in *17th IEEE International Conference on Advanced Thermal Processing of Semiconductors – RTP 2009, ISBN 978-1-4244-3815-0/09 IEEE ,xx (2009)*

122. **Petrik P**, Milita S, Pucker G, Nassiopoulou A, Van den Berg J, Reading M, Fried M, Lohner T, Theodoropoulou M, Gardelis S, Barozzi M, Ghulinyan M, Lui A, Vanzetti L, Picciotto A: "Analytical Techniques for Semiconductor Materials and Process Characterization", *Preparation and Characterization of Nanocrystals - ECS Trans., 25(3) ,373-(2009)*

123. **Petrik P**, Szilagyi E, Lohner T, Battistig G, Fried M, Dobrik G, Biro LP: "Optical models for ultra-thin oxides on Si-terminated and C-terminated faces of thermally oxidized SiC", *Journal of Applied Physics, 106, 123506-(2009)*

124. **Pfeifer J**, Horváth E, Vértesy Z, Arató P, Balázsi C: "Chemical methods for scanning electron microscope characterization of non-oxide ceramics and composites", *Key Engineering Materials, 409, pp.382-385 (2009)*

125. **Pietralunga SM**, Fere M, Lanata M, Piccinin D, Radnoczi G, Misjak F, Lamperti A, Martinelli M, Ossi PM: "Heteroepitaxial sputtered Ge on Si (100)", *Nanostructure and interface morphology EPL, 88(2), 28005 (2009)*

126. **Pődör B**, Horváth ZJ, Rakovics V: "Electrical and optical properties of InGaAsSb/GaSb" in *Proc. 32 th Int. Spring Seminar on Electronics Technology, Brno, CZ , ISBN 978-1-4244-4260-7, pp.328-329 (2009)*

127. **Pődör B**: "Defect thermal ionization energies in Cu-III-VI2 compound semiconductors", in *Proc. 32 th Int. Spring Seminar on Electronics Technology ISSE2009, ISBN9781424442607, Brno, pp.330-331 (2009)*

128. **Pongracz A**, Hoshino Y, D'Angelo M, Deville Cavellin C, Ganem JJ, Trimaille I, Battistig G, Josepovits K, Vickridge I: "Isotopic tracing study of the growth of silicon carbide nano-

crystals at the SiO_2/Si interface by CO annealing", *Japanese Journal of Applied Physics, 106, 024302 (2009)*

129. **Popa M**, Preda S, Fruth V, Sedlácková K, Balázsi C, Crespo D, Calderón-Moreno JM: "$BiFeO_3$ films on steel substrate by the citrate method", *Thin Solid Films, 517(8), pp.2581-2585 (2009)*
130. **Rácz M**, Eppeldauer GP: "Directional error correction of radiometric and photometric standard detectors" in *Optical Radiation Measurements Based on Detector Standards (Eds.: Eppeldauer GP), Gaithersburg, NIST Technical Note 1621, pp.211-215 (2009)*
131. **Rácz M**, Serényi M, Hámori A, Hidasi J: "Képalkotó reflexiómérő berendezés vízfelületen megjelenő folyékony szénhidrogén-származékok kimutatására", *Országos Környezetvédelmi Konferencia, Siófok, pp.47-50 (2009)*
132. **Rajta S**, Szilasi S, Fürjes P, Fekete Z, Dücső C: "Si Micro-turbine by Proton Beam Writing and Porous Silicon Micromachining", *Nuclear Instruments and Methods in Physics Research Section B, 267, pp.2292-2295 (2009)*
133. **Rakovics V**: "Félvezető vékonyrétegek kémiai leválasztása vizes oldatból", *Műszaki Kémiai Napok '09 (Nagy E), Veszprém, pp.98-103 (2009)*
134. **Ramsden JJ**, Horvath R: "Optical biosensors for cell adhesion", *Journal of Receptors and Signal Transduction, 29(3-4), pp.211-223 (2009)*
135. **Riesz F**: "Makyoh topography for the studies of extended defects: possibilities and limitations", *Physica Status Solidi C, 6(8), pp.1948-1952 (2009)*
136. **Sáfrán G**, Reinhard C, Ehiasarian AP, Barna PB, Székely L, Geszti O, Hovsepian PE: "Influence of the bias voltage on the structure and mechanical performance of nanoscale multilayer CrAlYN/CrN physical vapor deposition coatings", *Journal of Vacuum Science & Technology A,27(2), pp.174-182 (2009)*
137. **Sedláčková K**, Grasin R, Ujvári T, Bertóti I, Radnóczi G: "Carbon-metal (Ni or Ti) nanocomposite thin films for functional applications*", Solid State Science, 11(10), pp.1815-1818 (2009)*
138. **Serényi M**, Makai J: "A vízfelületen megjelenő folyékony szénhidrogén-származékok kimutatására szolgáló optikai berendezés", *Siófoki Országos Környezetvédelmi Konferencia, pp.51-57 (2009)*
139. **Shikimaka O**, Grabco D, Balázsi K, Danitsa Z, Mirgorodscaia I, Balázsi C: "Influence of microstructure on mechanical response of silicon nitride ceramic composites in nano-, micro- and macro-volume of material", *Key Engineering Materials, 409, pp.346-349 (2009)*
140. **Simon A**, Sulyok A, Novák M, Juhász G, Lohner T, Fried M, Barna Á, Huszank R, Menyhárd M: "Investigation of an ion-milled Si/Cr multilayer using micro-RBS, ellipsometry and AES depth profiling techniques", *Nuclear Instruments and Methods in Physics Research Section B: Beam Interactions with Materials and Atoms, 267(12-13), pp.2212-2215 (2009)*
141. **Somodi F**, Borbath I, Hegedus M, Lazar K, Sajo IE, Geszti O, Rojas S, Fierro JLG, Margitfalvi JL: "Promoting effect of tin oxides on alumina-supported gold catalysts used in CO oxidation", *Applied Surface Science, 256(3), pp.726-736 (2009)*

142. **Stueber M**, Ziebert C, Leiste H, Ulrich S, Sanz C, Fuentes E, Etxarri I, Solay M, Garcia A, Barna PB, Hovsepian P: "Wear Studies and Cutting Tests of Ti-Al-N-C Nanocomposite Coatings", *Machining Science and Technology, 13(1), pp.122-141 (2009)*

143. **Süle P**, Heinig KH: "The molecular dynamics simulation of ion-induced ripple growth", *Journal of Chemical Physics, 131, pp.204704-204712 (2009)*

144. **Szabó G**, Szolnoki A, Vukov J: "Selection of dynamical rules in spatial Prisoner's Dilemma games", *Europhysics Letters, 87, 18007/1-5. (2009)*

145. **Szabó G**, Szolnoki A: "Cooperation in spatial Prisoner's Dilemma with two types of players for increasing number of neighbors", *Physical Review E, 79, 016106/1-4. (2009)*

146. **Szabó G**: "A tisztességes magatartás kialakulása: játékelméleti elemzés", *Fizikai Szemle, 2009/3, 118 (2009)*

147. **Szekeres A**, Lohner T, Petrik P, Huhn G, Havancsak K, Lisovskyy I, Zlobin S, Indutnyy IZ, Shepeliavyi PE: "Ellipsometric characterization of SiOx films with embedded Si nanoparticles", *Vacuum, 80(1), pp.115-118 (2009)*

148. **Szekeres A**, Vlaikova E, Lohner T, Petrik P, Cziraki A, Kovacs G, Zlobin S, Shepeliavyi P: "Effect of high-temperature annealing on evaporated silicon oxide films: A spectroscopic ellipsometry study", in *Analytical Techniques for Semiconductor Materials and Process Characterization VI, Vienna, pp.379-384 (2009)*

149. **Szentpáli B**, Németh Á, Lábadí Z, Kovács G: "The Low-Frequency Noise in Al Doped ZnO Films", in *Proc. of the 20th International Conference on Noise and Fluctuations, Pisa, Italy, American Institute of Physics, AIP Conference Proceedings: 1129, pp.129-132 (2009)*

150. **Szilagyi IM**, Madarasz J, Pokol G, Hange F, Szalontai G, Varga-Josepovits K, Toth AL: "The effect of K^+ ion exchange on the structure and thermal reduction of hexagonal ammonium tungsten bronze", *Journal of Thermal Analysis and Calorimetry, 97(1), pp.11-18 (2009)*

151. **Szilágyi IM**, Wang L, Gouma PI, Balazsi C, Madarász J, Pokol G: "Preparation of hexagonal WO_3 from hexagonal ammonium tungsten bronze for sensing NH_3", *Materials Research Bulletin, 44(3), pp.505-508 (2009)*

152. **Szolnoki A**, Perc M, Szabó G, Stark HU: "Impact of aging on the evolution of cooperation in the spatial prisoner's dilemma game", *Physical Review E, 80, 021901 (2009)*

153. **Szolnoki A**, Perc M, Szabó G: "Phase diagrams for three-strategy evolutionary prisoner's dilemma games on regular graphs", *Physical Review E, 80, 056104 (2009)*

154. **Szolnoki A**, Perc M, Szabó G: "Topology-independent impact of noise on cooperation in spatial public goods games", *Physical Review E, 80, 056109 (2009)*

155. **Szolnoki A**, Perc M: "Emergence of multilevel selection in the prisoner's dilemma game on coevolving random networks", *New Journal of Physics, 11, 093033 (2009)*

156. **Szolnoki A**, Perc M: "Promoting cooperation in social dilemmas via simple coevolutionary rules", *European Physical Journal B, (DOI: 10.1140/epjb/e2008-00470-8),67(3), pp.337-344 (2009)*

157. **Szolnoki A**, Perc M: "Resolving dilemmas on evolving random networks", *Europhysics Letters, (DOI: 10.1209/0295-5075/86/30007), 86, 30007 (2009)*

158. **Szolnoki A**, Vukov J, Szabó G: "Selection of noise level in strategy adoption for spatial social dilemmas", *Physical Review E, 80, 056112 (2009)*

159. **Tomáš I**, Vértesy G, Kobayashi S, Kadlecová J, Stupakov O: "Low Carbon Steel Samples Deformed by Cold Rolling – Analysis of the Magnetic Adaptive Testing", *Journal of Magnetism and Magnetic Materials, 321, pp.2670-2676 (2009)*

160. **Tomáš I**, Vértesy G: "Influence of rate of change of magnetization processes on sensitivity of magnetic adaptive testing", *Journal of Magnetism and Magnetic Materials, 321, pp.1019-1024 (2009)*

161. **Tompos A**, Margitfalvi JL, Szabó EG, Pászti Z, Sajó I, Radnóczi G: "Role of modifiers in multi-component MgO-supported Au catalysts designed for preferential CO oxidation", *Journal of Catalysis, 266(2), pp.207-217 (2009)*

162. **Tóth AL**: "Elektronsugaras Mikroanalizis Restaurátoroknak (I) SEM", *ISIS-Erdélyi restaurátor füzetek, 8-9, pp.13-25 (2009)*

163. **Tóth AL**: "Elektronsugaras Mikroanalizis Restaurátoroknak (I) SEM", *ISIS-Erdélyi restaurátor füzetek, 8-9, pp.118-125 (2009)*

164. **Vancsó P**, Bíró LP, Márk GI: "Kvantum Főnix – hullámcsomag dinamika az Interneten", *Fizikai Szemle, 59, pp.233-238 (2009)*

165. **Vassányi I**, Gaál B, Fülöp K, Mák E, Kozmann G: "Personalized Dietary Counseling for Tele-care using Evolutionary Programming and Ontological Reasoning Med-e-Tel in Global Telemedicine and eHealth", *Updates: Knowledge Resources (Eds.Jordanova M) (ISSN 1998-5509), pp.272-276 (2009)*

166. **Vértesy G**, Tomáš I, Kobayashi S: "Nondestructive evaluation of low carbon steel by magnetic adaptive testing", *Nondestructive Testing and Evaluation, 53, pp.1-8 (2009)*

167. **Vértesy G**, Ueda S, Uchimoto T, Takagi T, Tomáš I: "Evaluation of plastic deformation in steels by magnetic hysteresis measurements", in *Proceedings of Sixth International Conference on Flow Dynamics, Sendai, Japan, pp.540-541 (2009)*

168. **Voelskow M**, Pecz B, Stoemenos J, Skorupa W: "Epitaxial 3C-SiC nanocrystal formation at the SiO_2/Si interface after carbon implantation and subsequent annealing in CO atmosphere Source", *Nuclear Instruments & Methods in Physics Research section B-Beam Interactions with Materials and Atoms,267 (8-9), pp.1364-1367 (2009)*

169. **Volk J**, Nagata T, Erdélyi R, Bársony I, Tóth AL, Lukács IE, Czigány Z, Tomimoto H, Shingaya Y, Chikyow T: "Highly Uniform Epitaxial ZnO Nanorod Arrays for Nanopiezotronics", *Nanoscale Research Letters, pp.699-704 (2009)*

170. **Zhou S**, Berndt M, Bürger D, Heera V, Potzger K, Abrasonis G, Radnóczi G, Kovács GJ, Kolitsch A, Helm M, Fassbender J, Möller W, Schmidt H: "Spin-dependent transport in nanocomposite C:Co films", *Acta Materialia, 57(16), pp.4758-4764 (2009)*

171. **Zolnai Z**, Deák A, Nagy N, Tóth AL, Kótai E, Battistig G: "A 3D-RBS study of irradiation-induced deformation and masking properties of ordered colloidal nanoparticulate masks", *Nuclear Instruments and Methods in Physics* Research *B(DOI: 10.1016/j.nimb.2009.09.039), 268, pp.79-86 (2009)*

172. **Zourob M**, Skivesen N, Horvath R, Mohr S, Goddard NJ: "Deep-Probe Optical Waveguides for Chemical and Biosensors in Advanced Photonic Structures for Biological and Chemical Detection", *Integrated Analytical Systems, Springer-Verlag New York (ISBN 978-0-387-98060-7.), pp.395-445 (2009)*